



ADDIS ABABA UNIVERSITY

SCHOOL OF GRADUATE STUDIES

SCHOOL OF EARTH SCIENCES

Rare metals mineralization in the Kilkile area of Kenticha Greenstone belt, Adola area, Southern Ethiopia



By: Mezmur Ayele

**A thesis submitted to Addis Ababa University in partial fulfillment of the requirements for
the degree of Master of Science in Earth Sciences**

(Mineral deposit)

**June, 2018
Addis Ababa, Ethiopia**

**ADDIS ABABA UNIVERSITY
SCHOOL OF GRADUATE STUDIES
SCHOOL OF EARTH SCIENCES**

**Rare metals mineralization in the Kilkile area of Kenticha
Greenstone belt, Adola area, Southern Ethiopia.**

**By
Mezmur Ayele**

ADVISOR: ZERIHUN DESTA (PhD)

**A thesis submitted to Addis Ababa University in partial fulfillment of the
requirements for the degree of Master of Science in Earth Sciences**

(Mineral deposit)

**June, 2018
Addis Ababa, Ethiopia**

**ADDIS ABABA UNIVERSITY
SCHOOL OF GRADUATE STUDIES
SCHOOL OF EARTH SCIENCES**

**Rare metals mineralization in the Kilkile area of Kenticha
Greenstone belt, Adola area, Southern Ethiopia.**

**By
Mezmur Ayele**

APPROVED BY EXAMINING BOARD

Dr. BALEMWAL ATNAFU

Head, School of Earth Sciences

Signature

Date

Dr. ZERIHUN DESTA

Advisor

Signature

Date

Dr. MULUGETA ALENE

Co-Advisor

Signature

Date

Prof. Dereje Ayalew

Examiner

Signature

Date

Dr. Worash Getaneh

Examiner

Signature

Date

**June, 2018
Addis Ababa, Ethiopia**

Declaration of Originality

This is to certify that this thesis entitled “Rare metals mineralization in the Kilkile area of Kenticha greenstone belt, Adola area, Southern Ethiopia”, is submitted in partial fulfillment of the requirements for the award of the degree of MSc, in Mineral deposit to the department of Earth Sciences, Addis Ababa University has been done by Mezmur Ayele, under the supervision of Dr. Zerihun Desta (2017/2018 academic year). This work has not been previously submitted to Addis Ababa University, or any other institution, for any degree, diploma or other qualification, and all sources of material used in this thesis have been duly acknowledged.

Mezmur Ayele

Signature

Date

This is to certify that the above declaration made by the candidate is correct to the best of my knowledge.

Dr. Zerihun Desta (Advisor 1)

Signature

Date

Dr. Mulugeta Alene (Advisor 2)

Signature

Date

Abstract

Rare metal bearing pegmatite of Kilkile contains a number of economically important minerals which attract economic interest by offering rare metals (Ta, Nb, Cs, Li and others), gemstones (emerald, aquamarine, tourmaline, beryl and Others) and industrial mineral (quartz and feldspar). The present study area is located in Adola area, southern part of Kenticha belt (southern part of Ethiopia). The main objective of the study is to evaluate the geology and geochemistry and characterize the rare metal bearing pegmatite of Kilkile area. To achieve the objective, field work and laboratory studies (thin and polished section) and geochemical analysis (ICP-MS and ICP-AES) have been conducted for whole rock and muscovite chemistry. Description of the geological structures and correlation with other rare metal bearing pegmatites have also been conducted for further examination of the genesis of the Kilkile rare metals. Based on field observation the Kilkile area predominantly consists of chromite, amphibolite gneiss and schist, biotite gneiss, serpentinite, chlorite-talc-tremolite schist, granites associated with barren & rare metal bearing pegmatites. Most of the pegmatite bodies of the area are striking nearly N-S direction, not more than a km long and have less than 200m width. Fractionation increases from south to north therefore rare metals like Rb, Li, Ga, Cs, and Ta concentration also increase towards north, while the Nb, Zn and Ba concentration decrease. Highly fractionated Kilkile I pegmatite plots in the zone of Ta-mineralization whereas Kilkile II and III plots in zone of Ta-prospect. REE chondrite normalized diagram shows all samples have enrichment in light rare earth element (LREE) contents relative to heavy rare earth elements (HREE) and shows negative Eu-anomaly. Kilkile rare metal bearing peraluminous granitic pegmatite is formed by partial melting of pre-existing metasedimentary rocks probably during post-Gondwana assembly, followed by hydrothermal-metasomatic enrichment of rare metals deposit. Muscovite chemistry, using Rb versus Tl and Rb versus K/Tl correlations, infers a cogenetic formation of Kilkile (I, II and III), Kenticha, Shuni and Bupo pegmatites and they are derived from same magma source most probably from Kilita Shumbela granite located on South of Kilkile III.

Key words: *Pan-African orogeny, Neoproterozoic, Arabian Nubian Shield, Kilkile area, Rare-element pegmatite, Magmatic fractionation, Muscovite chemistry, Ta-mineralization.*

Acknowledgment

First and foremost, praise is to Almighty God, without his mercy and support, this research could never have been achieved. I would like to acknowledge Ethiopia Ministry of Education for giving me the chance to join Master of Science in Mineral deposit at Addis Ababa University. My special thanks go to Addis Ababa University, school of Earth Sciences for funding this project.

I am indeed grateful to my advisors, Dr. Zerihun Desta and Dr. Mulugeta Alene for their invaluable encouragement, comment, assistance, fruitful discussion and guidance.

Special thanks go to to EMPBC for providing me all necessary data including borehole samples. This gratitude also included those who works in that company specially Mr. Tsegaye, Mr. Birhanu, Mr. Abdellah, Mr. Sadik, Mr. Yafet, Mr. Leta, Mr. Demelash, Mrs Hiwot and Mr. Gizaw all who helped me in every activity during field and office.

I would also like to extend my gratitude to the administrator of Dermi Woreda specially Mr. Hagela who is working on the head of Water super vision deserves big thanks. I am greatly indebted to Local people how live in and around Kenticha specially for Mr. Chala, Sister Kassech, Mrs. Wudase and Mr. Negeasa for helping me during undesirable field work.

My acknowledgement goes to my family for giving me courage and unforgettable support while I 'm in the project work specially my beloved sister Meron Ayele and her husband Zenebe Chaka as well as my brother Firew Ayele for their valuable support. My greatest appreciations also go to my dear friends' colleagues especially for Mr. Abera Birhanu for his valuable courage and limitless supports.

Table of content

Contents	Page No
ABSTRACT	I
ACKNOWLEDGMENT	II
TABLE OF CONTENT.....	III
LIST OF FIGURES.....	VI
LIST OF TABLES.....	VIII
LIST OF ACRONYMS.....	IX
CHAPTER ONE	
1. INTRODUCTION	1
1.1 RATIONALE	1
1.2. GEOGRAPHIC SETTING	3
1.2.1. <i>Location and accessibility</i>	3
1.2.2. <i>Physiography and climate of the study area</i>	4
1.3. STATEMENT OF THE PROBLEM.....	5
1.4. OBJECTIVES.....	6
1.4.1. GENERAL OBJECTIVE	6
1.4.2. <i>Specific objectives</i>	6
1.5. METHODOLOGY	6
1.5.1. <i>Pre-field work</i>	6
1.5.2. <i>Field work and sampling methods</i>	7
1.5.3. <i>Post-Field Work</i>	9
1.7. CHAPTER SCHEME	12
CHAPTER TWO	
2. LITERATURE REVIEW ON THE RARE METAL GRANITIC PEGMATITES	13
2.1. RARE METALS BEARING GRANITIC PEGMATITE.....	13
2.2. FORMATION OF RARE METAL BEARING GRANITIC PEGMATITES.....	13
2.3. ORIGIN OF RARE METAL BEARING GRANITE PEGMATITE	15
2.4. CLASSIFICATION OF GRANITE PEGMATITES	16
2.5. METHODOLOGY.....	19
2.6. ECONOMIC IMPORTANCE	20
2.7. EXPLORATION, MINING AND PROCESSING OF RARE METALS	22
2.7.1. <i>Exploration</i>	22
2.7.2. <i>Mining</i>	24
2.7.3. <i>Processing</i>	24
2.8. PREVIOUS WORKS ON RARE METALS DEPOSITS OF ETHIOPIA	25
CHAPTER THREE	
3. REGIONAL GEOLOGICAL SETTING	27
3.1. INTRODUCTION TO EAST AFRICAN OROGENY (EAO)	27

3.2. ARABIAN-NUBIAN SHIELD (ANS)	28
3.3. THE PRECAMBRIAN BASEMENT OF SOUTHERN ETHIOPIA.....	30
3.4. THE ADOLA BELT.....	31
CHAPTER FOUR	
4. GEOLOGY OF KILKILE AREA	34
4.1. INTRODUCTION	34
4.2. LOCAL GEOLOGY AND ROCK-FORMING MINERALS.....	34
4.2.1. <i>Biotite gneiss</i>	36
4.2.2. <i>Amphibolite gneiss</i>	36
4.2.3. <i>Amphibolite Schist</i>	38
4.2.4. <i>Chromitite</i>	38
4.2.5. <i>Serpentinite</i>	39
4.2.6. <i>Chlorite-Talc-Tremolite Schist</i>	41
4.2.7. <i>Granite</i>	43
4.2.8. <i>Pegmatite</i>	44
4.3. ALTERATION.....	49
4.4. GEOLOGIC STRUCTURES	52
4.4.1. <i>Foliation</i>	52
4.4.2. <i>Lineation</i>	53
4.4.3. <i>Fault</i>	54
4.4.4. <i>Joint and vein</i>	55
4.4.5. <i>Micro structure</i>	56
CHAPTER FIVE	
5. GEOCHEMISTRY OF THE KILKILE RARE METALS DEPOSIT.....	58
5.1. WHOLE-ROCK COMPOSITION	58
5.1.1 <i>Major Element Geochemistry</i>	60
5.1.2 <i>Trace Elements Geochemistry</i>	62
5.1.3 <i>REE composition of Kilkile area</i>	64
5.2 MUSCOVITE CHEMISTRY	64
5.2.1. <i>Major element</i>	66
5.2.2. <i>Trace elements and REE</i>	66
CHAPTER SIX	
6. DISCUSSION.....	71
6.1. GEOLOGY OF KILKILE RARE METAL DEPOSIT	71
6.2. ZONING.....	72
6.3. WHOLE-ROCK GEOCHEMISTRY	75
6.3.1. <i>Major elements</i>	75
6.3.2. <i>Trace elements</i>	76
6.3.3. <i>REE pattern</i>	77
6.4. MUSCOVITE CHEMISTRY	78
6.5. COMPARISON OF PEGMATITES IN THE ADOLA BELT.....	81
6.6. GENESIS AND PARAGENESES OF KILKILE RARE METAL DEPOSIT	84
6.6.1. <i>Genesis of Kilkile tantalite deposit</i>	84

6.6.2. *Parageneses of Kilkile tantalite deposit*88

6.7. OTHERS ECONOMIC IMPORTANT COMMODITIES IN GRANITIC PEGMATITES OF THE STUDY AREA90

CHAPTER SEVEN

7. CONCLUSIONS AND RECOMMENDATIONS.....92

7.1. CONCLUSIONS92

7.2. RECOMMENDATIONS94

REFERENCES.....95

APPENDIX I103

APPENDIX II106

List of Figures

Figures	Page No
Figure 1.1. <i>Location map of the study area</i>	3
Figure 1.2. <i>Photograph on Kilkile area</i>	4
Figure 1.3. <i>Physiographic map of Kilkile area</i>	5
Figure 1.4. <i>Flow sheet outlining the steps in the preparation of polished sections</i>	10
Figure 3.1. <i>Tectonic evolution Diagram of the East African Orogeny</i>	27
Figure 3.2. <i>The east Africa Orogeny</i>	28
Figure 3.3. <i>Simplified geological map of NE Africa and Kenticha pegmatite field</i>	32
Figure 4.1. <i>Geological map and cross section of the study area</i>	35
Figure 4.2. <i>Biotite gneiss and glimmerite from Kilkile area</i>	36
Figure 4.3. <i>Amphibolite gneiss</i>	37
Figure 4.4. <i>Micro photo picture of amphibolite gneiss rock unit sample</i>	37
Figure 4.5. <i>Amphibolite schist rocks on kilkile area</i>	38
Figure 4.6. <i>Chromite on Kilkile area</i>	39
Figure 4.7. <i>Serpentinite rocks on Kilkile area</i>	40
Figure 4.8. <i>Microscopic photo picture of serpentinite rock unit on Kilkile area</i>	41
Figure 4.9. <i>Chlorite- Talc-Tremolite schist from Kilkile area</i>	42
Figure 4.10. <i>Microscopic photo picture of Chlorite- Talc-Tremolite Schist</i>	43
Figure 4.11. <i>Weathered outcrop of granite from Kilkile area</i>	44
Figure 4.12. <i>Pegmatite rock on Kilkile area</i>	45
Figure 4.13. <i>Microscopic photo picture of pegmatite rock unit on Kilkile I and II</i>	47
Figure 4.14. <i>Ore microscopic photo picture of pegmatite rock unit on Kilkile area</i>	49
Figure 4.15. <i>Shows alteration of mineral in Kilkile area</i>	51
Figure 4.16. <i>Pervasive foliation in biotite gneiss</i>	52
Figure 4.17. <i>Stereo-plot of foliations</i>	53
Figure 4.18. <i>Geologic structure in Kilkile area shows intersection lineation</i>	53
Figure 4.19. <i>Geologic structure in Kilkile area(fault)</i>	54
Figure 4.20. <i>Stereo-plot of fault</i>	54
Figure 4.21. <i>Kilkile area joints photo</i>	55
Figure 4.22. <i>Stereo-plot for selective joints</i>	56

Figure 4.23. <i>Microscopic photo-pictures of microstructure and textures</i>	57
Figure 5.1. Classification diagrams for whole-rock samples (after Middlemost, 1985).....	60
Figure 5.2. <i>Classification and Discrimination diagrams</i>	60
Figure 5.3. <i>Discrimination diagrams (Clarke, 1992 and Chappel and White, 1974)</i>	62
Figure 5.4. <i>Classification diagrams samples of Feldspar triangle (after O’connor, 1965)....</i>	62
Figure 5.5. <i>geotectonic discrimination diagrams (Pearce et al., 1984)</i>	63
Figure 5.6. <i>Multi-element spider diagram Sun and McDonough (1989).</i>	63
Figure 5.7. <i>Chondrite normalized REE pattern (Boynton 1984)</i>	64
Figure 5.8. <i>Bivariate logarithmic diagrams (Beus 1966, and Gordiyenko 1971)</i>	67
Figure 5.9. <i>Rb/Sr Vs. some selected trace elements.</i>	68
Figure 5.10. <i>Nb/ Ta versus selected trace element variation in muscovite samples</i>	69
Figure 5.11. <i>Sun and McDonough, (1989) and Boynton, (1984) of the Kilkile muscovite</i>	69
Figure 6.1. <i>Borehole log of Kilkile I and II area.</i>	74
Figure 6.2. <i>Zoning redrafted from Fetherston (2004) and Černý (1991)</i>	75
Figure 6.3: <i>Triangular plot of Rb-Ba-Sr (El Bouseily and El Sökkary, 1975)</i>	77
Figure 6.4. <i>Bivariate plots showing geochemical variation in muscovite</i>	82
Figure 6.5. <i>Beus 1966, and Gordiyenko 1971 for Kenticha rare muscovite</i>	83
Figure 6.6. <i>Conceptual diagram to illustrate the genesis pegmatite (McKeough et al., 2013).</i>	87
Figure 6.7. <i>Paragenetic scheme of Kilkile pegmatite</i>	90
Figure 6.8. <i>Gem and Industrial minerals of Kilkile area</i>	91

List of Tables

Tables	Page No
Table 1.1. <i>List of samples and their name</i>	9
Table 1.2. <i>Chapters scheme</i>	12
Table 2.1. <i>The four classes of granitic pegmatite</i>	17
Table 2.2. <i>Classification of pegmatites of Rare-Element class after</i>	18
Table 2.3. <i>Internal structure and mineral assemblages of Kenticha pegmatite</i>	25
Table 4.1. <i>Minerals and texture of the pegmatite in some selected samples</i>	57
Table 5.1. <i>Major elements and trace elements from Kilkile pegmatite</i>	59
Table 5.2. <i>Major elements in weight and trace elements from Kilkile muscovite</i>	65
Table 6.1. <i>Average major and trace element composition of muscovite in from Kilkile (I, II, III), Kenticha, Bupo and Shuni, pegmatites</i>	81

List of Acronyms

AAS:	Atomic Absorption Spectrometry
ALS:	Australia Laboratories Service
ANS:	Arabian Nubian Shield
a.s.l	Above mean sea level
CGM:	Columbite Group Mineral
COLG:	Collisional Granite
EAO:	East African Orogeny
EMPBC:	Ethiopian Mineral Petroleum Biofuel Company
HFSE:	High field strength element
HREE:	Heavy rare earth element
ICP-MS:	Inductively Coupled Plasma-Mass Spectrometry
ICP-AES:	Inductively Coupled Plasma-Atomic Emission Spectrometry
ICP-OES:	Inductively Coupled Plasma-Optical Emission Spectrometry
LCT:	Lithium-cesium-tantalum family
LILE:	large ion lithophile element
LOI:	Loss of Ignition
LREE:	Light rare earth element
NYF:	Niobium-yttrium-fluorine family
ORG:	Orogenic Granites
PPL:	Plane polarized light
Ppm	Part per million
REE:	Rare earth elements
VAG:	Volcanic Arc Granites
WPG:	Within Plate Granites
XPL:	Cross polarized light

CHAPTER ONE

1. Introduction

1.1 Rationale

Ethiopia endowed with substantial amounts of metallic and non-metallic mineral resources and has a long history of traditional mining (Solomon et al., 2002). Metallic mineral resources that occur in various parts of the country include gold, platinum, copper, lead, zinc, tantalite columbite, manganese, molybdenum and iron (Aspermont, 2011). Out of all these, only one gold deposit (Legedembi, Medroc) and one columbo-tantalite deposit (Kenticha, Ethiopia Mineral Petroleum and Biofuel Corporation (EMPBC)) are under industrial scale mining operation. Regarding Industrial mineral resources and gemstones like emerald in Kilkile, sapphire in Tigray and opal in Amhara region are being exploited and some information sources indicate that the production of this commodities are offering some positive contribution to the country's economy.

The remaining mineral resources are not still exploited because some of them are not identified yet and some of them are in the exploration and reserve estimation stages. However, some individuals have already started to mine emerald, aquamarine, beryl and rare metals in Kenticha belt specially in Kilkile (the project area). The productions of these materials are not managed properly due to lack of knowledge and appropriate technology. Consequently, they are contributing very little to the country's economy.

The fastest growth of the world's population combined with an improving standard of living greatly increases the demand for different types of mineral-related products. Therefore, pursuing modern mineral exploration system in coupled with well-developed mineral resource management system play vital role for one country. According to Solomon (2009), in Ethiopia, modern mineral exploration related activities have been started very late in the 1960s with the establishment of the Ethiopian Geological Survey as a department within the Ministry of Mines and Energy to undertake surveys for geological mapping and to assess potential mineral resources of the country.

Strategic element occurrences reported in the country (Ta, Nb, Be, W, rare earth elements (REEs), and Co) are important to the country's economy in the near future (Solomon, 2009). For the follow up exploration program, complex-type of pegmatites need special focus because they are known to host important classes of rear element pegmatites which hosts LCT (Li–Cs–Ta) family elements (Cerný et al. 2012). According to the above writer such type of pegmatites contains enormous amount of Rb, Cs, Be, Ta, Nb, and Sn, and high quantity of fluxing components (Li, P, F, and B).

In Ethiopia, existence of rare metals was known some 38 years ago in southern Ethiopia (Adola region) particularly in Kenticha rare metal belt (covering area of more than 100 km length and 20 km width). A pocket of deposits found in different part of this rare metal belt are: Kilkile, Dermidama, Bupo, Katawicha, Bombawoha, Chembi, Angedi, etc. However, this pegmatite-hosted rare metals have not yet been totally studied and properly used. In order to ensure economic benefit from these minerals, this situation should be changed in the near future, and this requires both intensive promotional activity and efficient geological exploration by professionals (Ethiopian Ministry of Mines, 2002). Within the Kenticha belt, some kilometers to the north of my study area, there is a tantalum mine owned by government company, EMPBC. The area has been proved have deposit of more than 6000 ton of Ta₂O₅, >6000 ton of Nb₂O₅ and more than 200,000 tone of LiO₂ (Oral communication with profesional from EMPBC).

Kilkile area which consists a number of rare metal bearing pegmatites is located on the southern part of Kenticha Ta mining company. The study includes major and traces element analysis on Kilkile pegmatite rocks, collected from the study area. Trace element analysis was carried out using lithium borate fusion along with Inductively Coupled Plasma Mass Spectrometry (ICP-MS) and Lithium Borate Fusion along with Inductively Coupled Plasma and Atomic Emission Spectrometry (ICP-AES) for major oxides. In addition to that composition of muscovite was used to characterize the rare metals. Thin and polished sections were also used to understand the geology, alteration, parageneses and genesis of the rear metal deposit in Kilkile area.

1.2. Geographic setting

1.2.1. Location and accessibility

A selected study area (Kilkile area) is located in southern part of Ethiopia, Oromia National Regional State, Guji zone, Seba Boru woreda, Sebicha kebele. It falls within Kenticha map sheet and geographically bounded between $39^{\circ}00'00''\text{E}$ - $39^{\circ}02'50''\text{E}$, and $5^{\circ}22'50''\text{N}$ - $5^{\circ}26'40''\text{N}$. It covers 30 sq. km and it is located at about 560 km from the capital, Addis Ababa. The study area can be accessed via the main asphalt road that joins Addis Ababa to Kibremengist and through Addis Ababa-Sashemene-Hawassa-Kibremengist. The road from Kibremengist that takes to the Kilkile area through Shakisso to Kenticha and then Kilkile is totally gravel road. The site has 62 Km distance from shakisso town and on average located at 5 km from Kenticha tantalum mine site in south.

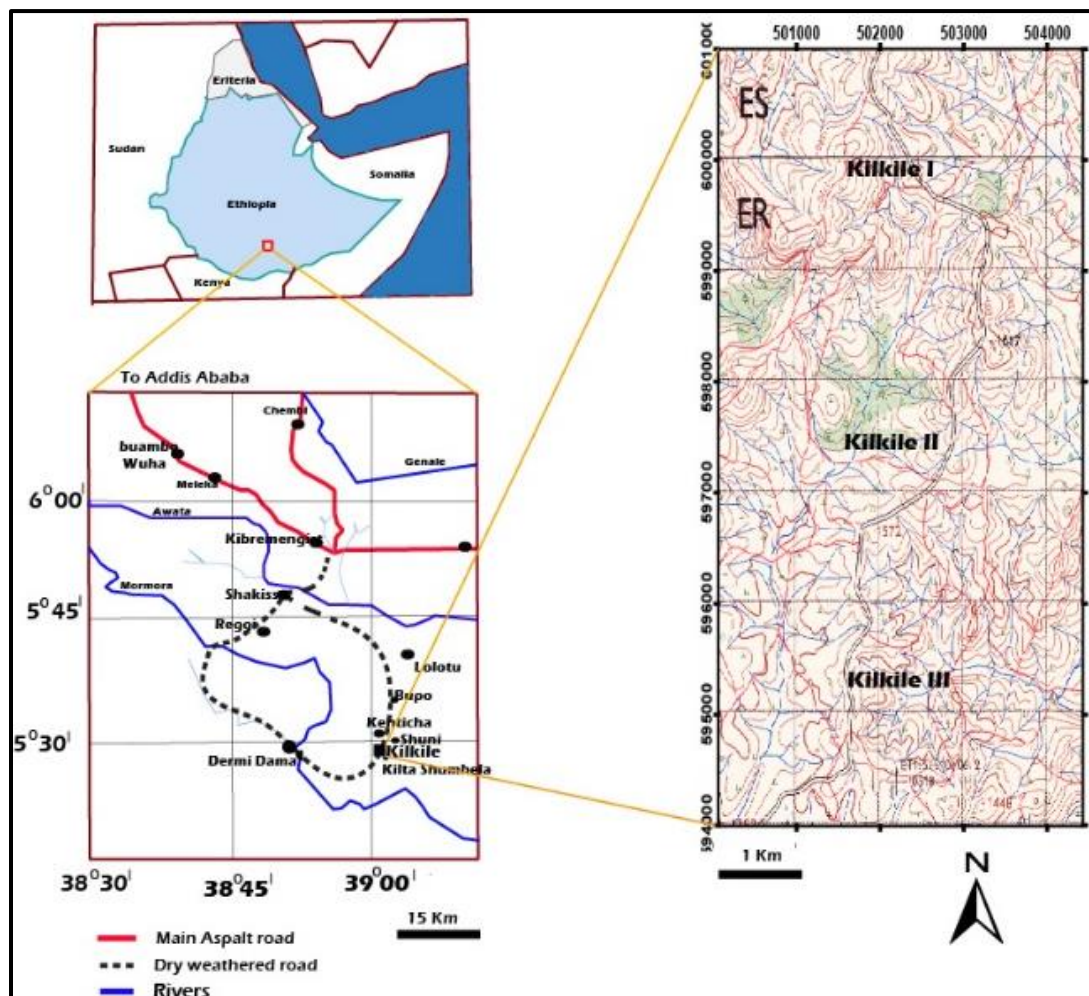


Figure 1.1. Location map of the study area.

1.2.2. Physiography and climate of the study area

The Dermi Dama, Killkile & Bupo area characterized by mountainous sloppy and rugged topography. The elevation ranges from 1400 to 1890m a.s. (EMPBC, 1997).



Figure 1.2. *photograph on kilkile area.*

The Mormora river, is the largest perennial river in the area. This river flows 12 km west of the deposit which provides sufficient water for drinking and industrial purpose. The drainage of the study area forms well developed dendritic pattern. The climate of the study area is equatorial monsoon type that includes both hot and humid condition and it accompanied by abrupt change of dry and rainy season respectively. The main rainy season are two: from March to May and September to November. The remaining months are generally characterized by dry weather condition. The annual precipitation ranges from 1100mm to 1300mm. The daily temperature varies from 11⁰C to 13⁰C minimum and 24⁰C to 30⁰C maximum (EMPBC, 1997).

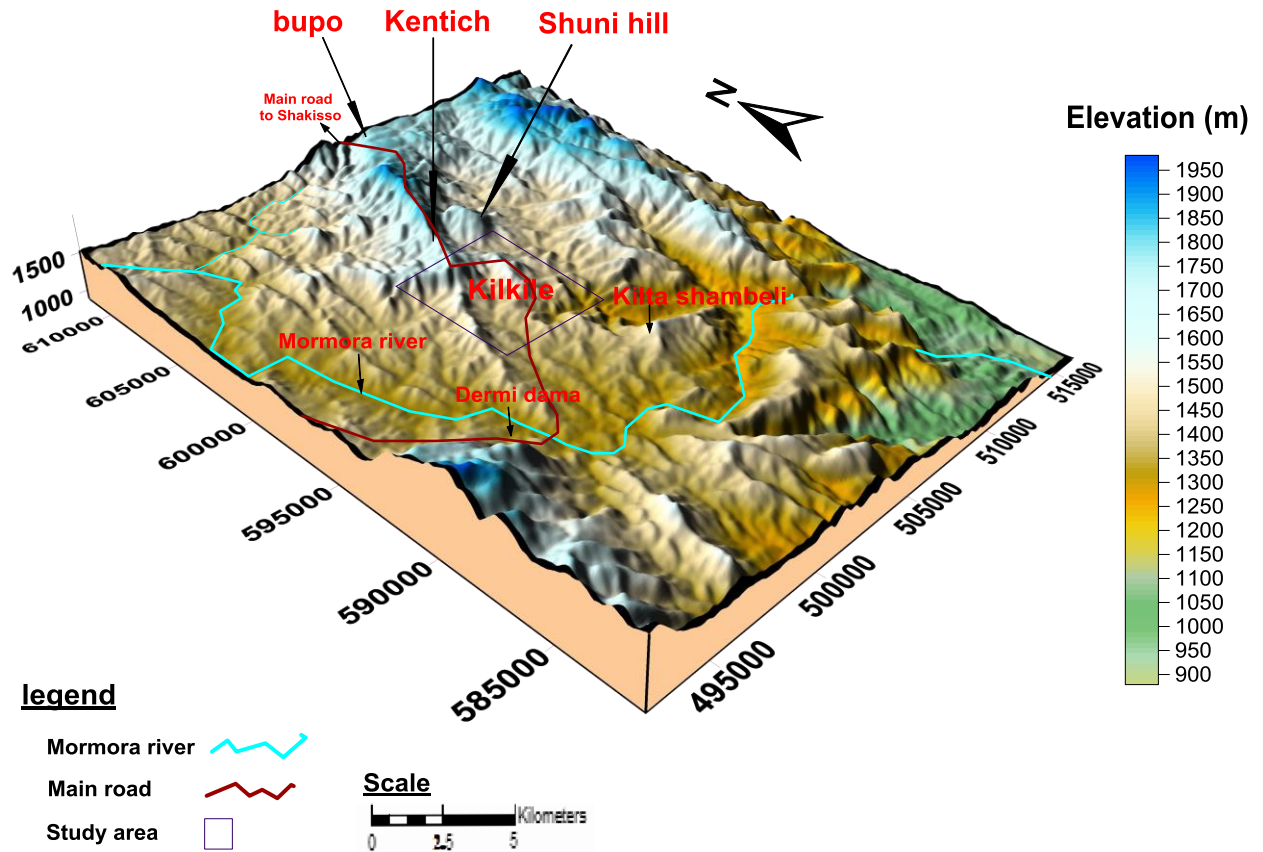


Figure1.3. Physiographic map of Kilkile area.

1.3. Statement of the problem

Rare metals are important in the modern world. Today many people use technological devices such as smart mobile phones, televisions, capacitors, computers, cars and others related devices. The growing demand for rear metals leads to strong interest in the search for economically viable deposits. The Kenticha area, is known for having a number of pegmatite bodies: mineralized and barren pegmatites. Therefore, discriminating between these types of pegmatites will assist exploration efforts in the search for rare–metal mineralization in the area (Zerihun et al., 1995).

Even though Kenticha belt consists a number of pegmatite occurrences it is not well studied (Zerihun, 1991; Zerihun et al., 1995; Küster, 2009; Solomon & Zerihun, 1996; Solomon, 2001) Due to its remote location, the Kenticha pegmatite has had little scientific study, those are limited to the weathering ore zone (Zerihun, 1991). Küster et al. (2009) has done some tasks on the geochemistry and age dating of the main Kenticha and Bupo using borehole data and little works on Kilkele and Shuni pegmatites using surficial pegmatite samples only for comparison. Therefore,

still more works are needed for both exploration of the deeper horizons of the primary ore zone and on surface pegmatite exposures.

Kilkile area consists a number of pegmatite deposit, which hosts rear metals like Li, Ta, Nb and Be. But there is no detail study conducted in relation to geology, petrography and geochemistry of mineralization, environment of deposition, genesis and alteration. Therefore, this thesis is proposed to fill this gap.

1.4. Objectives

1.4.1. General objective

The general objective of this project is to characterize rear metal mineralization in Kilkile area of Kenticha green stone belt.

1.4.2. Specific objectives

The specific objectives of the research are proposed to:

- Produce geological map of the study area at a scale of 1: 20,000.
- Characterize the petrology and geochemistry of the mineralized rocks.
- Describe associated structures at both microscopic and megascopic scales.
- Understand the genesis and parageneses sequence of rear metal mineralization.
- Correlate the rear metal bearing pegmatite from other area.

1.5. Methodology

Literature review, several field sampling and laboratory analyses were required to achieve the proposed thesis research; the whole activities are classified in to three phases such as the pre-field activity, the fieldwork and the post-field activity.

1.5.1. Pre-field work

Base map (topographic maps) 1:50,000 scale, GPS, compass, digital camera, sample bags, geological hammer, hand lenses, plastic bags, stationery materials and others that are essential for the field work were collected before actual fieldwork. In order to have a general overview about

the geology and mineralization of the study area and surrounding regions, the researcher has made review of relevant published and unpublished papers and technical reports. These latter helped the researcher as sources during preparation of research proposal (prepared at this stage) and thesis. Preliminary field visit had been conducted to have a general overview of the area, to select traverses and to assign data collection mechanisms.

1.5.2. Field work and sampling methods

Rare metal (Ta, Nb, Li, Be, Sc, Rb) bearing granitic pegmatite are known to occur in Adola area. Most of these pegmatites and granites are located in the Kenticha synclinal belt. In 1988-1989 various geologists of EMPBC conducted preliminary exploration works in southern part of Kenticha rare metal bearing pegmatite field such as Kilkile, Kenticha, Bupo, Kilta, Dermi Dama and Shuni. The Kilkile area consists parallel pegmatite bodies; some of them contain quartz rich core and greisen units while the others contain secondary albite and muscovite. According to EMPBC (2001) these pegmatites are rich in columbite-tantalite crystals relatively with higher content of TaO₅.

To characterize this rare metal pegmatite a number of activities has been conducted including gathering primary data in the field. The field work was conducted for 23 days in two phases: on October 9 to 24, 2017 and on April 22 to 28, 2018. Sample collection and geological map production at the scale of 1: 20,000, was done during the field work.

Degree of rare metal mineralization can be directly compared to that of the degree of fractionation. High content of Ta and Nb mineralization can be formed at the last stage of magma differentiation, (Černý, 1997). This is directly related with geographical location by which one can infer where the parent granite found. The distal ones being most fractionated (Breaks and Tindle, 1997). Based on geographical location, the study area divided in to three localities: Kilkile I (relatively the Northern part), Kilkile II (relatively the Central part) and Kilkile III (Southern part) (Fig. 1.1 & 4.1). Kilkile I and II pegmatites have borehole samples but Kilkile III pegmatites do not have, consequently all Kilkile III sample are surficial. Pegmatite rock consists very big crystals size, for this resion representatives whole rock specially muscovite mica was taken to represent study area.

Borehole samples and their locations were occupied from Ethiopian Mineral Petroleum and Biofuel Corporations. Every whole rock sample represent unique occurrence out of K1B14

(K1B14A & K1B14B) and K2A24 (K2A24A & K2A24B). K1B14B and K2A24B represent surficial samples which were taken relatively near to the surface and K1B14A and K2A24A represent the samples were taken relatively are at some depth.

Two types of data were collected for this research: primary and secondary. Most of the secondary data were collected before field work on pre-field work time whereas primary data was obtained mainly during field work. During field work preparing a geological map of the area at the scale of 1:20,000 finalized by using Arc GIS, Adobe illustrator and CorelDraw software. Identifying and measuring of the geologic structures (like faults, joints, lineation, foliation and other structures) were also conducted throughout the study.

Collection of representative samples for farther laboratory studies (like for thin section, polished section (Ethiopian Geological survey) and geochemical analysis (Australian laboratory science)), and recording GPS reading at each sampling station were conducted. Those samples described based on colour, texture and mineralogy similarly, their location has been plotted on the base map. Taking photograph of the lithology as well as transferring the data in to the topomap has been done.

No	Sample name	Description
Whole rock		
1	K1A7	Kilkile I area borehole A7
2	B14 }	K1B14B
3		K1B14A
4		K2T6S2
5	B24 }	K2A24A
6		K2A24B
7		K2C31
8		K2C30
9		K3T3S2
Muscovite chemistry		

10		K1B11	Kilkile IB borehole 11
11		K1A2A	Kilkile IA Borehole 2A
12		K2T4S1	Kilkile II travers four station one
13		K3T2S3	Kilkile III travers two station one

Table 1.1. *List of samples and their name*

1.5.3. Post-Field Work

The major tasks that were conducted during the post-field work includes: Geochemical analysis of rear metals (Li, Ta, Nb and associated rare metals) using ICP-MS and ICP-AES. Petrographical studies were undertaken by means of both thin and polished sections, under both plane polarized light (PPL) and cross polarized light (XPL). Both methods were used to understand the detail mineral assemblages, zoning, alteration and paragenetic relationships, genesis of the deposit and structural analysis of rare metal and their host rock.

1.5.3.1. Petrography

Petrography consists two major sub divisions such as: preparation of thin and polished sections and extraction of relevant information using transmitted light microscopy and ore microscope.

1.5.3.1.1. PREPARATIONS

Representative rock samples that have been collected from the study area and borehole were used for both thin and polished section at laboratory of Geological Survey of Ethiopia. Ten samples were sliced by the rock cutter and polished by DAP-U polishing machine to obtain the required size not greater than 4 cm to fit the mould size which has a maximum diameter of 4 cm. The rock samples were ground mechanically using carbide abrasive until the slice reaches the conventional thickness of 30 microns. This is carried out using petro-discs with 400-grit aluminum oxide powder. The general flow sheet outlying the steps in the preparation of polished sections is as follow.

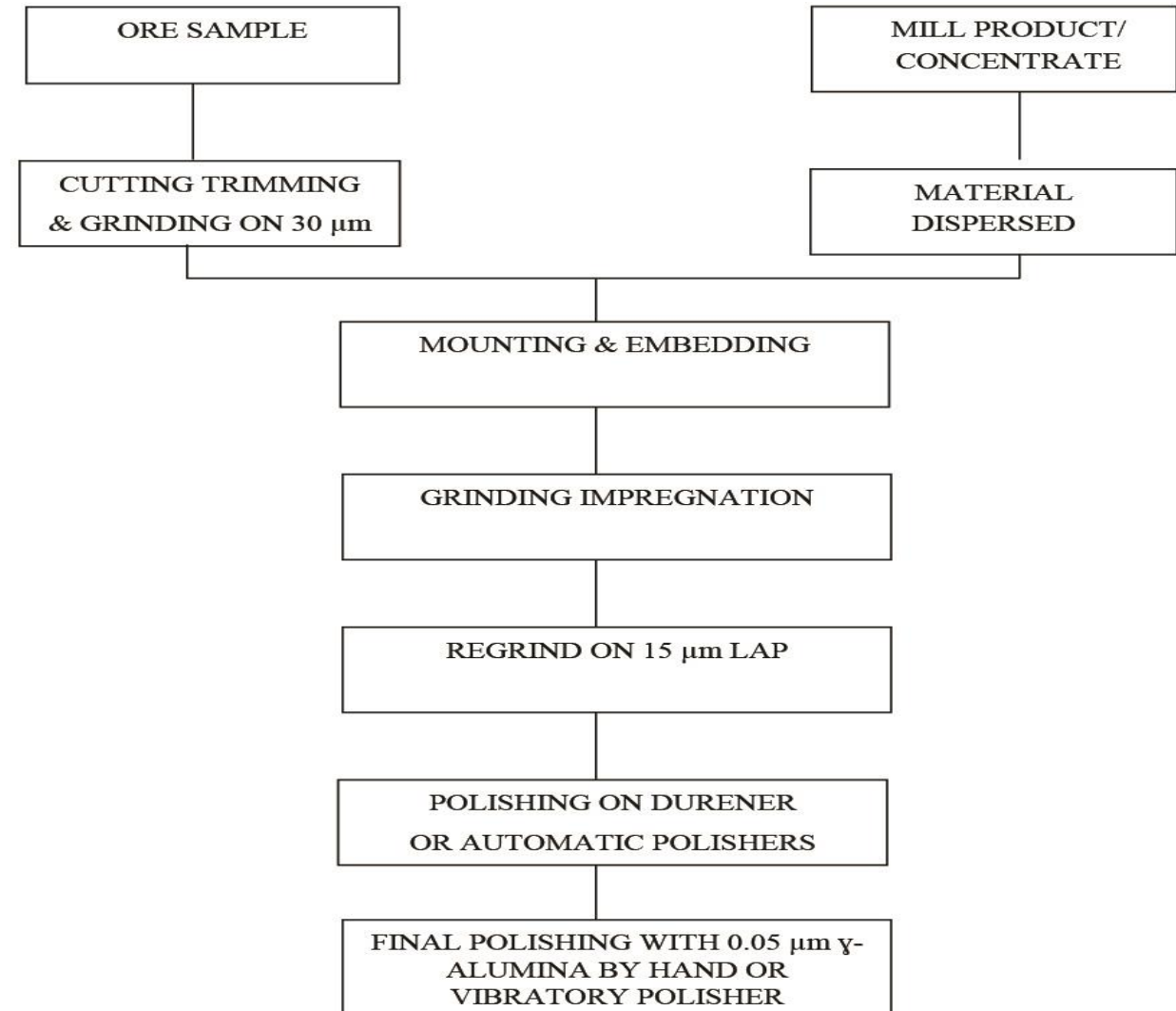


Figure 1.4. Flow sheet outlining the steps in the preparation of polished sections (after Craig, 1994).

1.5.3.1.2. MICROSCOPY

Ore microscopy and petrographic microscopy studies were conducted at laboratories of School of Earth Sciences, Addis Ababa University. Modal proportions and classifications, texture, grain size and micro structural features were studied under thin section and this value compared with normative value. For the purpose of ore minerals, reflected light microscope was used to identify the occurrence of ore minerals, their assemblage, alteration, parageneses and texture.

1.5.3.2. Geochemical Analyses

Thirteen rock samples, collected from surface and boreholes were submitted to ALS geochemical laboratory, Addis Ababa for preparation of geochemical analyses. The samples were crushed until 70% pass by less than 2mm sieve, after the sample split by sample splitter it again pulverized until 85 % pass by less than 75 microns. Finally, the pulverized samples were shipped to ALS Services, Loughrea located at Dublin road, Louhrea, Co. Galway, Ireland for whole rock and muscovite chemistry using ME-MS81d (for ICP-MS and ICP-AES) and ME-4ACD81(for Add-on Only). Codes are given by ALS services PLC to represent the methods.

1.5.3.2.1. ICP-MS

This method is a 30 Element Package which uses a minimum sample size of 1g. It comprises lithium borate fusion of the sample prior to acid dissolution which delivers the most quantitative analysis approach for a broad suite of trace elements. A prepared sample (4.00g) was added to lithium metaborate flux (0.90 g) in some cleaned PTFE microwave sample vessels and mixed well and fused in a furnace at 1000°C for 30 minutes. The melt is then cooled for 15 minutes and diluted in 100 mL of 4% HNO₃ or 2% HCl solution so that mineral species including those that are highly refractory are solubilized. The solution is then analyzed by inductively coupled plasma mass spectrometry for 30 trace elements including Ba, Ce, Cr, Cs, Dy, Er, Eu, Ga, Gd, Hf, Ho, La, Lu, Nb, Nd, Pr, Rb, Sm, Sn, Sr, Ta, Tb, Th, Tm, U, V, W, Y, Yb and Zr. For the code ME-4ACD81 Add-on Only Ag. As, Cd, Co, Cu, Li, Mo, Ni, Pb, Sc, Ti and Zn (Leta, 2016).

1.5.3.2.2. ICP-AES

The ICP-AES was used to analyze major elements in their oxide forms including SiO₂, Al₂O₃, Fe₂O₃, CaO, MgO, Na₂O, K₂O, Cr₂O₃, TiO₂, MnO, P₂O₅, SrO, BaO. Each of prepared solid samples (2g) was dissolved and mixed with water and sample solution was transformed into an aerosol by a nebuliser. After having been dissolved, the sample is then, topped off with dilute HCl and the solution containing the sample is analyzed using inductively coupled plasma-atomic emission spectrometry (ICP-AES) (Leta Amena., 2016).

1.7. Chapter scheme

This thesis is structured into seven chapters such as: Introduction, Review of literature, Regional geological setting, Local Geology and structures, Result and interpretation of geochemistry of Kilkile tantalite deposit, Discussion, and Finally conclusions and recommendations respectively. The content of each Chapter is highlighted in the table below.

Chapters	Contents
Chapter One	This chapter gives general information about the study area. The research problem and objectives and methods are included.
Chapter Two	Chapter two focus on literature review of rare metal bearing granitic pegmatites.
Chapter Three	This chapter provide a regional scale overview of geology and tectonic evolution of the ANS, Precambrian rocks of southern Ethiopia and mineralized Adola belt.
Chapter Four	Chapter four gives a detail description about the lithology, geological structures and geochemistry of tantalite deposit of study area.
Chapter Five	On this chapter geochemical results of whole rock and muscovite were interpreted and analyzed in the form of table and diagram.
Chapter Five	All results and findings are discussed hear. Geological, structural and geochemical data combined hear in order to know the genesis and parageneses of rare metals. Comparison on Kilkile rare metal bearing pegmatite with other area also included in this chapter
Chapter Six	Finally, the main conclusions and recommendations of this thesis is allocated in this chapter.

Table 1.1. Shows chapters scheme.

CHAPTER TWO

2. Literature review on the rare metal granitic pegmatites

2.1. Rare metals bearing granitic pegmatite

Pegmatite is “an essentially igneous rock, commonly of granitic composition, is distinguished from other igneous rocks by its extremely coarse but variable grain-size, or by an abundance of crystals with skeletal, graphic, or other strongly directional growth-habits.” (London, 2008). According to Bradley and McCauley (2013) geochemically, pegmatites typically have granitic composition and a pegmatite dyke will have a different trace element composition with greater enrichment in large-ion lithophile (incompatible) elements, boron, beryllium, aluminum, potassium and lithium, uranium, thorium, cesium, etc. Pegmatite is difficult to quantify the mineralogy in simple terms because it contains various mineralogy and difficulty in assessing the modal abundance of mineral species which are of only a trace amount, this is because of the difficulty in counting and sampling mineral grains in a rock which may have crystals centimeters, decimeters, or even meters across (New World Encyclopedia,2008).

Rare-element granitic pegmatites are well recognized and studied for the variety and concentrations of metal ores they host, supply of some of these elements recently designated metals such as (Nb, Ta, Ga, Zr, Hf, Li, Cs, Ti and Mn) from those tantalum and niobium are “critical materials” or “strategic resources”, these metals are very essential for once country economy’s (Linnen et al., 2011). According to Černý et al., (1985) high trace element concentrations, is affected by the style of partial melting and the degree of volatile saturation. Hydrothermal and metasomatic processes, also plays an important role on the accumulation of essential elements.

2.2. Formation of rare metal bearing granitic Pegmatites

Pegmatite is a very coarse-grained rock, which is mostly composed of quartz, feldspar and mica. Crystal size is the most striking feature of pegmatite, with crystals usually over 50mm in size. However, individual crystals over ten meters across have been found, consequently the world largest crystal was found within a pegmatite. For this crystal growth rates in pegmatite must be

incredibly fast to allow gigantic crystals to grow within the confines pressures of the Earth's crust. For this reason, the following processes are combined: Low rates of nucleation of crystals coupled with high diffusivity to force growth of a few large crystals instead of many smaller crystals, high vapor and water pressure to assist the enhancement conditions of diffusivity, high concentrations of fluxing elements such as boron and lithium which lower the temperature of solidification within the magma and low thermal gradients coupled with a high wall rock temperature (New World Encyclopedia,2008). In the early stages of a magma's crystallization, the melt usually contains a significant amount of dissolved water and volatiles such as chlorine, fluorine, and carbon dioxide, during crystallization in progresses the concentration of water in the melt become higher and higher eventually, pockets of superheated and rich in dissolved ions water separate from the melt (Hobart, 2018). Ions in the melt are not mobile as ions in the water, this allows them to move about and form crystals rapidly.

Pegmatite dikes are formed when the residual material released from the magma, many of those that had been stable at a higher level of heat become subject to etching or alteration take place, as the temperature become lower and lower, the cooling of these final fluids leads to the formation different rare metals, gems and valuable mineral take place, and this succession of minerals results in a concentric zoning of the pegmatite body (Ralph, 2015). These small pockets of pegmatite form from a magma in the late stages of crystallization along the margins of a batholith, and in fractures (Hobart, 2018).

According to London and Morgan (2012), fractional crystallization of the melt and interaction of aqueous fluid with the melt are the two competing models among the various proposed models that explain the formation of pegmatites and strategic resources. Field relationships, mineral chemistry, and experimental constraints indicate that these strategic resources are concentrated dominantly by magmatic processes (Linnen et al., 2011). The granitic melts involved in these processes are very unusual because they contain high concentrations of fluxing compounds, which play a key role at both the primary magmatic and late stage metasomatic process, fluxing components concentration and other incompatible elements increase towards the center of the magma chamber resulting increasing chemical fractionation from the margin to the center of the pegmatites (Cameron, 1949).

Two end member models have been proposed for the formation of fertile pegmatites i.e., continuous crystallization and partial melting. Partial melting of compositionally distinct protoliths produces wide compositional spectrum of granite magmas with the same degree of partial melting. Depending on the degree of fractional crystallization collective reservoir produces variety of granitic magmas (Shearer et al., 1992). Simmons et al., (1995) suggests that ghost and relict textures in the minerals, effect of fracturing in the mineral grains and the pattern of REE in the wall zone can be used as evidence for partial melting.

2.3. Origin of rare metal bearing granite pegmatite

The origin of rare metals bearing granitic pegmatite is still debatable. It is clear that some pegmatites represent the most highly fractionated products of a parental granite body, whilst others have formed by anatexis of local crust (Shaw et al., 2016). The compatibility of the elements in granitic pegmatites depends on the temperature, pressure and mineral phases in the system, and modified by fractional crystallization and assimilation processes. Incompatible elements in the rock forming minerals further increases until they form their own distinctive minerals such as spodumene, beryl and feldspars (Černý et al., 2012).

The provenance of pegmatites need to be traced back from their source granite, and can be mantle or crustal origin. According to (Černý et al., 2012) the origin of the pegmatites and their genetic link with the granites is controlled by the pressure-temperature condition, metamorphic grade and depth of emplacement. For instance, miarolitic pegmatites of shallow-level have no igneous control whereas the rare-element pegmatites of intermediate-depth are generally linked with the granites and are emplacement along deep-seated fault in tectonically active regimes.

Partial melting of mica rich pre-existing metamorphic rocks in collisional zones commonly forms LCT granitic pegmatites and gives high concentration of trace and rare earth elements. Muscovite and biotite carry most of the trace elements and these mica-bearing pegmatites are formed both by anatexis (Simmons, 2007) and igneous fractionation (e.g., Černý et al., 1985). The term NYF family is based on compositional characteristics that are related to the source (provenance) of the original magma and the chemical evolution of the magma as some components are removed and while others are concentrated (Rakovan, 2008).

2.4. Classification of granite pegmatites

The most geological classification of granitic pegmatite is provided by Ginsburge et al., (1979) This classification based on depth of emplacement and their relationship to metamorphism and granitic plutons. These pegmatites categorized in to four formations: a) Pegmatite formation of shallow depth (less than 3.5 km; Mirolitic pegmatites) it is immediate vicinity to parental granite has lowest metamorphic grade and contains rock quartz, optical fluorite, gem-quality beryl, topaz etc. b) Pegmatite formation in intermediate depth (3.5-7 km; rare element pegmatite) with Li, Cs, Be, Ta (Sn, Nb) mineralization in Precambrian shields. Rare-element pegmatites are commonly separated from their sources due to their intrusion into tectonically active regimes along deep fault system. C) Pegmatite formation of great depth (7.8-11 km mica bearing pegmatites) hosted by metamorphic rock of almandine-amphibolite facies which carry rare element mineralization. These pegmatites are commonly dispersed with in large volume of kyanite-bearing metamorphic sequences. (D) Pegmatite formation of maximal depth (>11 km) in granulite facies terrains, usually barren pegmatite which lack any parent/product relationship to the granites.

Based on depth of emplacement, metamorphic grade and minor element content Černý's (1991) revised the classification of granite pegmatites as Abyssal (high grade, high to low pressure), Muscovite (high pressure, lower temperature), Rare-Element (low temperature and pressure), and Mirolitic (shallow level).

THE FOUR CLASSES OF GRANITIC PEGMATITE ČERNÝ 1991						
CLASS	Family	Typical minor elements	Metamorphic environment	Relation to Granite	Structural features	Examples
Abyssal		U, Th, Zr, Nb, Ti Y, REE, Mo Poor to moderate mineralization	(upper amphibolite to) Low-to high-P Granulite facies 4-9 kb 700 - 800 °C	None (segregations of anatectic leucosome)	Conformable to mobilized cross-cutting veins	Rae and Heame provinces. Sack (remblay, 1978) Aldan and Nabar shields Siberia (bushev and Koplus 1980 Eastern Baltic shield Kalita 1965)
Muscovite		Li, Be, Y, REE, Ti, U, Th. Nb>Ta Poor /to moderate/ mineralization micas and ceramic minerals	High-P Barrovian amphibolite facies (kyanite-sillimanite) 5-8 Kb 650-580 c	None (anatectic bodies) to marginal and exterior	Quasi-conformable to cross cutting	White sea region USSR (Gorlo 1975/ Application province [Jahns et al., 1952) Rajahstan India (Shmakin 19 76)
Rare-Element	LCT	Li, Rb, Cs, Be, Ga, Nb<>Ta Sn, Hf, B, P, F Poor to abundant mineralization gem stock industrial minerals	Low-P Abu Kuma amphibolite to upper greenschist facts (andalusite-sillimanite 2-4kb 650-500°c	/interior to marginal to exterior	Quasi conformable to cross cutting	Yellow knife field NWT (Meintzer 1987) Black Hills south Dakota Shearer et al., 1987) Cat Lake Winnipeg River field. Manitoba (Cerny at 1981)
	NYF	Y, REE, Ti, U, Th, Zr, NB> Ta, F Poor to abundant mineralization ceramic minerals	Variable	Interior to marginal	Interior pods conformable to cross cutting exterior bodies	Liano Co. Texas (Lands 1932) South Platte district Colorado (Simmons et al., 1987) western Keivy Kola USSR (Bous 1960)
Miarolitic		Be, Y, REE, Ti U, Th, Zr, Nb> Ta, F Poor mineralization gem stock	Shallow to sub-volcanic 1-2 kb	Interior to marginal	Interior pods and cross cutting dikes	Pikes peak Colorado (food 1982). Sawtooth batholith Idaho (Boggs 1986) Korosten pluton Ukraine (Lazarenko et al., 1973)

Table 2.1. *The four classes of granitic pegmatite (after Černý, 1991).*

The Rare-Element Class further subdivided into five types and subtypes (Černý's, 1991). Rare-Earth, Beryl, Complex, Albite Spodumene and Albite rare element types, these types also have sub types as shown in the table below (Table 2.2).

CLASSIFICATION OF PEGMATITES OF THE RARE ELEMENT CLASS			
Pegmatite type	Pegmatite subtype	Geochemical signature	Typical minerals
RARE-EARTH	Alunite –monazite	REE, U, Th (P, Be, Nb,>Ta)	Alunite Monazite
	Gadolinite	Y, (H) REE, Be, Nb>Ta, F, (U, Th, Ti, Zr)	gadolinite, fergusonite Euxenite, (beryl) (topaz)
BERYL	beryl-columbite	Be, Nb ><Ta, P (±Sn, B)	beryl Columbite –tantalite
	Beryl- columbite-phosphate	Be, Nb> <Ta. P (Li, F= Sn, B	Beryl columbite –tantalite triplite triphylite
COMPLEX /rare element/	Spodumene	Li, Rb Cs, Be, Ta >< Nb (Sn, P, F ± B)	Spodumene (Amblygonite) Beryl (lepidolite) Tantalite (pollucite)
	Petalite	Li, Rb Cs, Be, Ta >< Nb (Sn, Ga, P, F±B)	Petalite (amblygonite) Tantalite Beryl (lepidolite)
	Lepidolite	F, Li, Rb, Cs, Be Ta >Nb (Sn, P±B)	lepidolite (lepidolite) Beryl Topaz (pollucite)
	Amblygonite	P, F, Li, Rb, Cs, Be Ta >Nb (Sn ± B)	Amblygonite (lepidolite) Beryl (pollucite) Tantalite
ALBITE SPODUMENE		Li (Sn, Be, Ta >< Nb ±B)	Spodumene (beryl) Cassiterite (tantalite)
ALBITE		Ta >< Nb, Be (Li=Sn, B)	Tantalite (cassiterite) Beryl

Table 2.2. Classification of pegmatites of Rare-Element class after (after Cerny’s, 1991).

A number of classification schemes have been proposed for granitic pegmatites, as recently summarized and critiqued by London (2008). For example, for the purposes of exploration or assessment, two simple distinctions are particularly helpful. The first is between the common pegmatites, which have the simple mineralogy of granites. The second distinction is among rare-element pegmatites, which are mineralogically complex and are grouped on petrologic grounds into two families, the LCT and NYF pegmatites (Bradley and McCauley, 2013). **LCT** is family for **L**ithium, **C**esium, and **T**antalum enrichment while **NYF** is for **N**iobium, **Y**trium, and **F**luorine enrichment (Table 2.1).

LCT pegmatites represent the most highly differentiated and last to crystallize components of certain granitic melts their parental granites are typically peraluminous granites (Martin and De Vito, 2005). S-type granite (derived from micas) constitutes mineral assemblages of muscovite, garnet, cordierite, sillimanite or andalusite, tourmaline, gahnite and rare-metal mineralization (Chappell and White, 2001). LCT pegmatite displays moderately to slightly HREE-depleted patterns, S-type and low REE abundances and negative Eu anomaly is occasionally well expressed but in most cases absent (Černý, 1997). This kind of pegmatites comes from the melt which enriched in fluxing components including water, fluorine, phosphorus, and boron; these reduce the solidus temperature, viscosity, and density while increasing the bulk diffusivity of the melt as a result the pegmatite become rich in incompatible elements lithium, cesium, tin, rubidium, tantalum and the melt (Bradley and McCauley, 2013). This all helps to distinguish LCT pegmatite from other rare-element pegmatites.

I-type granites are usually affiliated with subduction-related magmatism, but they can be generated from the metamorphic products of any mafic to intermediate igneous rocks or volcanoclastic sedimentary rocks. This type of sources granite is lacking of fluxing components (London and Morgan, 2012).

Most of NYF families are sourced from A-type granites, where “A” means “an orogenic” (e.g. Eby, 1990). The source of such granites is generally thought to be gneissic granulite’s deep in the continental crust, with some contribution from the mantle in the form of basaltic melt or low-density carbonic fluid (Černý and Ercit, 2005). A-type granites is enriched in F, which derived from amphiboles and biotite’s with strong tendency to accumulate significant Li, Rb, Cs, Ta, Be and Sn, (Cerny, 2012).

2.5. Methodology

Modern analytical techniques and petrographic works are being used for geological resource researching. Thin and polished sections used to understand the geology, alteration, parageneses and genesis of the rare metal deposit. Rock samples should be selected from all localities at different depths to characterize major and trace elements distribution as well as to demonstrate the zonal pattern of geochemical fractionation. The actual sampling points able to determine with the

use of Global Positioning System (GPS) which later helps to produce geological map of the study area (Abiola, 2014). Carefully selected representative drill core and surficial samples are can be crushed and pulverized into 75 mm size, then these powdered samples used for whole-rock analysis. This can be determined by a combined method of Inductively coupled Plasma-Mass Spectrometry (ICP-MS) for trace element analysis and Atomic Emission Spectrometry (ICP-AES) for major oxides by decomposing the sample using lithium metaborate (LiBO₂) fusion at the different laboratory services (Mohammed, 2017; Abiola, 2014 and Good enough et al., 2014). In addition to the above methods Zhu et al., (2005) used X-ray fluorescence (XRF) spectrometer on their powder pellets and glass discs. Küster et al., (2009) also used to ICP-MS, ICP-AES and XRF methodology for both whole rock and muscovite chemistry.

“Selected mineral grains can be analyzed using electron microprobe (also known as electron-probe microanalysis, EPMA) and laser ablation inductively coupled plasma mass spectrometry techniques (LA-ICP-MS). A CAMECA SX 100 electron microprobe equipped with five wavelength-dispersive spectrometers and an energy-dispersive system (Princeton Gamma Technologies) can be used to determine major and minor element concentrations. The instrument able to operate at a 30-kV acceleration voltage, 40 nA sample current and appropriate counting times to reach a detection limit of 200 ppm for minor and trace elements” (Melcher et al., 2013). Even though there are a number of methods are available and used regarding to rear metals bearing pegmatite, the above methods are more adapted by most researchers.

2.6. Economic importance

The critical rare metals and metalloids, all exhibit a diverse range of chemical and physical properties. These properties allow the rare metals to be used in a wide range of energy and technology applications. Tantalum and Niobium is the most chemically linked pair of RMs (rare metals). They are typically found together in the ore columbite-tantalite ("coltan"), after we separate one other's we can use them for several purposes (Ralph,2015).

According to Ralph (2015) both LCT and NYF pegmatite have remarkable uses for industries, but the size and the commercial value of NYF pegmatites are generally of lower than those of the LCT type. LCT contains large amount of rare metal ore bodies those are economic interest and also a

number of high value attractive gemstones (pink, red, green and blue as well as multi-colored crystals) like beryl in the form of emerald, heliodor, and aquamarine; spodumene in the varieties known as kunzite and hiddenite; topaz and garnets are found dispersedly around the world. For example, aquamarines and topaz found in pegmatites in the mountains of Colorado and Idaho and beautiful crystals of emerald found in Ethiopia, Kilkile area. Pegmatites are also mined for ultrapure quartz crystals, potassium feldspar, albite and muscovite mica.

Strategic metals like Tantalum and Niobium play great role for once country economy. Tantalum has a high strength at elevated temperature (melting point 3020°C) and electrical conductivity makes tantalum predominantly to be used in the electronics industry in the production of capacitors (utilized in computers, smart phones, and automobiles), high-power resistors, rectifier, amplifier, oscillators, signal devices, alarm systems timing devices, jet engines and recently for drones. Historically much of the world's Ta production has come from complex-type pegmatites (e.g. Tanco(Canada); Greenbushes (Australia); Altai #3 (Mongolia); Bikita (Zimbabwe), albite-type pegmatites Wodgina (Australia), and albite–spodumene pegmatites (Mt. Cassiterite, Australia) (Černý and Ercit, 2005).

Pegmatites are also important sources of lithium, it occurs as a series of minerals in pegmatites, the most common are (1) lepidolite ($\text{K}[\text{Li}, \text{Al}]_3[\text{Si}, \text{Al}]_4\text{O}_{10}[\text{F}, \text{OH}]_2$), or lithium mica (four percent lithia) which also can constitute Rb ore; (2) spodumene($\text{LiAlSi}_2\text{O}_6$), a lithium-aluminum silicate mineral belonging to the pyroxene family that is converted to lithium carbonate or lithium hydroxide (eight percent lithia); (3) petalite($\text{LiAlSi}_4\text{O}_{10}$), another lithium aluminum silicate (five percent lithia); (4) triphylite, a lithium, iron and manganese phosphate (nine percent lithia); and (5) amblygonite($\text{LiAlPO}_4[\text{F}, \text{OH}]$), a fluophosphate of aluminum and lithium (ten percent lithia) (Ralph, 2015). By far the most important Li pegmatite is the Greenbushes deposit, which produced roughly one-third of the world's lithium in 2009 and contains 70.4 million tons grading 2.6 wt. % Li_2O , it is the major source of technical-grade Li, where spodumene is used directly in the ceramics or glass industries without processing; Li lowers thermal expansion and and decrease firing temperature (Ralph, 2015).

Cesium formate is fabricated for the applications of high-pressure and high-temperature drilling intended for petroleum exploration. Because of its photo emissive properties, it is used in solar

photovoltaic cells, beryllium and copper alloys are in components of aerospace, automotive, and electronic devices (Linnen et al., 2011).

2.7. Exploration, mining and processing of rare metals

2.7.1. Exploration

If the company already knows the ore content, they will begin sampling and conducting feasibility studies. However, they will begin mineral exploration if they don't have prior sufficient information about potential of the areas of good bedrock exposure. Pegmatite is essentially restricted to Barrovian facies sequence metamorphic rocks of at least middle greenschist facies, and often intimately associated with granites intruding into such terranes (New World Encyclopedia, 2008). Encyclopedia further illustrated that, worldwide, notable pegmatite occurrences are within the major cratons and greenschist-facies metamorphic belts. Within the metamorphic belts pegmatite tends to concentrate around granitic bodies within zones of low mean strain and extension, for example strain shadow of a large rigid granite body. Similarly, pegmatite is often found within the contact zone of granite, transitional with some greisen's, as a late-stage magmatic-hydrothermal effect of syn-metamorphic granitic magmatism. Some skarns associated with granites also tend to host pegmatites (New World Encyclopedia, 2008).

There are two way of rare metal exploration: regional and geochemical methods. Basal-till sampling, flat-chiseling and reconnaissance techniques are regional program such approach are more time consuming and expensive methods for rare metal exploration, stream-sediment geochemistry technique yields twofold information than the above method (Cerny et al., 1982). Tantalum and Nb are highly incompatible in quartz and feldspar; thus, their bulk distribution coefficients are typically very small. However, they are compatible in muscovite and partition strongly into Ti-bearing minerals, notably rutile and titanite (Linnen and Cuney, 2005). Content of muscovite has been used as an exploration tool, and pegmatites that contain muscovite with greater than ~80 ppm Ta are considered as economic (Černý, 1989).

Identification of possible granitic parents is a key step in evaluating a region for LCT pegmatite potential. Coarse-flaked yellowish-green and silvery muscovite is typical of Be, Nb and Ta bearing

and spodumene pegmatites (Cerny et al., 1982). However, Selway et al., (2005) illustrate that, fertile, peraluminous granites typically contain coarse muscovite that is green rather than silvery; potassium feldspar that is white rather than pink; and accessory garnet, tourmaline, fluorite, and (or) cordierite. The above writer further illustrated that fertile granites have high cesium, lithium, rubidium, tin, and tantalum, and low calcium, iron and magnesium; they also have unusual elemental ratios (for example, Mg/Li <10 and Nb/Ta <8).

The most fractionated pegmatites contain >3000 ppm Rb, K/Rb <30, and >100 ppm Cs. Similarly, muscovite's from the most fractionated pegmatites contain >2000 ppm Li, >10,000 ppm Rb, and >500 ppm Cs (Selway et al., 2005). According to the above writer, garnets change both in color and composition with increasing fractionation from red, iron-rich almandine to orange, manganese-rich spessartine. Tourmaline in fertile granites and the outer zones of LCT pegmatites is black and low in lithium and manganese content; whereas the inner zones of the most fractionated pegmatites commonly bear tourmaline as pink to green variety elbaite, which is high in lithium and manganese. Beryl shows color changes with increasing fractionation, from greenish or brownish in less evolved pegmatites, to pale, white, and pink in more evolved bodies (Trueman and Černý, 1982).

Most LCT pegmatites are known to form as far as 10 km from the parental granite (Breaks and Tindle, 1997). The distal ones are most fractionated and the proximal one is the least fractionated which contain only the standard rock-forming minerals of S-type granite. These pegmatites typically occur in groups which consist of tens to hundreds of individuals and cover areas up to a few tens of square kilometers (Černý, 1991). In the most fractionated pegmatites successive regional zones appear. But these highly fractionated rare-element-enriched pegmatites only constitute 1 or 2 percent of regional pegmatite populations (Ginsburg et al., 1979). Pegmatites commonly take the form of tabular dikes, sills, sheets, pipes, pods and irregular masses intruded into metamorphic or igneous rocks. Most LCT pegmatite bodies, no matter their shape, are concentrically zoned, but in an irregular manner. Four main zones of pegmatites are: the border, wall, intermediate and core zones (Ralph, 2015).

Weathering of LCT pegmatites can result in both soil anomalies and indicator minerals. Smith et al. (1987) demonstrated that arsenic, beryllium, antimony, and tin form a 12- by 20-km halo in lateritic soils around the Greenbushes pegmatite; niobium, tantalum, and boron form a smaller, 1- by 5-km halo. Cassiterite, tantalite, elbaite, and spessartine are sufficiently dense and durable to serve as heavy indicator minerals. Highly mobile elements such as lithium, rubidium, and cesium, and volatile components like boron and fluorine tend to alter the adjacent country rocks during LCT pegmatite emplacement. (Bradley and McCauley, 2013). The presence of anomalous Cs and/or Ta can be indicative of enriched Li mineralization due to their common direct correlation in pegmatite-type mineralization (Moller & Mortenai, 1987).

2.7.2. Mining

Mining is the extraction of minerals and elements of economic interest from the earth's surface. Most of pegmatite dikes and pockets are small in size. Therefore, the mining operations to exploit rare metals usually small in size and uses underground mining that follows a dike or exploits a small pocket (Hobart, 2018). It can also be done by using open-pit mining like Kenticha Ta mining factory in Ethiopia which is now proposed to use underground mining. A combination of both mining method is preferably in use. Significant amount of rare metals is also extracted by artisanal and small-scale mining (ASM).

2.7.3. Processing

After mining, the ore must be processed to separate the mineral from host rock. Initial concentration is normally undertaken at or close to the mine site and involves crushing the ore followed by separation of niobium and tantalum ore from gangue material using a combination physical and chemical method (British Geological Survey, 2011) is essential. The purification of extracted ores requires a variety of techniques unique to each ore. New processes for refinement of rare metals in particular area are still under experimentation to reduce multiple extensive processes and lower the waste of energy, time and materials (British Geological survey, 2011).

Processing techniques vary from one company to another. For example, Kenticha Ta mining factory uses gravity and magnetic separation system.

2.8. Previous works on rare metals deposits of Ethiopia

Regional geological, geochemical and geophysical prospecting work conducted in 1979-1981 and revealed the occurrence of tantalum and gold mineralization in megado and Kenticha belt. The Kenticha rear-metal pegmatite deposit was discovered in 1980 during the course of geological mapping and prospecting, at scale of 1:100,000 (Kozyreva et al 1982). Zerihun (1991) and Zerihun et al. (1995) used mineral parageneses and trace element geochemistry of Adola belt, Kenticha rare metal field.

	Grain Size	Major minerals	Accessory and rare minerals	Ta ore minerals
Exomorphic zone	Fine grained	contact assemblage in serpentinite and talc–tremolite schist, glimmerite (phlogopite–quartz–Holmquist–talc–tremolite–actinolite)		
Upper Zone	Coarse Grained	Albite–quartz–spodumene–muscovite Microcline–pegmatite with large spodumene and quartz crystals	Amazonite, apatite amblygonite beryl Li–muscovite, topaz, Kunzite cassiterite petalite?	Mn–tantalite Axialite / wodginite Ta>Nb
Discontinuous Lenses and Spherical bodies	Variable fine grain coarse grained	Monomineralic quartz and quartz- mica assemblages (lepidolite- zinnwaldite) saccharoidal albite Blocky microcline with graphic quartz- feldspar intergrowth		
Intermediate zone		Medium grained	muscovite–quartz–albite Microcline pegmatite	Pyrite limonite magnetite Arsenopyrite Fe–columbite Mn–columbite Nb>Ta
Lower zone	Fine to medium grained	Alaskitic muscovite –albite granite to layered albite – quartz aplite	Green tourmaline, garnet- magnetite pyrite, limonite	Columbite Nb > TA

Table 2.3. Internal structure and mineral assemblages of Kenticha pegmatite, after Solomon and Zerihun (1996); Polytaev et al., (1991).

The current local mining company Ethiopian Mineral, Petroleum and Biofuel Corporation is exploring and developing the mineral resources existing in the Kenticha greenstone belt. These exploration activities have proved the existence of economic tantalum mineralization in Kenticha pegmatite belt. The area of occurrences include bupo, Shuni hill and Killkile for rare metal and Dermi-dama for both rear metals and gold exploration.

According to Solomon and Zerihun (1996); Kuster (2009) the ore mineralogy of columbo-tantalite crystals from pegmatites around Kenticha show compositional variability and internally zoned.

They recognised that the minerals studied display progressive change from niobium- and iron-rich to tantalum- and manganese-rich members. The crystals relatively rich in tantalum and manganese are associated with highly fractionated pegmatites. They further demonstrated that this compositional variation of the columbo-tantalite pegmatites reflect an over all regional zoning.

CHAPTER THREE

3. Regional geological setting

3.1. Introduction to East African Orogeny (EAO)

The East Africa Orogeny (EAO) about 900 Ma to 550 Ma, (Vail, 1985; Berhe, 1990; Abdelsalam and Stern, 1996). “East African Orogen (EAO)” is introduced by Stern (1994) and the stages of tectonic evolution suggested are shown in Fig 3.1.

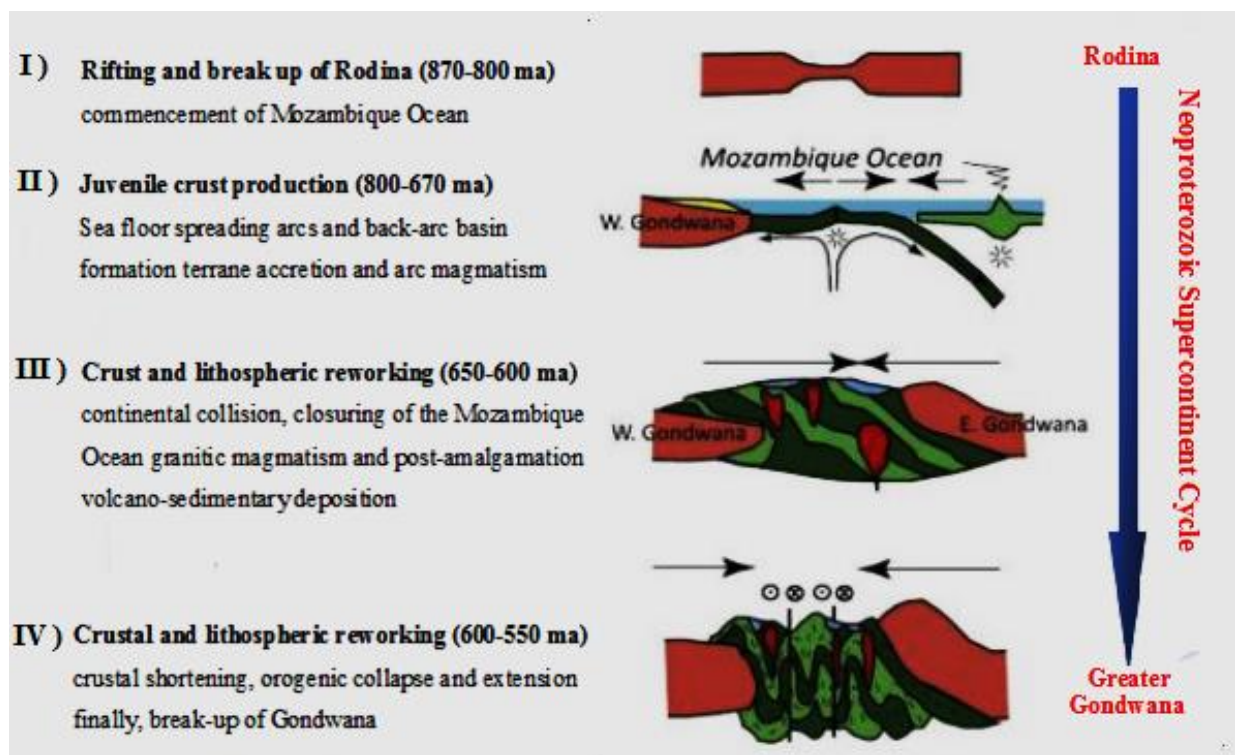
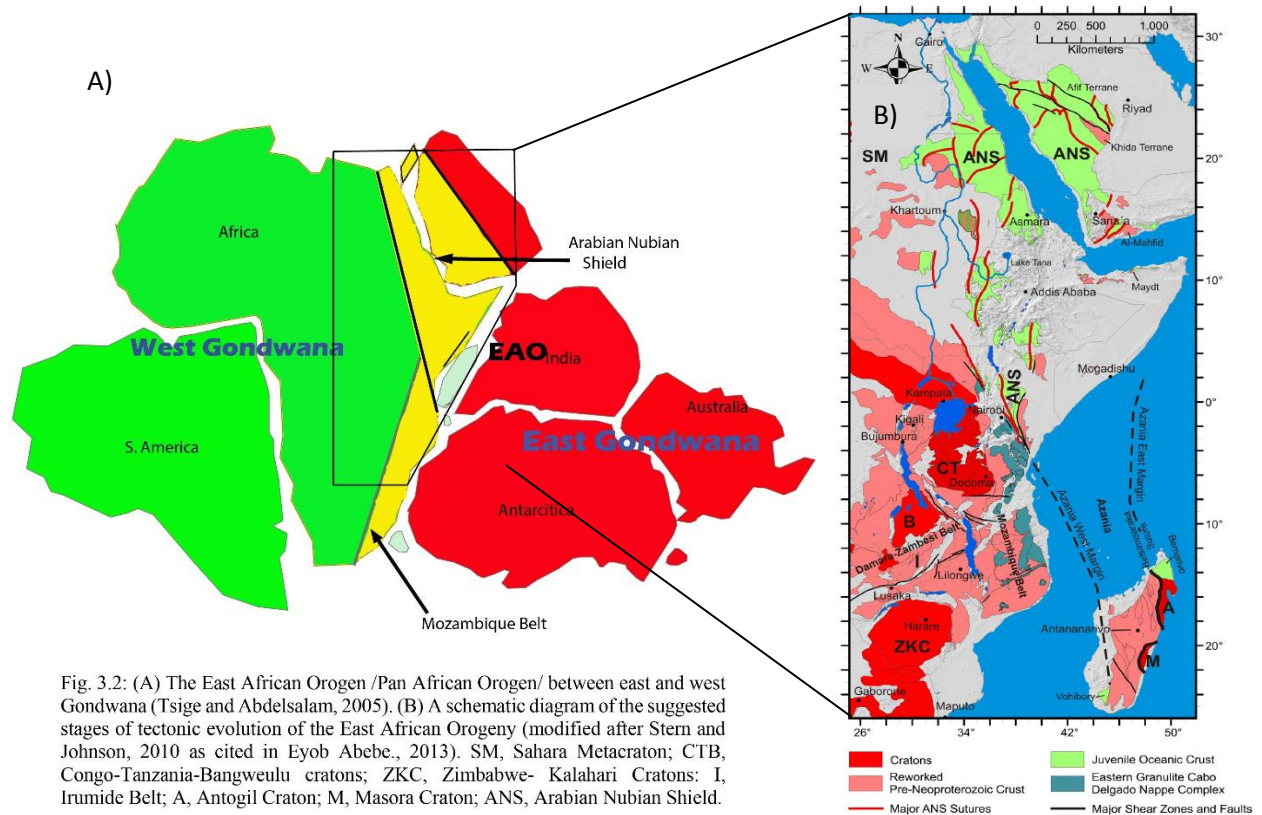


Figure 3.1. A schematic diagram of the suggested stages of tectonic evolution of the East African Orogeny (modified after Stern and Johnson, 2010).

Similarly, Kröner and Stern (2005) also explained the tectonic evolution of East African Orogen (EAO). First rifting and breaking up of the supercontinent Rodina into West and East Gondwana which is the beginning of Mozambique Ocean (~900 – 850 Ma); secondly sea-floor spreading, juvenile crust production, arcs and back-arc basin formation, terrane accretion and arc magmatism

(870 - 690 Ma); thirdly continental collision between West and East Gondwana forming the East African Orogen, closing of the Mozambique Ocean, granitic magmatism and post-amalgamation volcano-sedimentary deposition (650-600 Ma), and Finally crustal shortening, orogenic collapse and extension leading to the break-up of Gondwana (600 to 540 Ma). which is responsible for the formation of the supercontinent Gondwana.



According to Kröner and Stern, (2005) this orogeny comprises two major segments namely Arabian–Nubian Shield (ANS) and Mozambique belt. These segments in Africa, extending from Mozambique in the south to southern Israel in the north. Geographically Arabian–Nubian Shield (ANS) makes up the northern sector extends from southern Israel to Ethiopia and Yemen whereas Mozambique belt covers relatively the southern sector of East African Orogen.

3.2. Arabian-Nubian Shield (ANS)

The Arabian-Nubian Shield forms the joint zone between East and West Gondwana at the northern end of the EAO (Johnson et al., 2003). It consists variety of rocks including gneisses, granitoids,

various metavolcanics and metasedimentary rocks (Blasband et al., 2000). ANS is distinguished from the Mozambique belt by its juvenile continental crust (mantle derived), relatively less deformed and less metamorphosed and abundance of ophiolites. (Asfawossen et al., 2001; Kröner and Stern, 2005). The Mozambique Belt comprises high-grade gneisses, migmatites and schists (Asfawossen et al., 2001). The abundance of island-arc rocks and ophiolites make ANS distinct from Mozambique Belt (Kröner & Stern, 2005).

The ANS is suggested to be a crust that was generated during the formation of smaller terrains of arc and back arc crust within and around the margins of a large oceanic tract known as the Mozambique ocean, which formed in association with the breakup of Rodina (~ 800–900 Ma (Stern, 1994)). Most of these ophiolites formation above a convergent plate margin, either as part of a back-arc basin or in a fore arc setting.

Notable geological features were formed with the gneissic domes such as granitoid intrusions, dykes, and sedimentary basins. Alkaline granites are found throughout ANS, on the basis of their geochemistry, these granites assumed to be derived from mantle and to have intruded in an extending and thinned crust (e.g. Beyth et al., 1994; Kessel et al., 1998). The ANS was subsequently buried by Phanerozoic sediments but has been exposed by uplift and erosion on the flanks of the Red sea in Oligocene and younger times. A broad region uplifting occurred in association with Cenozoic rifting and formed the Red sea, exposing a large tract of mostly juvenile Neoproterozoic crust which comprises ANS (Kröner & Stern, 2004).

According to Abdulsalam and Stern (1996); Johnson and Woldehaimanot, (2009) the sequence of Neoproterozoic evolution, has a number of tectono-metamorphic and igneous cycles has been occurred in ANS; but two major tectono-metamorphic phases were the most prominent. The first phase is the older phase at around 750 Ma followed the cessation of most island-arc igneous activity and probably pertains to the accretion and assembly of ANS island arcs. The second phase is subsequent tectono-metamorphic phase which followed a period of reduced igneous activity at around 700 Ma causing thickening of the previously stitched island-arc complexes and formed tight, roughly N–S trending upright folds.

The ANS consists of three principal units, the first one is gneissic terrenes dominated by quartzo feldspathic gneisses, migmatites, and meta-sediments of amphibolite to granulite facies, which are

found in the western part of the Nubian shield, eastern Arabian shield and in some regions of the central part of the shield (Vail 1985; Johnson and Woldehaimanot, 2003). According to the above writers these high-grade rocks were derived from continental crust recycled during the East African Orogen(EAO).

The second one is green schist to lower amphibolite metamorphosed volcano-sedimentary terranes including calc-alkaline basaltic and andesitic lavas, tuffs, pyroclastic, and rhyolites, which are intruded by various pre-, syn-, and post-tectonic granitoids and occurred between the western and eastern gneissic terrain (Vail, 1985). The meta volcanic rocks are considered to have mainly derived from a depleted mantle source (Kröner et al., 1991; Stern, 2002).

The third one is mafic-ultramafic suites comprising ophiolite assemblages, narrow discontinuous belts of dismembered serpentinites, gabbro, sheeted dikes, pillow lavas, and ultramafic rocks. These mafic-ultramafic suites are interpreted to represent suture zones between intra-oceanic plates or continent-island arc margins (Kröner ,1985; Vail 1985; Berhe 1990).

3.3. The Precambrian basement of southern Ethiopia

The Precambrian shield of southern Ethiopia occupies an important position because they occur at the interface between the Mozambique Belt (MB) in the south and the Arabian– Nubian Shield (ANS) to the north (Stern, 1994). The tectonostratigraphic classification of the Precambrian terrane of Ethiopia into Lower, Middle and Upper Complexes (Kazmin, 1975; Kazmin et al., 1978) has long been in use, it was mainly based on metamorphic grade and deformational differences. This classification suggested a prevalence of Archaean gneisses in the Precambrian of southern Ethiopia, but was not based on absolute geochronological data.

Lower Complex accompanying high-grade gneisses and migmatites and it is a part of the Mozambique Orogenic Belt. It generally consists of amphibolite facies (locally granulite facies), migmatites, ortho-gneisses, para-gneisses, amphibolite and bands of marble which mainly exposed in southern part of the country. The Middle Complex represented by psammitic and pelitic meta-sediments (quartzites, biotite and quartz muscovite schists, meta-arkoses,) with subordinate marbles, calc-silicates and amphibole schists this mainly exposed in the southern, eastern, and western parts of the country. The low-grade volcano-sedimentary rocks with associated mafic to

felsic intrusive, which is referred to as Upper Complex associated meta-sediments, clastic and to less extent carbonate sediments (Kazmin, 1971; 1975) belongs to the Pan-African Arabian-Nubian Shield.

Recently, the above Kazmin's theory has been revised on the basis of field geochronological, thermochronological, geochemical and lithotectonic data. The Ethiopian basement rocks are thus regrouped into two major blocks; (1) Volcanic-sedimentary-ophiolite terrain and (2) Gneissic-migmatitic terrain (Asfawossen et al., 2001 and Yibas et al., 2002).

The granite-gneiss terrane consists of para- and ortho-quartzo-feldspathic gneisses and granitoids, intercalated with amphibolite and sillimanite–kyanite-bearing schists. The granitoid gneisses form an integral part of the granite-gneiss terrane, but are rare in the ophiolitic fold and thrust belts. The granite-gneiss terrane is classified into the Burji–Moyale and Adola–Genale granite-gneiss sub-terrane, which are separated by the major Sebeto–Chelanko fault zone. The Burji–Moyale sub-terrane is further divided into the Burji–Finchaa and the Moyale–Sololo complexes. The Adola–Genale sub-terrane is divided into the Adola and Genale–Dolo Complexes.

The mafic–ultramafic–sedimentary assemblages have been referred to as “fold and thrust belts” (Yibas, 2000). Geochemistry of the mafic rocks of the ophiolitic fold and thrust belts of southern Ethiopia constraints on the tectonic regime during the Neoproterozoic (900–700 Ma) (Yibas, 2003). The undeformed granitoids developed in these belts. Four ophiolitic fold and thrust belts have been recognized. These are the Bulbul, Kenticha, Megado and Moyale–El Kur fold and thrust belts, which are composed of mafic, ultramafic and metasedimentary rocks in various proportions. Felsic volcanic rocks are virtually absent in these belts.

Kenticha and Megado form two N–S trending linear belts, separated by quartzo-feldspathic gneisses and granitoids of the Adola granite-gneiss complex and together called Adola belts.

3.4. The Adola Belt

Adola area is proposed to be a two fold subdivision of rocks into Gneissic terrain and Green stone belt. The Gneissic terrain consists relatively high grade rocks which consists three NS trending anticlinal zones separated by two intervening narrow N-S trending synclinal green stone belt. Reference to the green stone belts, Western, Central and Eastern gneissic terrains are

distinguished. The two greenstone belts can be divided into western side called Megado Green stone belt and eastern side called Kenticha green stone belt (Woldai, 1989). According to Kuster et al. (2009), the Kenticha pegmatite field situated within the Neoproterozoic Adola belt, which constitutes the southernmost extension of the Arabian-Nubian Shield.

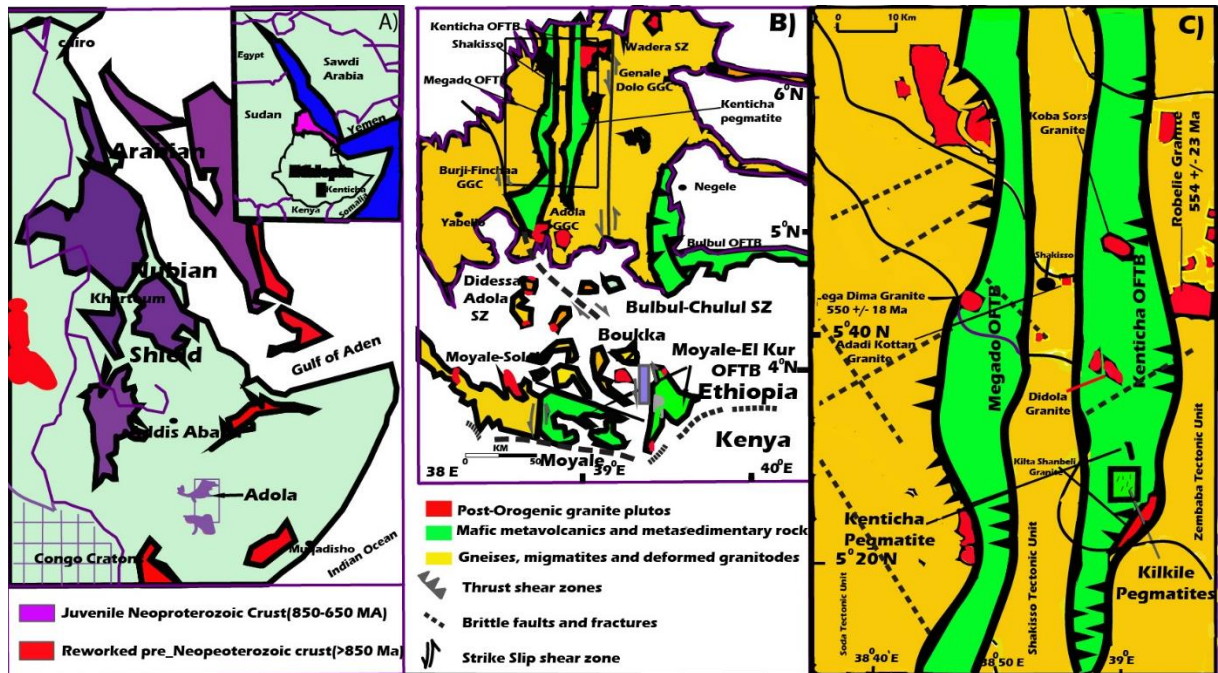


Figure 3.3. (a) Simplified geological map of northeastern Africa and location of the Kenticha pegmatite field (modified after Küster, 2009) (b) southern Ethiopia (modified after Worku and Schandelmeyer 1996; Yibas et al. 2002; Tsige and Abdulsalam 2005) and (c) the Adola belt (modified after after Kozyrev et al. 1988; Worku and Schandelmeyer 1996).

The Kenticha and Megado ophiolitic fold and thrust belts (OFTBs) are made up of greenschist to lower amphibolite facies meta-sediments (garnet–mica schists, graphite schists, quartzites, marbles) and metamorphosed mafic–ultramafic rocks (amphibolite, talc–tremolite schists and serpentinites) (Worku and Schandelmeyer 1996; Yihunie 2002; Yibas et al. 2003). In Kenticha belt ultramafic rocks (serpentinite, talc–tremolite and talc–anthophyllite schists) are dominant over the mafic rocks. Staurolite, sillimanite-bearing biotite schists, minor occurrences of Fe–Mn quartzites, marbles and siliceous metapelites are also recognized in the Kenticha belt. Meta-basic and metasedimentary rocks are dominant over ultramafic rocks in the Megado Belt. (Kazmin et al., 1978; Yibas et al., 2000a).

Metamorphic conditions of Adola granite–gneiss complexes and Kenticha OFTB reached 600–650°C, 6–7 Kb and 520–580°C and 4–5 Kb respectively (Yihunie et al. 2004; Tsige 2006). Deformation and metamorphism of the lithotectonic units of the Adola belt likely occurred in a collisional setting (Worku and Schandelmeier 1996; Yihunie 2002). East-directed thrusting of the ophiolite associations was followed by right-lateral strike slip movements along these thrust shear zones between 610 and 554 Ma (Yihunie 2002).

CHAPTER FOUR

4. Geology of Kilkile area

4.1. Introduction

The ore bearing granitic pegmatites are associated with the mafic to ultramafic rocks such as serpentinite, talc tremolite, biotite gneiss and amphibolite rocks. Kenticha rare metal field pegmatites are lithologically and structurally controlled i.e. they were emplaced by a process of magmatic injection within the metamorphosed volcano-sedimentary rocks and their emplacement were controlled by the regional north south trending deep fault system (Polytaev et. al., 1989).

The study area is located within the Precambrian basement of southern Ethiopia (Fig.3.4C). This basement constitutes the southernmost part of the Arabian–Nubian Shield (ANS), which covers an area of around 30 km². Kilkile rare metal pegmatite is located in the southern part of Kenticha belt on which a number of sub parallel pegmatite veins are available (Fig.4.1).

4.2. Local geology and rock-forming minerals

Based on field observation the geology of the prospect site, as part of main kenticha – Dermi Dama area, predominantly consists of amphibolite schist and gneiss, talc tremolite schist, biotite gneiss, serpentinite, granites associated with barren & rare metal bearing pegmatites. The mappable lithological unites found in the Kilkile area are the following.

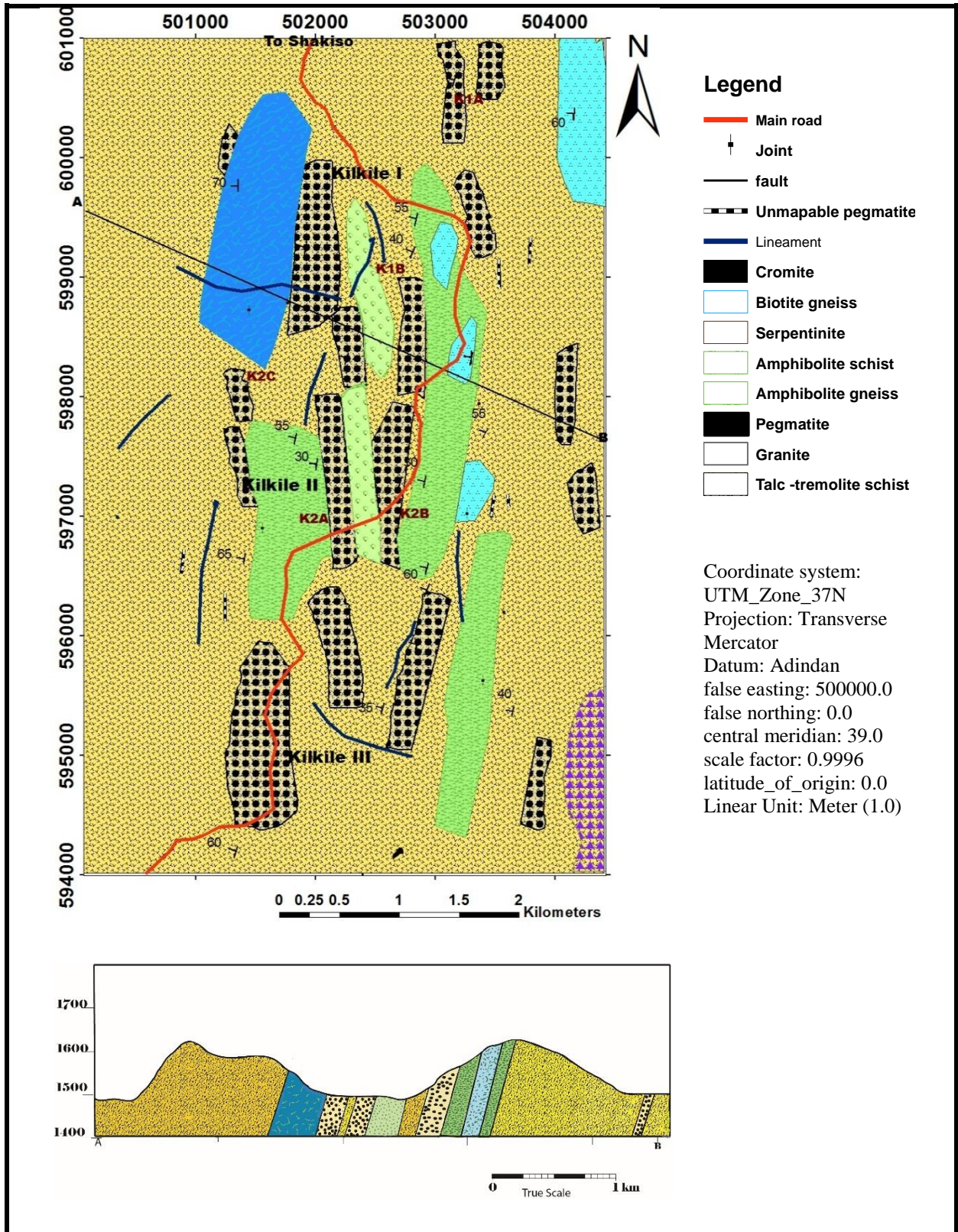


Fig 4.1. Geological map and cross section of the study area.

4.2.1. Biotite gneiss

This rock unit is dominantly found in the North-West part of the study area. Like other rock units this unit also trends nearly N-S direction. The fresh out crop of biotite gneiss has gray to dark gray color whereas the weathered part shows light yellow color. The rock has medium- to coarse-grained texture massive nature. Quartz, biotite and feldspar are the main minerals constituents in the biotite gneiss.



Figure 4.2. *Outcrop of biotite gneiss of Kilkile area.*

4.2.2. Amphibolite gneiss

Amphibolite gneiss is found in three distinct places, striking nearly N-S direction, more than a km long and have less than 200m width. This rock unit consists of hornblende, pyroxene and plagioclase minerals which are coarse enough for the individual mineral grains to be seen with unaided eye. Fresh part of this rock unit has dark gray to light green color while weathered part has red to brown color.

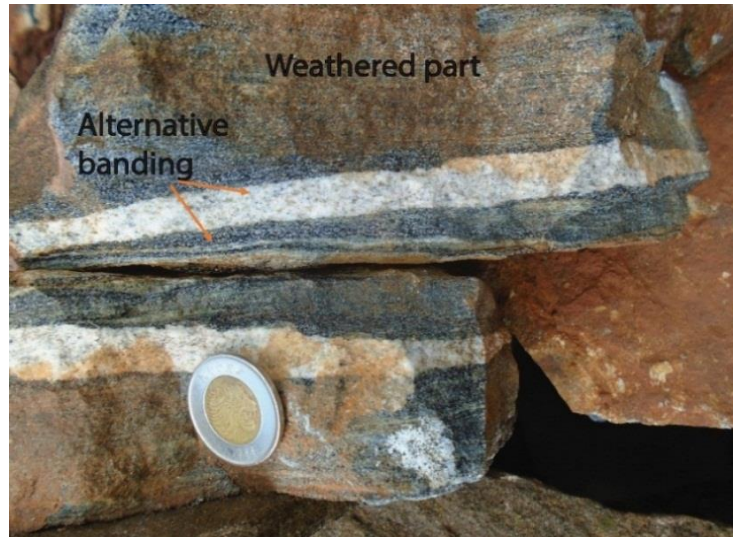


Figure 4.3. Amphibolite gneiss rocks on Kilkile area shows alternative banding.

Petrographic study indicates that (Fig.4.4) this rock composed of 50% amphibole (hornblende), 25% pyroxene, 24% plagioclase and the remaining covered by others small constituents. Most of the minerals specially amphibole and pyroxene have more or less uniform orientation. Plagioclase minerals in xpl (cross polarized light) show white to gray to pale in color with black and white strip (Fig.4.4), Pyroxene shows short prismatic and tabular crystal habits in variable color nevertheless most of the time it shows light brown in xpl and dark green and brown in ppl (plane polarized light) with relatively having high relief. On the other hand, high relief hornblende shows dark green to black color and have short stocky prismatic as well as long thin crystal forms.

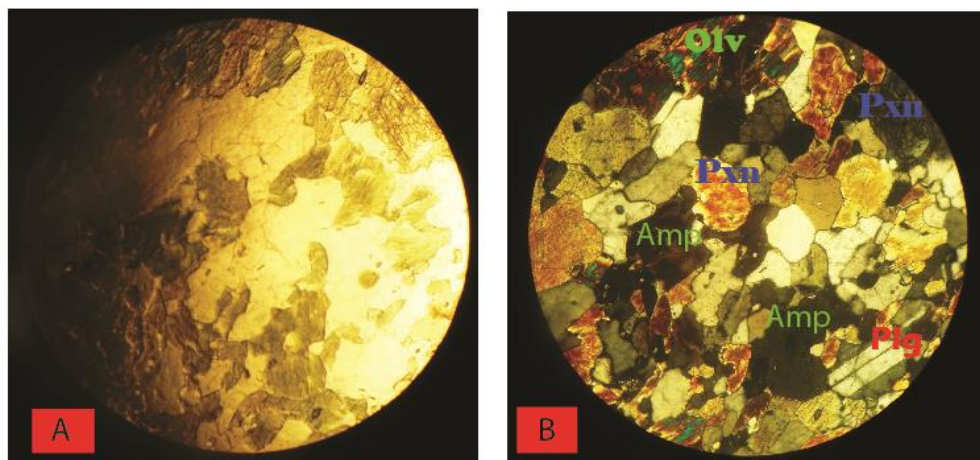


Figure 4.4. Micro photo picture of amphibolite gneiss rock unit sample; (A) under PPL (B) under XPL. The labels stand for; Amp-Amphibole, Plg-Plagioclase feldspar, Pxn- pyroxene. The photo picture is taken at 10X magnification.

4.2.3. Amphibolite Schist

On the study area amphibolite schist occurrence found in two distinct places, relative to amphibolite gneiss it covers small and central part of the study area. This rock unit trends N-S direction, occurs as lenses and have more than a kilometer along strike but few tens of meters to few hundreds of meters across the strike. Lineation, foliation, joints and veins are dominant structure in these rocks units.

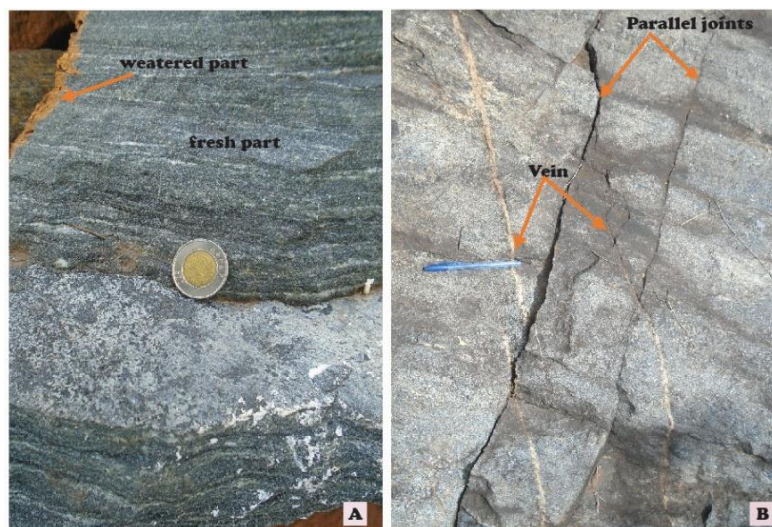


Figure 4.5. Amphibolite schist rocks on kilkile area. (A) schistose structure (B) Amphibolite schist which contain two parallel joints dissects two sub parallel vein at around 30° .

Petrographic study of this rock indicates that it is composed of Amphibole (hornblende), plagioclase and pyroxene minerals. Mineral content of this rock unit in microscopic photo-pictures shows more or less similar to amphibolite gneiss. Amphibole and pyroxene shows uniform orientation. plagioclase minerals show relatively low relief.

4.2.4. Chromitite

Chromite in the study has dark gray to black color with a metallic to sub metallic luster, coarse grained and have high specific gravity. This unit is found as small outcrop around 100m^2 diameter in the southern part of the study area. At a time, there is a quarry site in which artesian miners are involving.

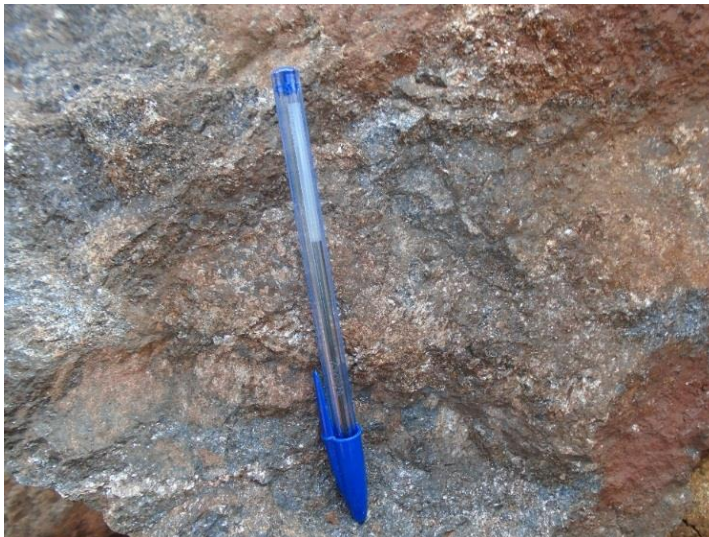


Figure 4.6. Chromite on Kilkile area.

4.2.5. Serpentinite

The serpentine occurs on ridges, hills and as small lenses and usually found in the northern and central part of the study area. It is pale green to dark green when it is fresh but weathered serpentinite shows yellowish brown color. This rock unit covers relatively smaller portions of the study area, and often found in association with talc tremolite rocks. The serpentinite is usually fractured and have many joints, also filled by secondary materials like silica, carbonate and asbestos (Fig 4.7). Serpentine is the most dominant mineral which commonly derived from the alteration of orthopyroxene and olivine.

The preexisting ultramafic rocks (serpentinite) is intruded by pegmatite body. During solidification of the pegmatite body, heat and volatiles (H₂O, CO₂, F, B) were lost from the consolidating magma into the hanging wall. The emanating volatiles lead to alteration of the ultramafic rocks along the hanging wall contact producing the exomorphic zone called glimmerite (Kuster 2009). Glimmerite”, is thin transitional zone between serpentinite & pegmatite body after metamorphism of serpentinite. It is highly foliated dark brown to black color of biotite schist comprise dominantly biotite.

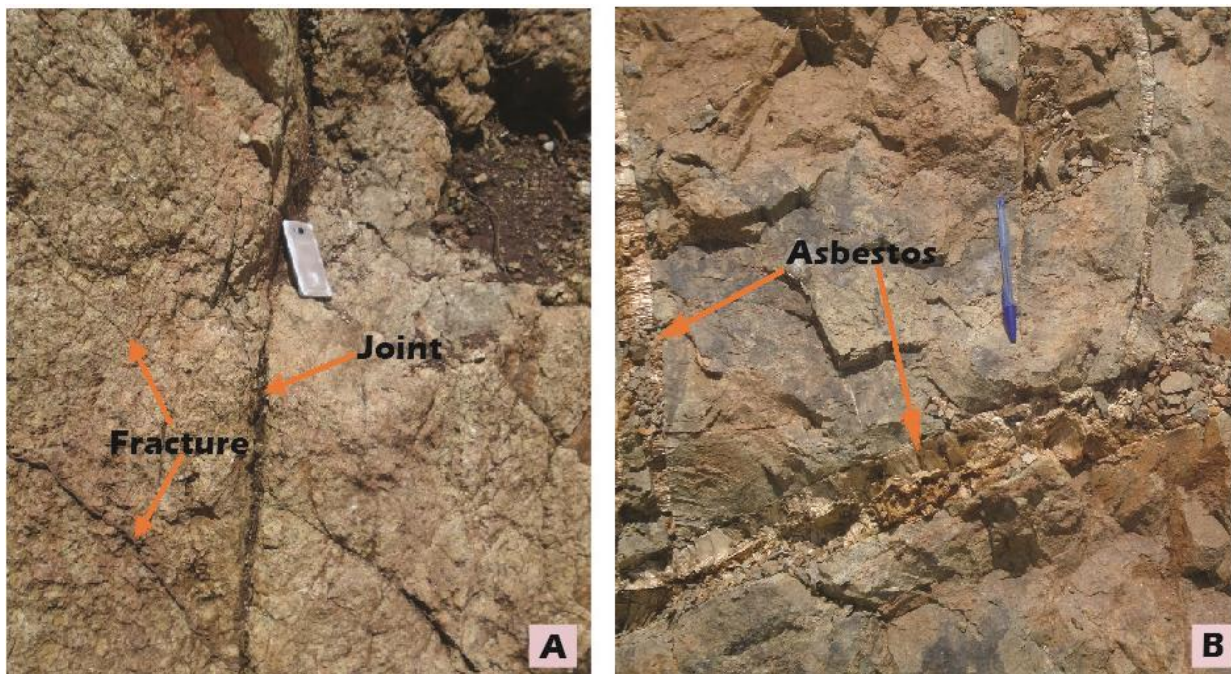


Figure 4.7. *Serpentinite rocks on kilkile area; (A)Serpentinite which shows joint and nonsystematic fractures. (B) Serpentinite and asbestos which crosses nearly perpendicular each other of kilkile area.*

Petrographic study indicates that (Fig.4.8) this rock composed of 70 % Serpentine, 15% of pyroxene, 10 % of Olivine and other small volume constituents (like opaque). Serpentine is the most dominant mineral in the sample with a noticeable alteration. The color of serpentine varies from light grey (PPL) to light green to black (XPL) with fibrous form. Olivine shows light green to pale yellow color and flatten tabular crystal which shows highly weathered appearance. Altered pyroxene also show light brown color, having sheet-like habit.

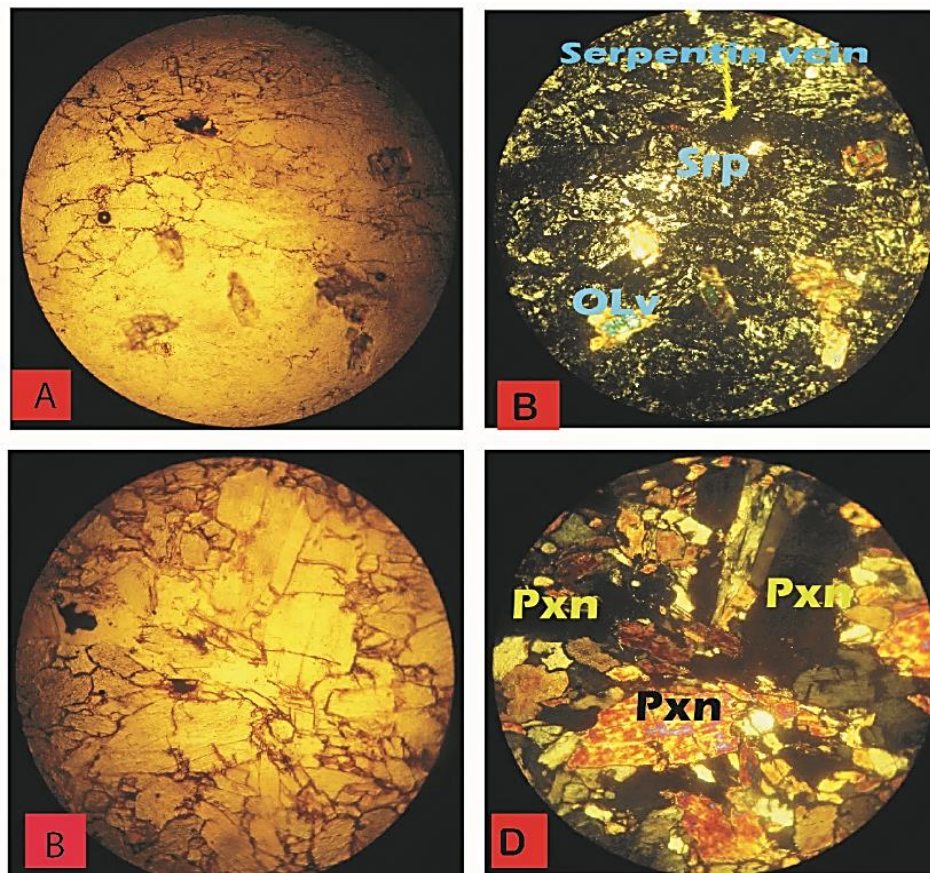


Figure 4.8. Microscopic photo picture of serpentinite rock unit on kilkile area; (A & C) under XPL whereas (B & D) under PPL the labels stands for; *srp*-serpentinite, *Olv*-Altered Oliven, *Pxn*-pyroxen. The photo picture is taken at 10X magnification.

4.2.6. Chlorite-Talc-Tremolite Schist

This rock unit occurs in large part of the study area and forms ridges. In most of the study area this rock unit is subjected to weathering that changed the rock to dark gray to yellowish brown color (Fig. 4.10A). Depending on the chlorite content, the fresh part has light to moderate green color. The out crop of this rock unit has massive and blocky nature and also is characterized by schistosity associated with radiated actinolite tremolite minerals. Joints, veins, lineation's, foliations and faults are the main structures in this rock unit.



Figure 4.9. Chlorite- Talc-Tremolite schist from kilkile area; (A) weathered, large and form ridges found on kilkile III. (B) greenish chlorite- talc-tremolite schist rocks on kilkile I. (C) highly weathered and covered by soil, shows foliation found in Kilkile II and (D) outcrop of predominantly talc schist.

In thin section it shows 35 % chlorite, 30% of talc, 15% of tremolite, 5% muscovite, 9 % opaque and the remaining covered by others. Chlorite and talc shows a noticeable alteration and align in one direction. The color of chlorite varies from light grey (PPL) to light green/blue to pink (XPL) with fibrous form whereas tremolite shows relative high relief with alternative yellow and blue color. These crystals are coarse and have anhedral shape with a noticeable alteration. Muscovite also shows yellow, light green and brown color, it is a sheet-like tabular crystals with a noticeable alteration. Relative to other units, on this rock opaque minerals have large amount and they shows euhedral shapes.

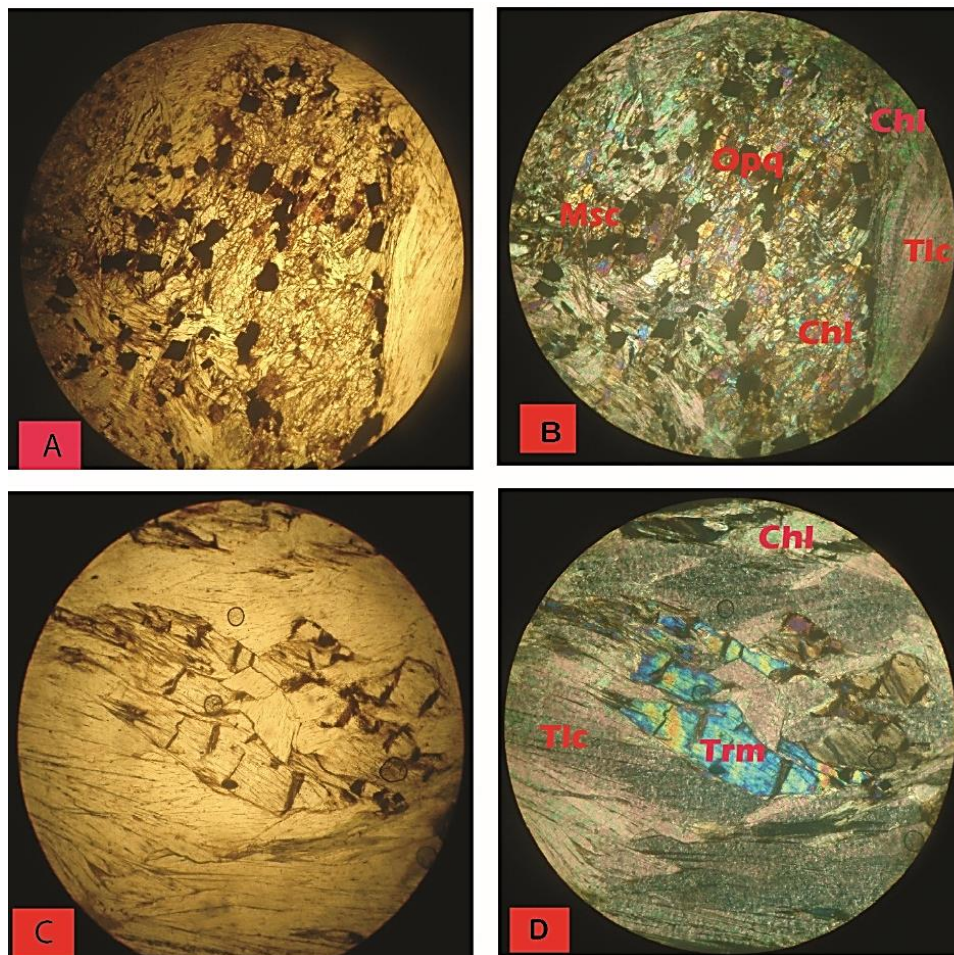


Figure 4.10. Microscopic photo picture of Chlorite- Talc-Tremolite Schist rocks on kilile area; (A &C) under PPL whereas (B &D) under XPL. The labels stand for; Tlc- Talc, MSc-Muscovite mica, Chl- Chlorite, Trm- tremolite and OPq- Opaque. The photo picture is taken at 10X magnification.

4.2.7. Granite

This rock unit is found in the southern part of the area. It has light pink color (depending on the content of feldspar) in fresh exposures but white, light grey to reddish brown when weathered. It is coarse grained, equigranular, predominantly composed of quartz, K-feldspar, plagioclase and mica.

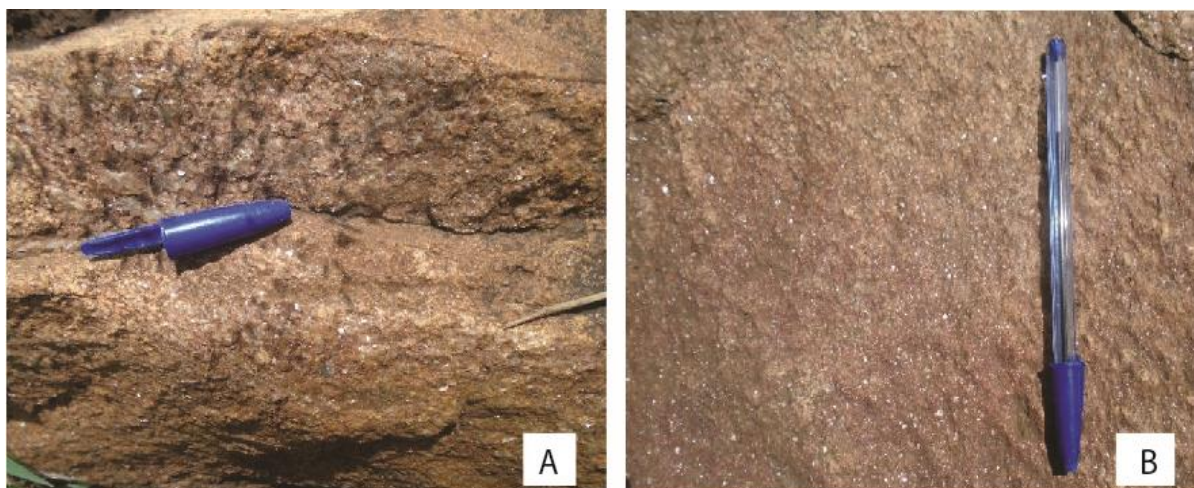


Figure 4.11. *Weathered outcrop of granite from Kilkile area.*

4.2.8. Pegmatite

The pegmatite exposures are characterized by large crystal of mica, microcline and quartz and often together with plagioclase. The rare metals bearing pegmatite in the study area have lenticular shape that elongate nearly N-S direction having variable width and composition (simple and complex), texture, degree of differentiation and intensity of alteration and weathering. Based on their location pegmatites in Kilkile area are divided in to three group, pegmatites in Kilkile I which covers relatively northern part, pegmatite in Kilkile II which covers relatively the central part and pegmatite in Kilkile III which covers the southern part of the study area (figure 4.1).

Most of the pegmatite bodies found in kilkile I are composed of quartz, muscovite, albite and microcline. Orthoclase also has relatively enormous amount, most of the time it shows cloudy heterogenous appearance with low relief and birefringence. These pegmatites usually albitized, kaolinized and greisenised. Most of the pegmatite bodies of the area are striking nearly N-S direction, not more than half of a km long and have less than 200m width. Whitish to dull white, glassy to smoky quartz are common; fine- to medium- grained colombite-tantalite crystals are observed, muscovite has mostly silver and brown color. Accessory minerals like magnetite, hematite, emerald, tourmaline and beryl are also available in these pegmatites



Figure 4.12. Pegmatite rock on Kilkile area. (A) pegmatite in Kilkile III, (B) pegmatite in kilkile II; (C) pegmatite in Kilkile I and (D) Pegmatite rock which dominantly consists silvery to green muscovite on Kilkile II area.

Muscovite, quartz, albite, k-feldspar and micas are the major mineral phases in Kilkile II pegmatite. Beryl, magnetite, hematite, tourmaline and pyrite are accessory minerals. Alkali feldspars of pegmatite are altered to albite, in some place these feldspars further altered to form kaolin. The intensity of albitization and kaolinization varies from place to place but most of the time they are high in Kilkile I than Kilkile II. In some Kilkile II pegmatites beryl crystals, glassy quartz and brown to silvery book muscovite are observed. These pegmatites bodies are like in Kilkile I, generally striking N-S direction, more than a km long and not more than 200m width.

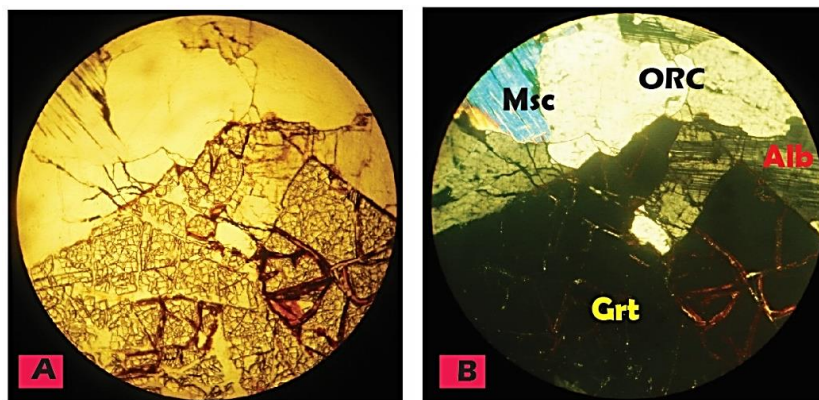
Kilkile III Pegmatites found in the southern part of the study area, this pegmatite bodies covers relatively large area. Morphologically, the pegmatite bodies have both tabular and lenticular shapes. Most of these pegmatites bodies are also generally striking N-S direction having more than a kilometer of length and its width varies from few meters to few hundreds of meters.

Even though the major mineral composition of most of Kilkile pegmatites is similar, they differ in minor constituents. In general, the Kilkile pegmatites are classified into two types: simple and complex spodumene pegmatite type. Simple pegmatites are barren pegmatite, it is mainly composed of feldspar, quartz, and mica. This barren granitoid pegmatite veins are usually found in Kilkile III and some of Kilkile II area. Complex pegmatite bodies consist of elevated Ta, Nb, Cs, Rb, Li and other rare metals. This type of pegmatite is usually found in Kilkile I and some of Kilkile II area. In general, the pegmatite bodies of the area show various degrees of mineralization, internal texture, intensity of alteration, and weathering.

4.2.8.1. Rock forming minerals in pegmatites

Pegmatite is a very coarse-grained rock, which is mostly composed of quartz, feldspar, and mica. For this crystal growth rates in pegmatite must be extremely fast to allow gigantic crystals to grow within the confining pressures of the Earth's crust. In Kilkile pegmatite, feldspar is present in a very large amount in different forms as microcline, orthoclase, and albite. Albite, orthoclase, and microcline are more dominant in pegmatites of Kilkile I and II.

Plenty of muscovite micas are available in Kilkile I and Kilkile II pegmatite as well. Ordinary silvery to greenish muscovite is most common, which appears as clear elongate crystals together with albite. High relief anhedral secondary garnet is observed in some of Kilkile pegmatite. These have fractures with purple to reddish color. Most of the garnet in ppl shows conchoidal fracture with spherical crystal shape but it appears black in xpl (Fig. 4.14). White (milky quartz), smoky, and transparent quartz appears in Kilkile pegmatites and most of them show xenoblastic texture with low relief.



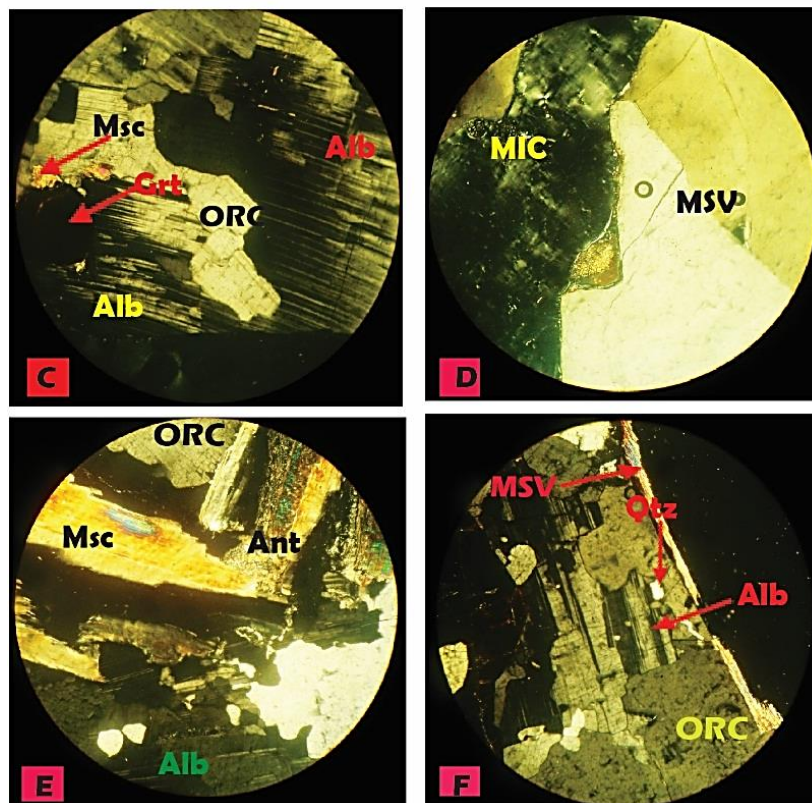
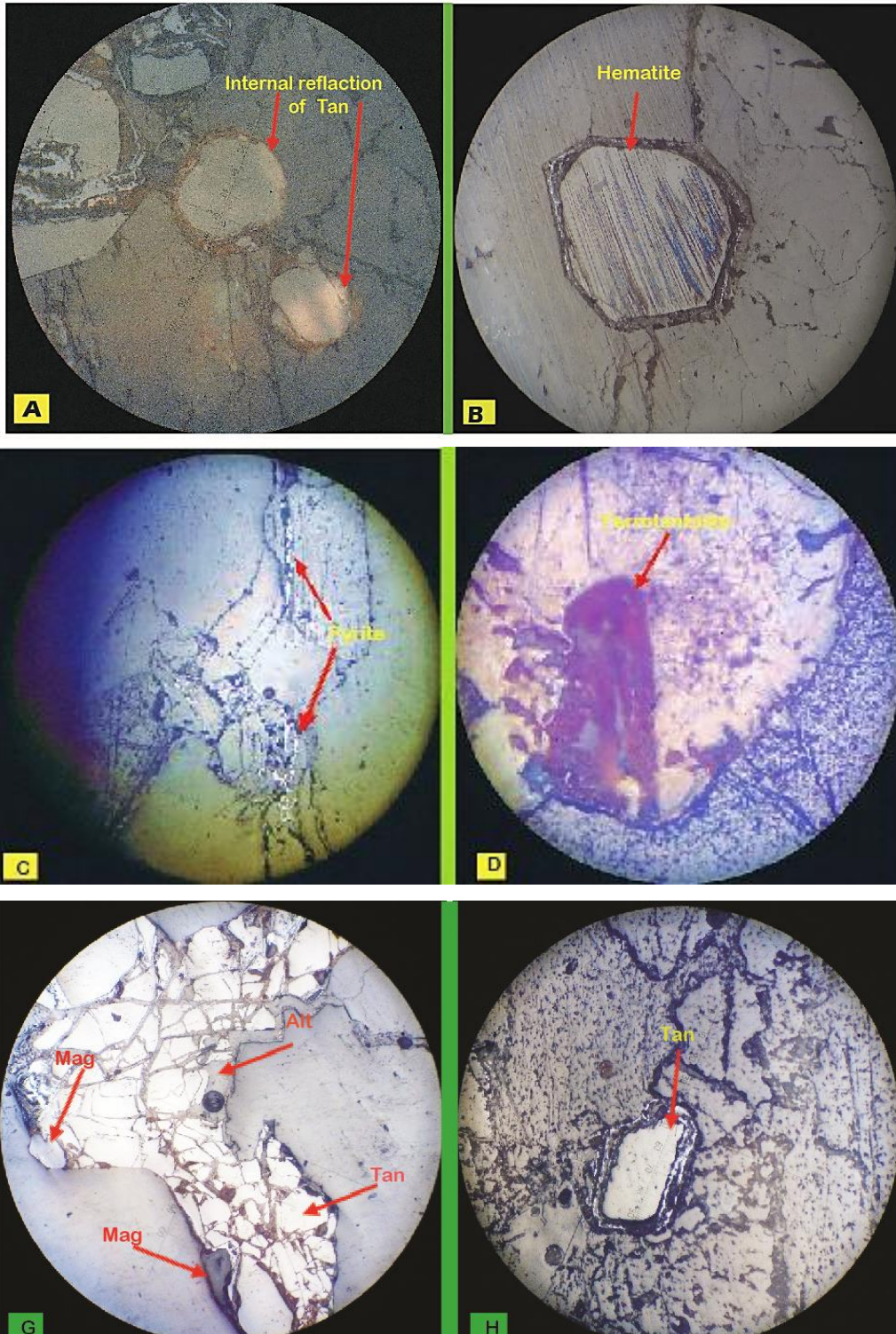


Figure 4.13. Microscopic photo picture of pegmatite rock unit on Kilkile I and II area; (A) under PPL whereas (B, C, D, E and F) under XPL the labels stands for; Msc-Muscovite, Alb-Albite, ORC-Orthoclase, Grt-Garnet, MIC-Microcline-Quartz and Ant-Anorthites. The photo picture is taken at 10X magnification.

4.2.8.2. Ore forming minerals in pegmatite

Ore microscope is used to identify and characterize ore minerals. Kilkile pegmatites under ore microscope typically shows ore minerals such as columbite-tantalite, pyrite, hematite and magnetite. Tantalite under ore microscope shows light gray, elongate, euhedral to subhedral mineral. Internal reflection in the columbite-tantalite crystal has been observed (Figure 4.15A). Dark brown with dark gray color is a typical characteristic of ferrotantalite crystal (Figure 4.15D).

Magnetite occurs frequently in small crystals and irregular nodules in the pegmatite (Figure 4.15E). Hematite shows gray white with bluish tint (Figure 4.15B) and pyrite and tourmaline occur abundantly especially in the northern part of the Kilkile area this is observed in microscope and field work as well.



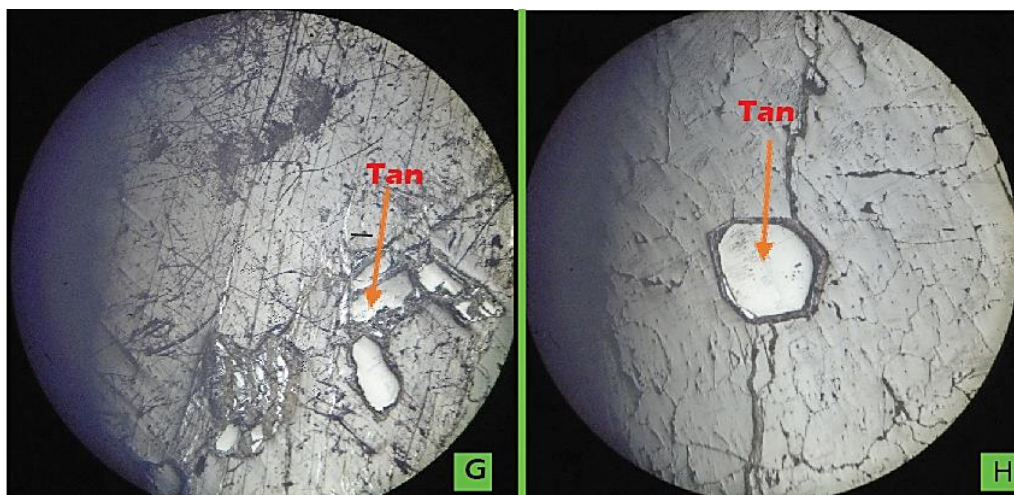


Figure 4.14. Ore microscopic photo picture of pegmatite rock unit on kilkile area. (A) Internal reflection in the columbite-tantalite crystal, (B) magnetite show lamellar texture, (C) pyrite, (D) ferrotantalite, (E) magnetite and columbite-tantalite crystals and (F, G, H) columbite-tantalite crystal. The labels stand for; Tan represent columbite-tantalite, Mag-magnetite, Spt-sphalerite and Alt-alteration. All the photo picture is taken at 10X magnification except figure A, which is at 20X.

4.3. Alteration

The term alteration refers to the effects that a hydrothermal fluid imparts upon a host rock on which mineralogical and/or textural changes exhibit. The hydrothermal fluid is normally channeled through the rock by either primary (pore space) or secondary porosity (fractures) and in general terms, the degree of alteration increases as the main channel way is approached (Taylor, 2009).

The alteration effects range from small selvages adjacent to cracks up to kilometer scale zones surrounding breccia pipes or porphyry systems. According to Taylor (2009) temperature, pressure, Eh, pH, wall rock composition, fluid composition, rate of flow and periodicity of flow are potential variables controlling the reactions. The above writer further stated that, hydrothermal fluid is constantly modifying in composition as a result of alteration along its path.

Detailed studies indicate that most widely reported replacement are replacements of perthite, quartz, muscovite, and spodumene by albite and replacements of quartz, feldspars, spodumene, and tourmaline by muscovite, lepidolite, or other sheet-structure minerals (Cerny, 1982). The types of alterations which encountered in the study area include chloritization, glimmeritization, kaolinization, serpentinization, albitization, silicification and phyllic alteration. Feldspar

components like albite and anorthite replaced by a buff-grey mineral fine -grained white mica called sericite. Sericite has no formal mineralogical definition and is best termed white, fine grained potassium mica this phenomenon of sericitization is called phyllic-alteration (Taylor, 2009). Albitization is partial or complete replacement of pre-existing alkali feldspar by albite. A common process involves the residual water-rich vapor released during the final stages of crystallization of a granite body. This vapor, which can carry high concentrations of Na in solution, rises through the granite body and reacts with the feldspars present in the granite, converting them to albite which is stable under the lower temperature vapor rich condition (Aallaby, 2008). Albite is more dominant in pegmatite sample of Kilkile I and II and usually shows twinning and elongate shape and most of them altered to sericite and less like to clay. Kaolinite represents the final product from the chemical weathering of alteration of aluminosilicates, especially feldspars to give clay. Pegmatites have higher input of k-feldspars as major constituent, the solid-state transformation of these aluminum-rich minerals into white color hydrous aluminosilicates produces the clay-type mineral kaolin and the process is called kaolinization. Kaolin is weakly structured, soft and friable and it shows a white soft clay appearance. The evidence of kaolinization is observed, on the surface and in borehole samples in the northern part of the study area.

Greisen is an altered, light-colored, granite rock consisting of white mica and quartz. This rock is formed by the reaction of crystalline granite with hot fluorine-rich vapor derived from the crystallizing granite at a deeper level in the intrusion (Aallaby, 2008). Greisenization mostly found in Kilkile I area. Silicification is the introduction of cryptocrystalline silica into a non-siliceous rock via groundwater or fluids of igneous origin (Allaby, 2008). The introduced silica either fills pore spaces in the rock or replaces pre-existing minerals. Most of kilkile area lithologies shows silicification. Chlorite is an alteration product of ferromagnesian minerals in igneous rocks. It is important group of phyllosilicate minerals and commonly occurs during green-schist facies metamorphism. The process of serpentinization is mainly the alteration of olivine and pyroxenes in the ultra-mafic rocks.

Glimmeritization describes the alteration reactions with the host rock (serpentinite) along the contacts of pegmatite characterized by the development of an exomorphic assemblage form glimmerite. Secondary garnet and muscovite also observed on kilkile pegmatite (Figure 4.15).

During interaction between crystallized granites and acidic late magmatic fluids secondary muscovitization and greisenization become prominent under sub-solidus conditions (Pirajno, 2013).

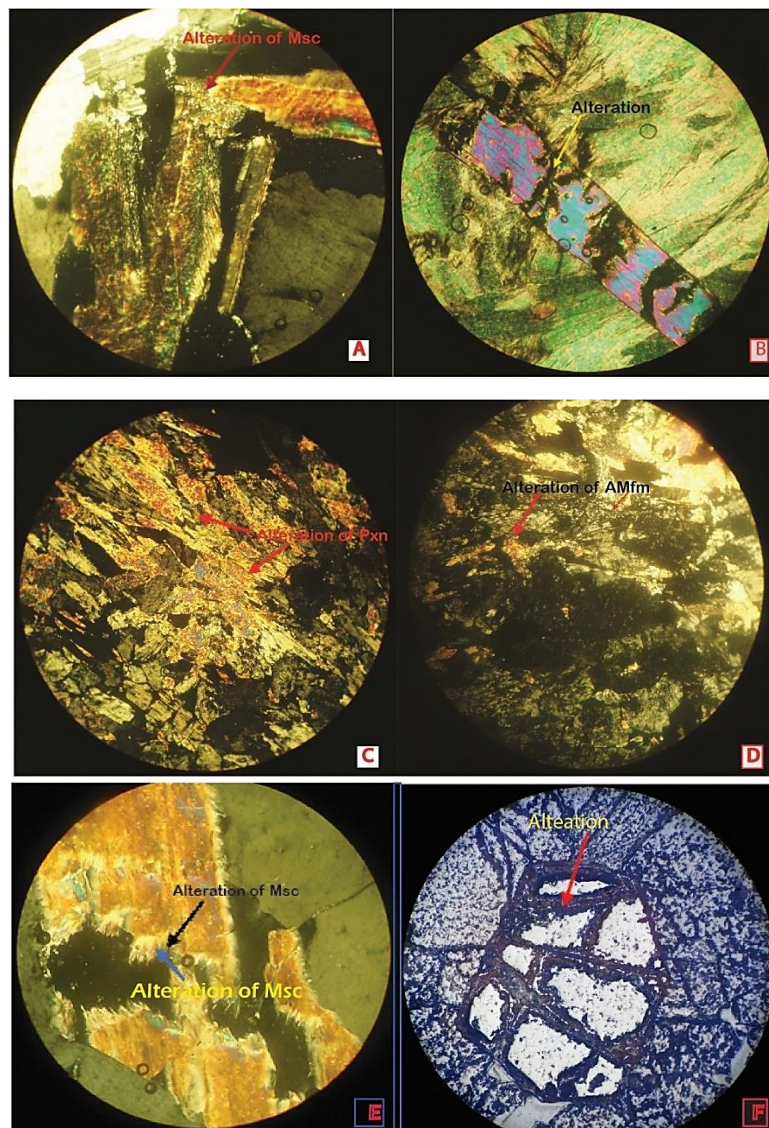


Figure 4.15. Shows alteration of mineral in kilkile area;(A) and (E) shows alteration of muscovite to sericite from pegmatite rocks, (B) shows alteration of tourmaline form chlorite-talc-tremolite schist, (C) Alteration from serpentinite rock of pyroxene from amphibolite schist, (D)Alteration of ultramafic mineral(pyroxene) to serpentine and (F) Alteration of tantalite crystal to gangue from pegmatite rock. The photo picture is taken at 10X magnification.

4.4. Geologic structures

Poly phase of deformation and metamorphism which affected the study area, have been a cause for various structural features formation, this area consists different structure like faults, joints, lineation's and foliations with variable size (micro, macro & mega scale).

4.4.1. Foliation

Most of the lithologic unit in the study area display NNE trending foliation specially in amphibolite schist and talc tremolite schist (Fig 4.16 & 4. 17). In the western and eastern part of the study area the foliation dips towards SW and in the central part rather represented by sub-vertically dipping. Amphibolite schist shows book like foliation (figure 4.16B).

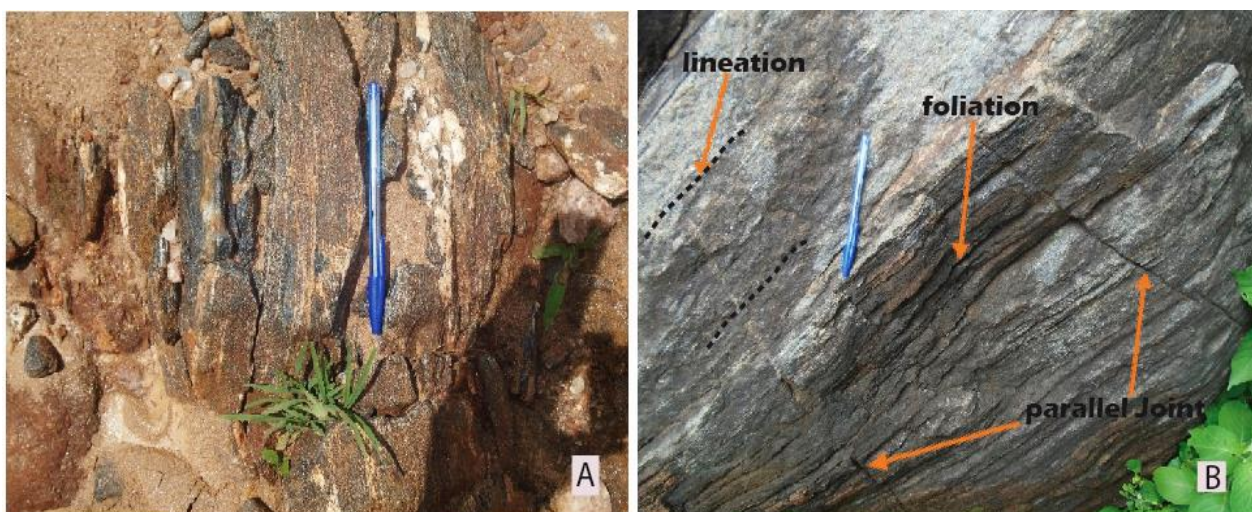


Figure 4.16. Pervasive foliation in biotite gneiss (A), and amphibolite schist (B).

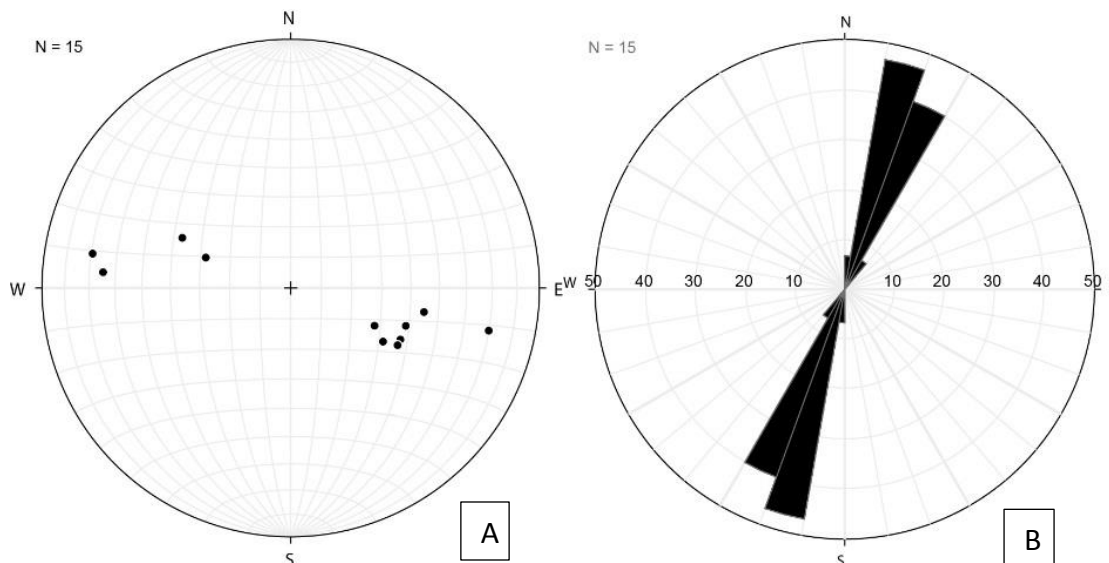


Figure 4.17. Stereo-plot of foliations. (A) The poles to the foliations. The dominant poles are clustered on the SE indicates that the foliations are dipping towards the NW. (B) Rose diagram for the foliations: The longest wedge of the rose diagram represents N10°- 20°E and this value indicates that the mean value of the strike direction of the foliations in the study area.

4.4.2. Lineation

Parallel alignment of biotite and amphibole minerals in biotite gneiss and amphibole schist as well as in amphibolite gneiss form linear structures. Parallel lineation stretching lineation and intersecting lineation are the major type that found in the study area. Most of the lineation in the study area are arranged down dip to the foliation.

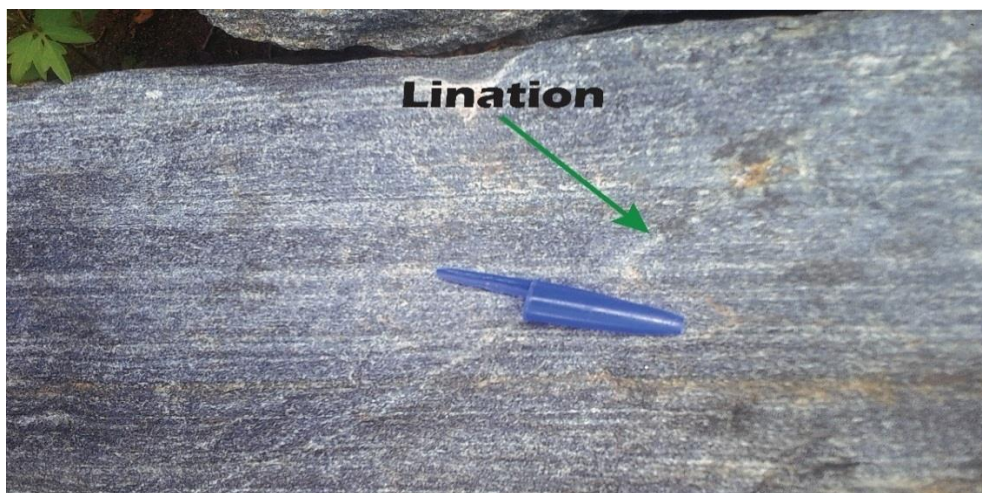


Figure 4.18. Geologic structure in Kilkile area shows intersection lineation on amphibolite rock units.

4.4.3. Fault

In Kenticha and Kilkile area, there are three sets of faults including the principal, older N-S trending ones (Fig 4.20). Two relatively younger faults, have NE-SW and NW-SE striking directions. These faults, were developed in the late Proterozoic–Paleozoic time giving way to the final stage of the structural development and the intersection of these younger faults with the N-S trending structures were the most favorable conditions for the ore formation (Kozyrev et al., 1982). The faults are the result of the development of various deformations of the green stone belt and enveloping gneisses (Beraki et al., 1989). Most rock units in the study area are affected by the faults.



Figure 4.19. Geologic structure in Kilkile area; (A) fault in Kilkile II and (B) fault in Kilkile I.

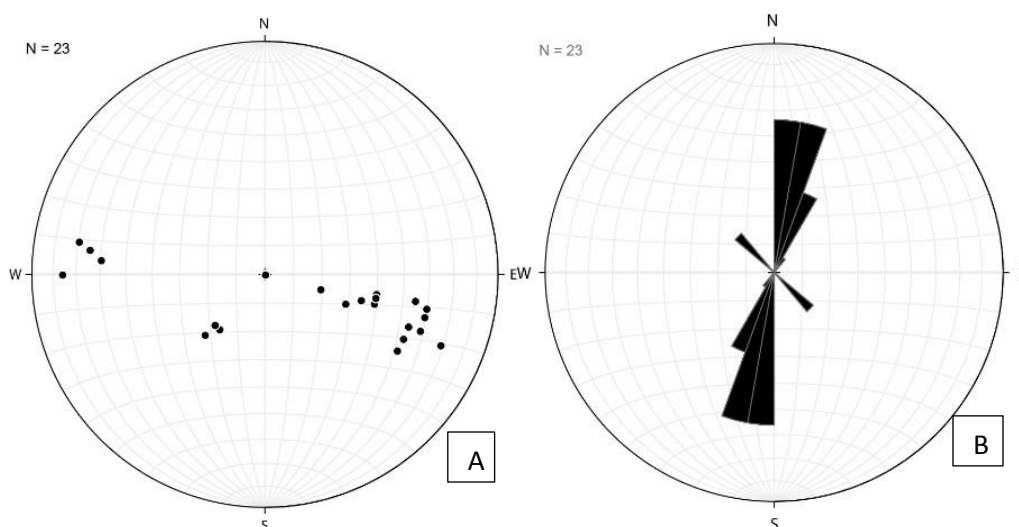


Figure .4.20. (A) Stereo-plot of fault, most of the pole clustered on NE which indicated the most of the fault dips to ward NW.(B) Rose diagram of the joints which shows which shows majority of the fault strike NNE to NE.

4.4.4. Joint and vein

In the study area numerous joints are available, and they dominantly trends in N-S direction, and other joints trend in NW-SE and NE-SW directions as well; most joints found in talc tremolite schist and amphibolite schist are sub horizontal. The joints in amphibolite gneiss, amphibolite schist and talc tremolite show different magnitude of joint openings with a maximum of 50 cm; in some case are field with secondary minerals, such as silica, carbonate and iron oxides. The orientation measurements of all joints and other structures are presented in Appendix I.

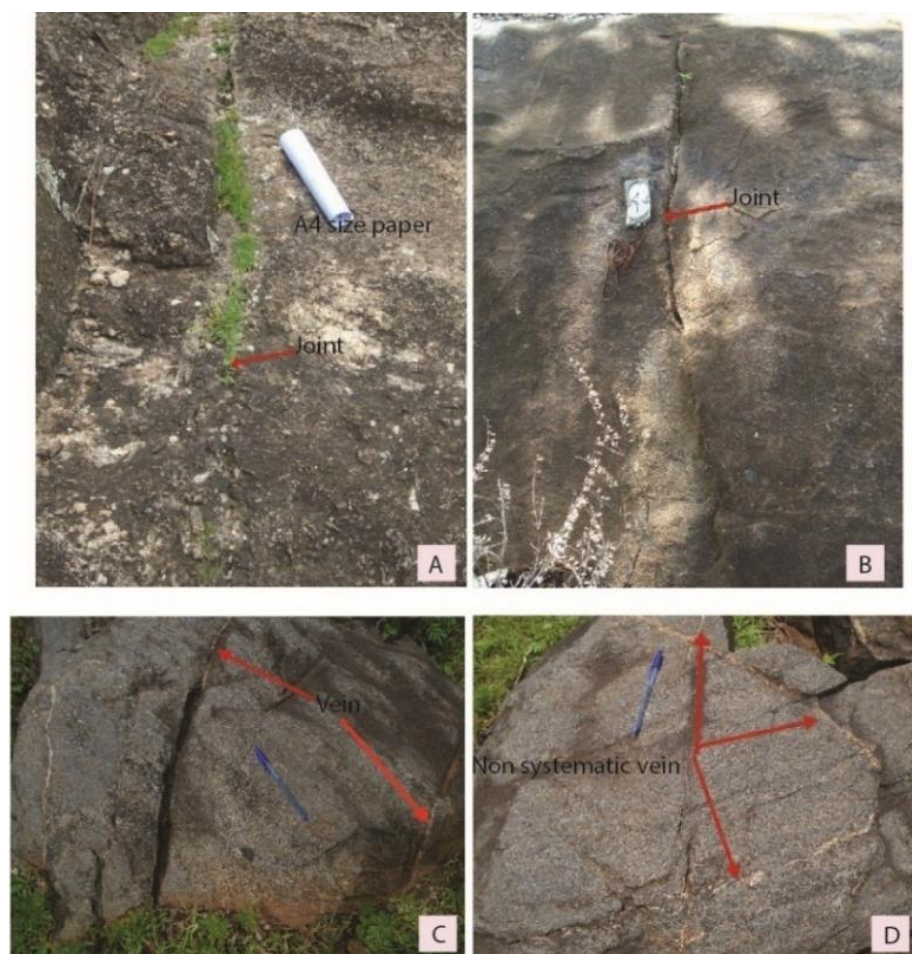


Figure 4.21. Geologic structure in Kilkile area; (A) Sub horizontal joint on talc tremolite schist in Kilkile III, (B) joint on Amphibolite rock unit in Kilkile II, (C) Sub parallel veins and (D) non-systematic veins on amphibolite schist.

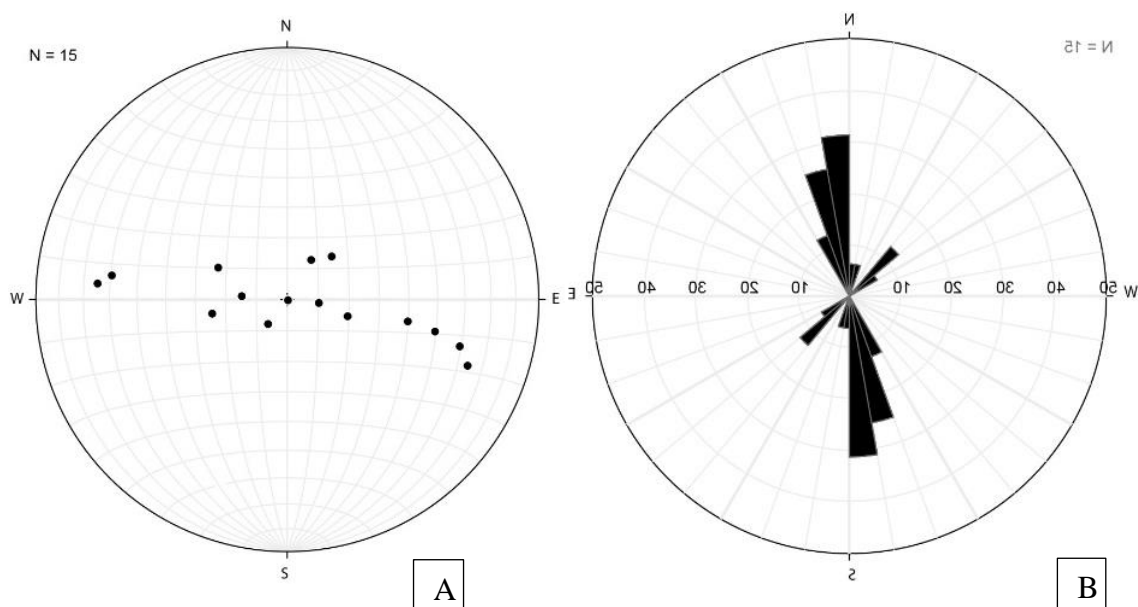


Figure 4.22. Stereo-plot for selective joints: (A) the poles of the joints show the dominant poles are clustered at the center. (B) Rose diagram of the joints which shows the longest wedge of the rose diagram is $N00^{\circ} - 10^{\circ}E$ this represents the mean value of the strike direction of the joint set. The second joint set have $N10^{\circ} - 20^{\circ}E$, implying that mean value of the strike direction of the second joint sets. The third joint set have $N40^{\circ} - 50^{\circ}W$ which also imply the mean value of the strike direction of the third joint sets.

4.4.5. Micro structure

Kilkile pegmatite minerals show mineral texture such as platy, idioblastic, xenoblastic, relict, flaky, fibrous, and veinlet textures (see Table 4.1, Fig 4.23).

Mineral	Texture	Description	Thin section number
Quartz	Xenoblastic	It dominantly occurs in pegmatite unit with low relief, have no cleavage and twinning.	K3T3S3
Muscovite	Flaky	Tabular and have pseudo hexagonal outline with perfect micaceous cleavage and usually altered to sericite	K2T5S1
Microcline	Xenoblastic	Anhedral with tartan twinning	K1B20
Albite	Xenoblastic	Tabular usually shows black and white stripes	K1B20

Chlorite	Platy	Felt like appearance	K2T5S7
Talc	platy	Occur as long fibers	K2T5S7
Tourmaline	Idioblastic to Xenoblastic	Prismatic	K2T5S7 & K2T6S2
Garnet	relict	High relief, internal fracture of grain is common and it is roughly spherical crystal	K1B20
Opaque	Xenoblastic	High relief, tabular, equant and euhedral. Usually they are magnetite and hematite	K2T5S7
Serpentine	Platy	Occur as long fibers.	K2T5S6

Table 4.1. Minerals and texture of the pegmatite in some selected samples.

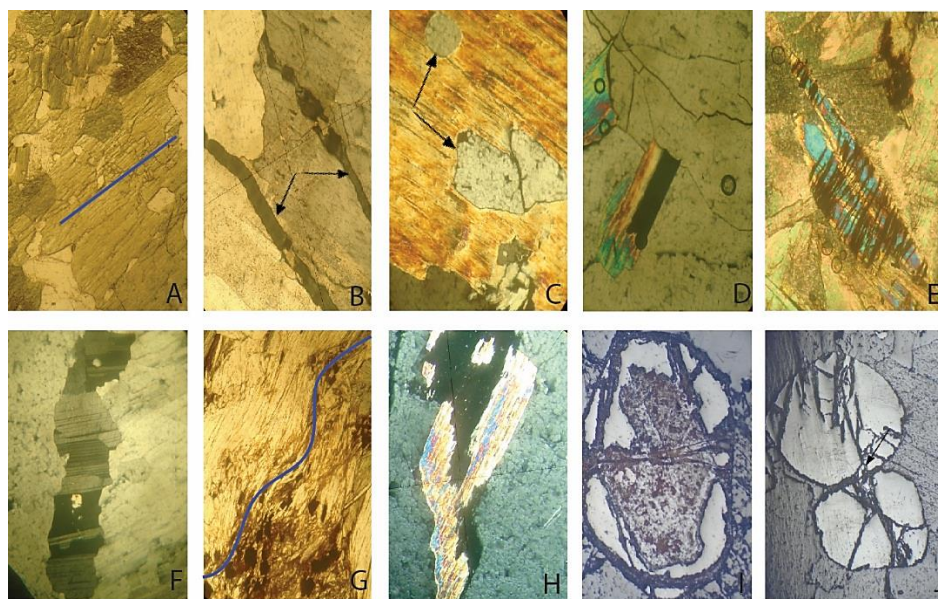


Figure 4.23. Microscopic photo-pictures of microstructure and textures. (A) preferred orientations of mineral grains, (B) sub parallel joints, (C) inclusions, (D) twining and microfractures, (E) replacement of tremolite, (F) well developed twining, (G) crenulation on talc tremolite schist, (H) vein filling, (I) Pseudomorphic replacement textures and (J) trans-granular microcracks. All pictures are from petrographic microscope except I and J which is taken from ore microscope.

CHAPTER FIVE

5. Geochemistry of the Kilkile rare metals deposit

5.1. Whole-rock composition

The chemical composition and mineralogy of the source region exerts a fundamental control over the chemistry of magmatic rocks, consequently major and trace element composition of a melt is determined by the type of melting process and the degree of partial melting, and composition of the melt can be substantially modified while it comes to the surface (Rollinson, 1993).

Major and trace element geochemical data are mainly used to understand the evolution of magma, and these elements can be analyzed using ICP-MS and ICP-AES. For the investigation of whole rock geochemistry, nine rock samples from both surface and borehole have been analyzed (table 5.1).

Sample	Kilkile I			Kilkile II				Kilkile III	
	K1A7	K1B14B	K1B14A	K2T6S2	K2A24A	K2A24B	K2C31	K2C30	K3T3S2
ICP-AES (Major oxides (wt.%))									
SiO ₂	75.6	73.8	69.8	85.5	75	77.5	75	74.5	95.1
TiO ₂	0.01	0.06	0.04	0.05	0.03	0.06	0.06	0.03	0.01
Al ₂ O ₃	14.05	15.5	16.9	8.13	15	13.45	16.05	15.75	2.66
Fe ₂ O ₃	1.34	1.9	1.88	1.49	1.79	2.28	1.53	1.23	0.99
MnO	0.03	0.2	0.18	0.02	0.25	0.19	0.02	0.13	0.01
MgO	0.08	0.28	0.19	0.17	0.08	0.17	0.26	0.12	0.03
CaO	0.23	0.64	0.3	0.01	0.3	0.24	0.03	0.59	0.01
Na ₂ O	4.9	6.53	5.15	0.2	5.64	3.83	0.29	7.38	0.06
K ₂ O	3.78	1.34	3.14	2.35	1.67	1.33	4.48	0.96	0.7
P ₂ O ₅	0.07	0.05	0.07	bdl	0.04	0.02	0.01	0.21	bdl
LOI	0.49	0.53	0.91	1.1	1.44	1.82	3.21	0.58	0.39
Total	100.58	100.84	98.56	99.02	101.24	100.9	100.94	101.48	99.97

Sample	Kilkile I			Kilkile II				Kilkile III	
	K1A7	K1B14B	K1B14A	K2T6S2	K2A24A	K2A24B	K2C31	K2C30	K3T3S2
ICP-MS (Trace element (ppm))									
Li	50	120	140	200	70	90	210	70	20
Sc	bdl	3	5	6	2	3	8	1	1
V	5	18	bdl	bdl	9	21	12	bdl	11
Cr	10	30	10	10	20	40	20	10	30
Ni	1	9	2	1	7	38	9	5	bdl
Cu	bdl	bdl	1	bdl	45	30	30	bdl	bdl
Zn	68	109	46	83	46	68	94	30	10
Ga	33.2	46.1	54	51.4	36	42.8	73	38.6	11.4
Rb	441	421	343	421	195.5	221	716	128.5	95.7
Sr	4	165.5	12.7	1	5.4	10	2.4	10.4	0.9
Y	3.4	13.6	11.6	11.8	8.3	6.8	2.2	11.3	0.6
Zr	13	48	63	4	71	34	8	48	3
Nb	124.5	87.5	134	118	69.1	58.6	158	153	29.3
Sn	6	20	32	16	10	7	30	5	8
Cs	4.55	9.42	10.3	6.97	4.87	9.04	10.95	4.32	2.03
Ba	7.8	42.4	13.3	5.8	24.7	41.5	10.1	20.5	11.1
Hf	1	3.8	4.7	0.2	5.5	1.9	0.5	4	0.2
Ta	17.4	8.7	8.8	5.8	11.1	5.1	9.7	21.4	7.9
W	3	2	2	4	54	167	128	1	2
Tl	Bdl	bdl	10	bdl	bdl	10	bdl	bdl	10
Pb	21	18	19	bdl	15	10	12	5	bdl
Th	5	22.4	13.8	0.63	7.24	3.8	2.32	5.47	0.05
U	3.12	6.21	27.8	0.81	8.75	2.04	0.44	4.24	bdl
K	31366	11119.2	26055.3	19500	13857.5	11036	37174.6	7966	5808.5
Mn	232.4	1549.3	1394	154.9	1936.6	1471.8	154.9	1007	77.5
Fe	9380	13300	1316	10430	12530	15960	10710	8610	6930
Mg	480	1680	1140	1020	480	1020	1560	720	180
Mg/Li	9.6	14	8.14	5.1	6.86	11.3	7.43	10.29	9
Nb/Ta	7.16	10.1	15.2	20.34	6.23	11.49	16.29	7.15	3.71
Zr/Hf	13	12.63	13.40	20	12.91	17.89	16	12	15
ICP-MS (REE(ppm))									
La	1.3	11.9	2.6	0.5	2.6	2.9	2	3.8	0.9
Ce	1.5	26.5	4.7	bdl	4.4	5.8	1.7	5.2	bdl
Pr	0.19	3.53	0.76	0.03	0.67	0.64	0.34	1	bdl
Nd	0.6	13.3	3.1	0.2	2.6	2.7	1.3	3.9	bdl
Sm	0.55	6.73	2.53	0.37	1.62	0.75	0.6	2.27	bdl
Eu	bdl	0.13	bdl	bdl	0.04	0.1	0.05	0.11	bdl
Gd	0.59	4.51	2.45	1.21	1.35	0.88	0.49	2.68	0.05
Tb	0.17	0.73	0.5	0.37	0.28	0.22	0.1	0.59	0.02
Dy	0.73	2.98	2.13	2.15	1.82	1.26	0.39	2.44	0.07
Ho	0.08	0.35	0.25	0.21	0.3	0.19	0.06	0.24	0.02
Er	0.15	0.86	0.55	0.57	0.77	0.54	0.14	0.38	0.03
Tm	0.03	0.15	0.06	0.07	0.18	0.12	0.03	0.01	0.02
Yb	0.19	1.29	0.83	0.36	1.49	0.88	0.18	0.57	0.05
Lu	0.03	0.16	0.09	0.04	0.23	0.11	0.01	0.05	0.01
Total	6.11	73.12	20.5	6.08	18.35	17.09	7.39	23.24	1.17

Table 5.1. Major elements in weight % (wt.%) and trace elements in parts per million (ppm) from Kilkile pegmatite both borehole and surficial samples. SrO and BaO and Cr₂O₃, Ag, As, Cd, and Mo are below the detection limit (bdl). NB: All samples are pegmatite

5.1.1 Major Element Geochemistry

The Kilkile area samples are mainly enriched in SiO₂ (69.8 to 85.5 wt. %) and Al₂O₃ (8.13 to 16.9 wt. %).

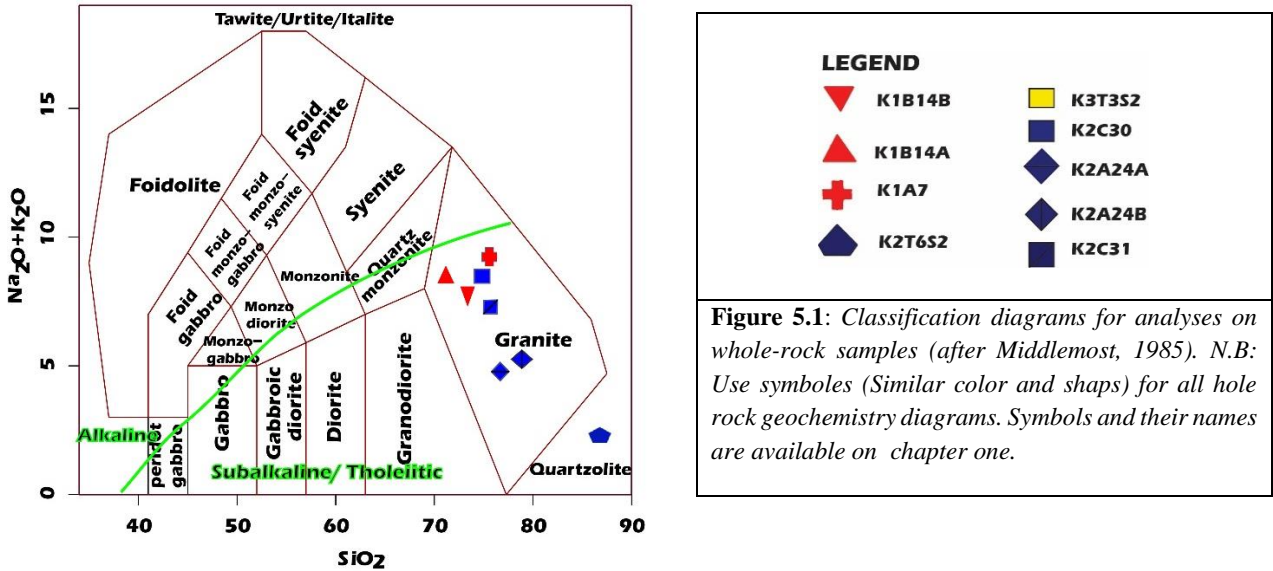


Figure 5.1: Classification diagrams for analyses on whole-rock samples (after Middlemost, 1985). N.B: Use symbols (Similar color and shapes) for all hole rock geochemistry diagrams. Symbols and their names are available on chapter one.

Middlemost (1985) demonstrates the nomenclature of normal igneous rocks on the basis of the weight percentages of SiO₂ versus total alkalis (Na₂O+K₂O). Accordingly, pegmatite rocks of the Kilkile area fall in the granite fields.

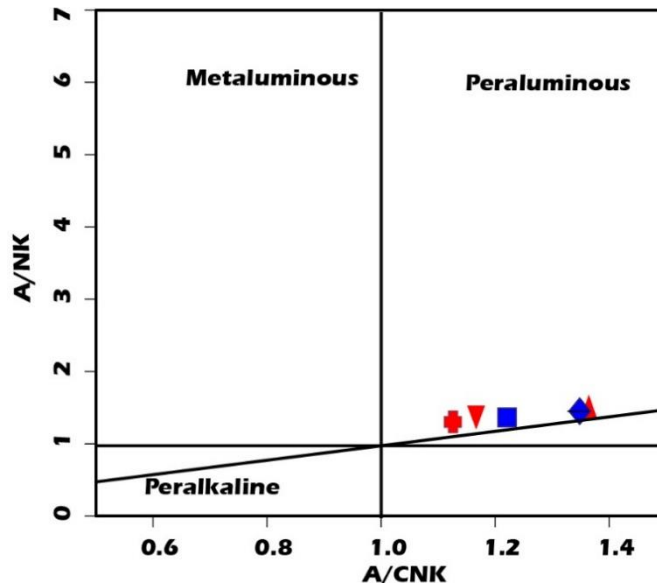
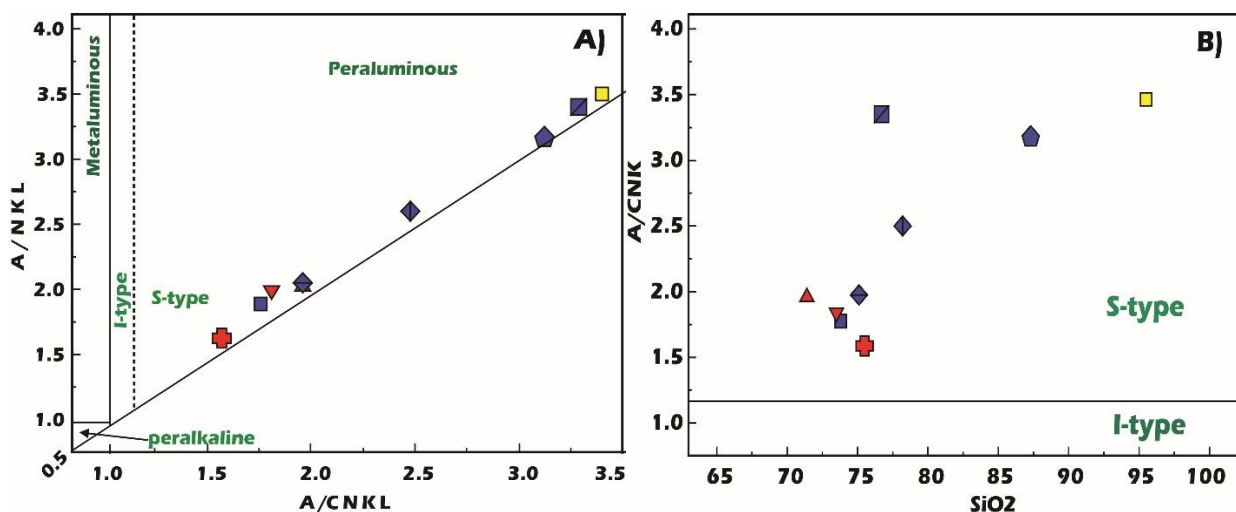


Figure 5.2. Classification diagrams for analyses on whole-rock samples: A/NK (A = Al₂O₃, N = Na₂O and K = K₂O) versus A/CNK (CaO) diagram (Shand, 1943)

Most of the LCT pegmatites have compositional affinity with the peraluminous S-type granites expressed by the mineral assemblages of muscovite, garnet, cordierite, sillimanite or andalusite, tourmaline and gahnite. On the other hand, pegmatites that belong to the NYF family are sourced from A-type granites (Chappell and White, 2001). A/CNK versus A/NK Classification diagrams (Shand, 1943) indicates that Kilkile granitic pegmatite comprises peraluminous as it has high amount of Al_2O_3 . (Figure 5.2A).

SiO_2 versus $\text{Al}_2\text{O}_3/\text{CaO}+\text{Na}_2\text{O}+\text{K}_2\text{O}$ diagram (Fig 5.3B) used to identify the source rock of the pegmatite (S-type or I-type). $\text{Al}_2\text{O}_3/\text{CaO}+\text{Na}_2\text{O}+\text{K}_2\text{O}+\text{LiO}_2$ versus $\text{Al}_2\text{O}_3/\text{Na}_2\text{O}+\text{K}_2\text{O}+\text{LiO}_2$ diagram also demonstration multi-functional classification of the granites on which we can infer that whether the granite sample is peraluminous, or metaluminous as well as peralkaline. This diagram can be also used to infer I-type or S-type granites. On both diagrams, the granitic pegmatite plot entirely within the field of S-type peraluminous granitoids (Figure 5.3A and B). On the other hand, whole-rock analyses of the Kilkile rock samples SiO_2 versus P_2O_5 diagram shows Low contents of P value.



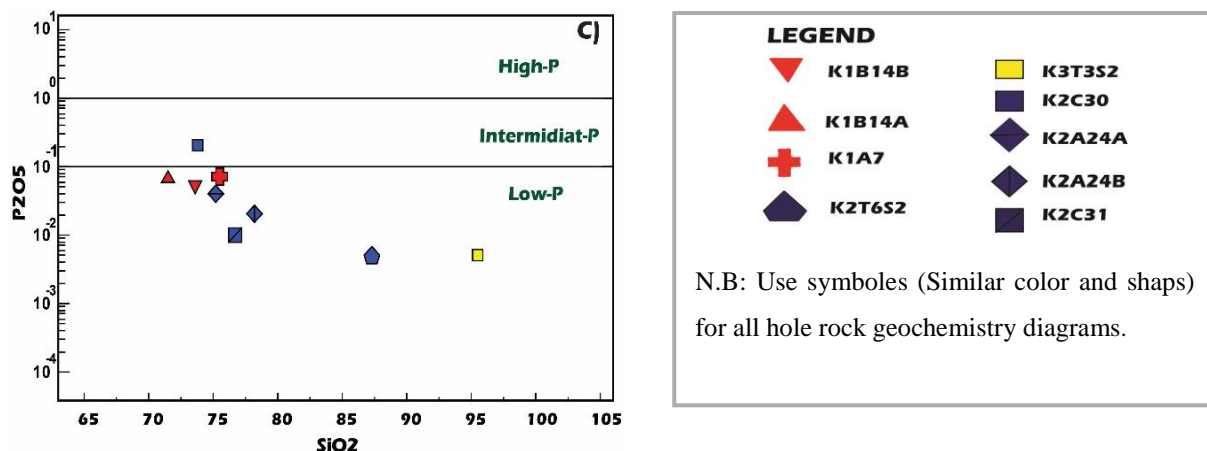


Figure 5.3. Discrimination diagrams of major element geochemistry of Kenticha pegmatite: (A) ANKL versus ACNKL index (fields for I- and S-type granites (Clarke, 1992); (B) Molecular $Al_2O_3/CaO+Na_2O+K_2O$ versus SiO_2 diagram showing the classification of the granites as S-type and I-type (after Chappel and White, 1974), and (C) major element geochemistry of Kilkile pegmatite: $\log P_2O_5$ versus SiO_2 (based on Linnen and Cuney, 2005).

5.1.2 Trace Elements Geochemistry

A trace element is an element which is present in a rock in concentrations of less than 0.1 wt. % that is less than 1000 parts per million (ppm). Variations of trace elements provides additional in sight in to the sources and major processes that control the nature of the products. Their relative abundances are also used to identify minerals present during melting or fractional crystallization.

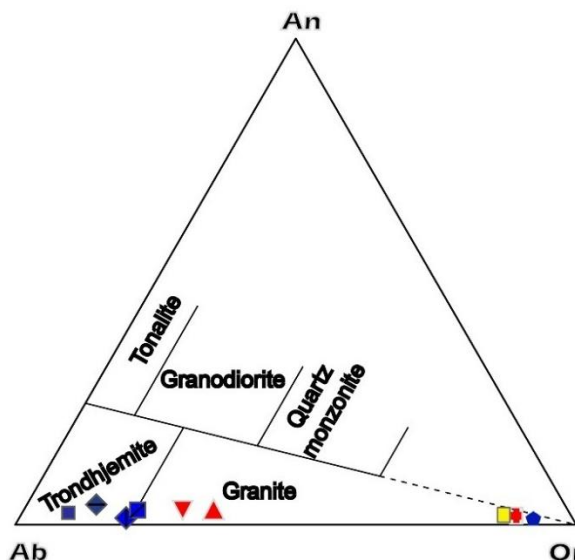


Figure 5.4. Classification diagrams for analyses on whole-rock samples of Feldspar triangle (after O’connor, 1965).

The Ab-An-Or classification diagram of O'Connor (1965) can be applied to felsic rocks chiefly used to classify plutonic rocks with more than 10% normative quartz (Appendix III) as in the case with Kilkile pegmatite (Fig 5.4).

Using geotectonic discrimination diagrams such as Y+ Nb versus Rb, Y versus Nb and Ta + Yb versus Rb and Yb versus Rb (Pearce et al., 1984), the Kilkile pegmatite samples are in the limit of WPG fields, thus in Y + Nb versus Rb, Y versus Nb almost all samples plot within WPG (Figure 5).

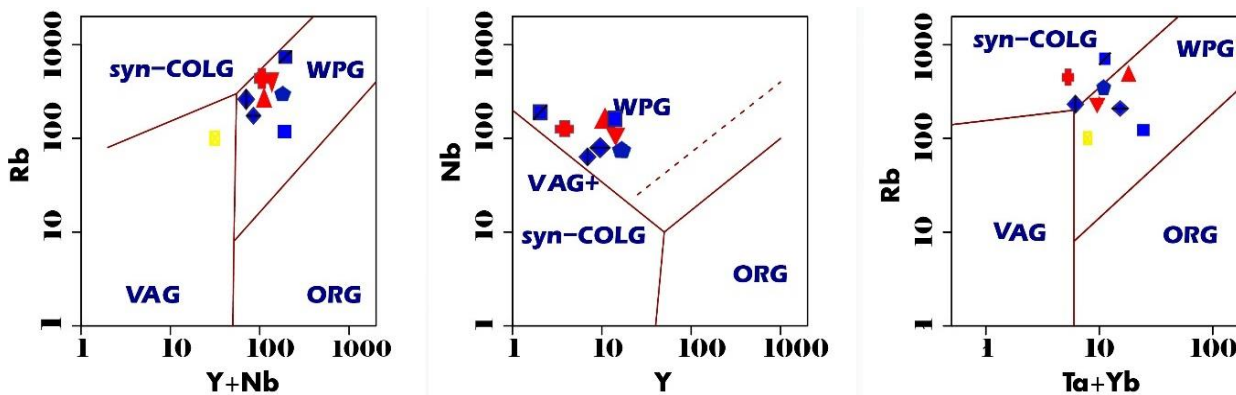
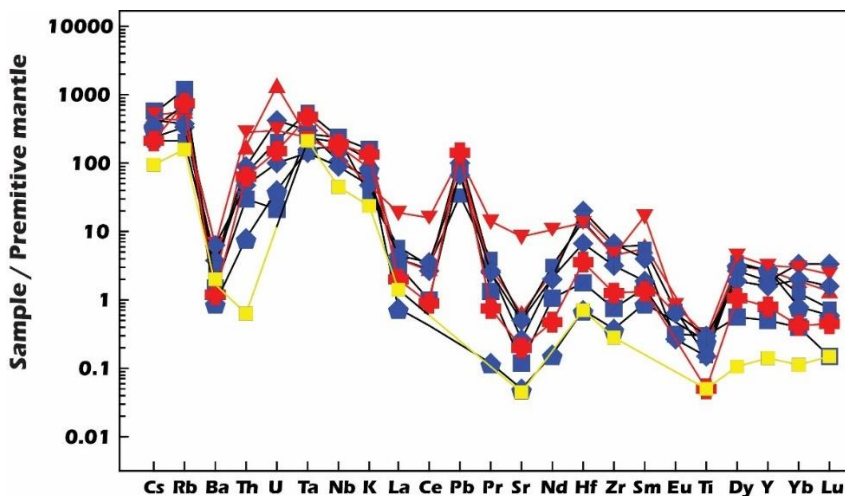


Figure 5.5. Geotectonic discrimination diagrams (Y + Nb versus Rb, Y versus Nb, Yb + Ta versus Rb and Yb versus Ta) (Pearce et al., 1984).



LEGEND	
▼ K1B14B	■ K3T3S2
▲ K1B14A	■ K2C30
⊕ K1A7	◆ K2A24A
◆ K2T6S2	◆ K2A24B
	■ K2C31

Figure 5.8. Multi-element spider diagram Sun and McDonough (1989). N.B: Use similar symbols for whole rock REE diagram.

In the multi-element diagram (Fig. 5.8) normalized to primitive mantle values of Sun and McDonough (1995), trace element data show, the concentration of large ion lithophile elements of Rb, Cs, K, Pb and some of high field strength elements (HFSE) like Ta, Nb comparatively high, since they are highly incompatible to the mineral phase, therefore their concentration increases at the last stage of fractionation. Ce, Ba, Sr, Nd and Ti have relatively very low content.

5.1.3 REE composition of Kilkile area

Chondrite normalized REE pattern (Boynton 1984) of the Kilkile pegmatite sample show negative Eu anomaly and almost all samples have similar pattern.

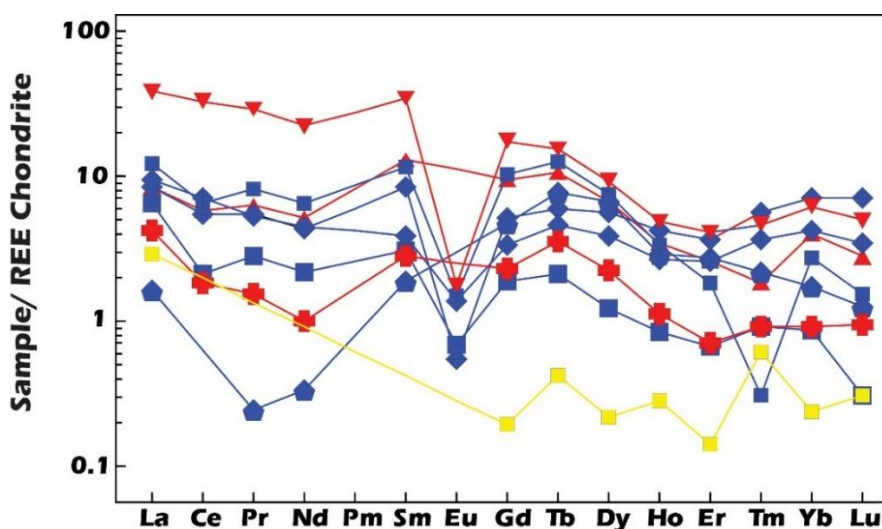


Figure 5. 9. Chondrite normalized REE pattern (Boynton 1984) of the Kilkile pegmatite sample.

5.2 Muscovite chemistry

The compositional attributes of muscovite can help to determine the degree of fractionation of the magma and the relationships among different pegmatites within a pegmatite. Furthermore, the trace-element contents of micas indicate economic potential of pegmatites (Trumbull 1995).

Representative compositions of muscovite both surface and core samples have been analyzed for mineral chemistry. One surficial and three borehole muscovite samples have been analyzed for major oxide, trace and rare earth element chemistry. These muscovite micas analyzed using ICP-MS and ICP-AES from Kilkile I, Kilkile II and Kilkile III pegmatites (Table 5.2).

Sample	Kilkile III	Kilkile II	Kilkile I	
	K3T2S3	K2T4S1	K1A2A	K1B11
ICP-AES (Major oxides (wt.%))				
SiO ₂	45.5	48.3	46.4	45.4
TiO ₂	0.12	0.06	0.05	0.08
Al ₂ O ₃	32.9	31.9	32.2	32.9
Fe ₂ O ₃	4.57	4.25	4.69	4.39
MnO	0.04	0.04	0.08	0.05
MgO	0.64	0.34	0.54	0.46
CaO	0.05	0.01	0.01	0.01
Na ₂ O	0.51	0.57	0.69	0.66
K ₂ O	9.09	9	9.62	9.75
P ₂ O ₅	0.01	0.01	bdl	bdl
LOI	6.44	5.44	5.27	5.26
Total	99.87	99.92	99.55	98.96
ICP-MS (Trace element (ppm))				
Li	310	250	900	430
Sc	12	4	2	10
V	32	13	5	19
Cr	20	10	10	10
Ni	8	2	18	Bdl
Cu	1	bdl	54	2
Zn	192	304	448	313
Ga	205	199.5	223	296
Rb	2230	2260	3200	3570
Sr	3.2	1.1	1.6	0.6
Y	2.4	1.1	bdl	0.6
Zr	18	13	4	4
Nb	567	491	562	432
Sn	316	355	348	129
Cs	42.8	70.2	97.3	246
Ba	14.4	7.8	3.9	7.4
Hf	1	1	0.4	0.8
Ta	38.7	36.5	55.8	169
W	8	6	82	17
Tl	10	10	10	20
Pb	18	16	8	14
Th	1.3	0.87	0.39	0.17
U	0.51	0.27	0.24	0.12
K	75427.9	74681	79825.8	80904.5
Mg	3840	2040	3240	2760
K/Rb	33.82	33.04	24.94	22.66
Mg/Li	12.38	8.16	3.6	6.41
Nb/Ta	14.65	13.45	10.07	2.56
Zr/Hf	18	13	10	5
ICP-MS (REE(ppm))				
La	2	1.44	bdl	0.7
Ce	2.5	2.4	bdl	bdl
Pr	0.38	0.16	0.04	bdl
Nd	1.5	0.7	0.2	0.1
Sm	0.44	0.21	0.06	0.08
Eu	0.07	0.03	bdl	bdl
Gd	0.33	0.21	bdl	0.09
Tb	0.08	0.03	bdl	0.01
Dy	0.49	0.21	bdl	0.09
Ho	0.07	0.04	0.01	0.01
Er	0.24	0.12	bdl	0.08
Tm	0.06	0.04	0.01	0.02
Yb	0.24	0.16	0.04	0.1
Lu	0.05	0.02	bdl	0.01
Total	8.45	5.77	0.36	1.29

Table 5.2. Major elements in weight % (wt.%) and trace elements in parts per million (ppm) from Kilkile muscovite borehole and surficial samples using ICP-AES and ICP-MS.

5.2.1. Major element

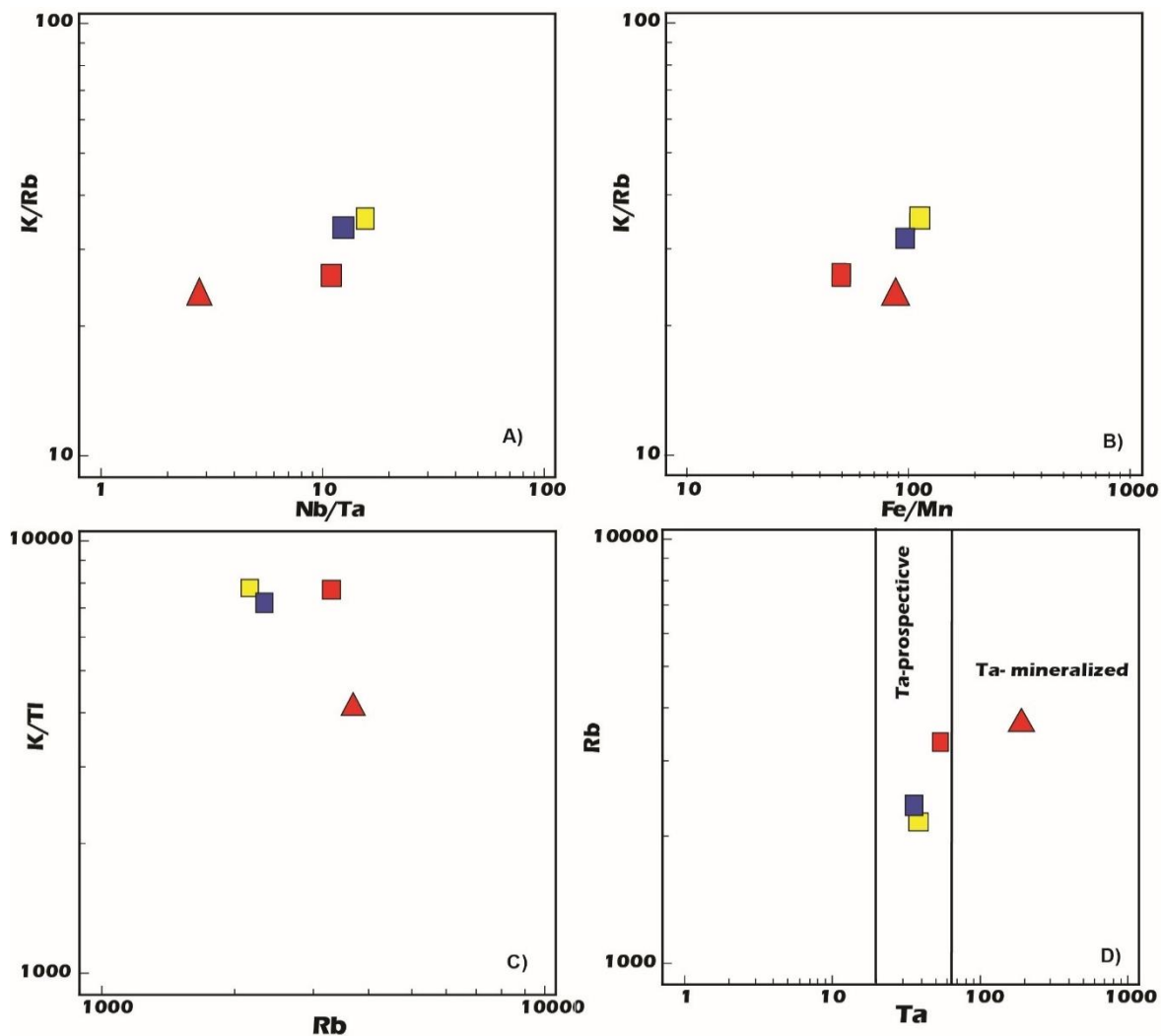
The data reveal that the chemical composition of muscovite from different location of Kilkile shows diverse chemical composition. Contents of the three major oxides are only slightly variable in the individual muscovite samples: SiO₂ (45.4–48.3 wt.%), Al₂O₃ (31.9–32.9 wt.%), K₂O (9–9.75 wt.%). The content of Fe₂O₃ show (4.25-4.69 wt. %) and MgO (0.34–0.64 wt.%). Lol also vary from (5.26-6.44 wt. %) and MgO (0.11–1.20 wt.%). Na₂O values of 0.51–0.69 wt. % might indicate the existence of a minor paragonite component.

5.2.2. Trace elements and REE

The Rb and Cs in muscovite show enrichment from Kilkile III to Kilkile I (Table 5.2). Kilkile I have also highest contents of incompatible trace elements (Ga and Ta) than Kilkile II and III. Pronounced enrichment of Rb (up to 3570 ppm) Cs (up to 240 ppm), Ga (up to 296 ppm) and Ta (up to 169 ppm) are the highest in Kilkile muscovite.

In general, the the Kilkile muscovite shows relatively high concentration of Rb, Nb, Sn Li, Ga, Cs, and Ta. The pairs element Hf and Zr, and Nb and Ta, are very similar in size and charge and show very similar geochemical behavior. Low field strength (LFS), large ion lithophile(LIL) cations include Cs, Rb, K and Ba to these may be added Sr, divalent Eu and divalent Pb these three elements have almost identical ionic radii and charge consequently show similar geochemical behavior (Rollinson, 1993).

The melt composition in granitic pegmatites is a function of K, Sr and Rb distribution in K feldspar which depend on the extent of fractional crystallization and the degree of differentiation of the parent magma before the emplacement of the pegmatite-forming melt (Larsen, 2002). Therefore, those elements and their ratio helps to infer igneous process as they are sensitive to igneous processes.



<p>LEGEND</p> <ul style="list-style-type: none"> ■ K1A2A ▲ K1B11 ◆ K2T3S1 ■ K3T2S3 	<p>Figure 5.10. Bivariate logarithmic diagrams showing chemical variation in muscovite from Kilile pegmatites: A) Nb/Ta versus. K/Rb, B) K/Rb versus. Fe/Mn, C) Rb versus. K/Tl D) Ta versus Rb (minimum Ta contents for Ta-prospective and Ta-mineralized pegmatites are from Beus 1966, and Gordiyenko 1971). N.B: Use symbols (Similar color and shaps) for all Muscovite Chemistry diagrams.</p>
---	---

The bivariate logarithmic diagrams shown in (figure 5.10) Rb shows positive correlations except for the K/Tl versus Rb plot which shows negative correlation.

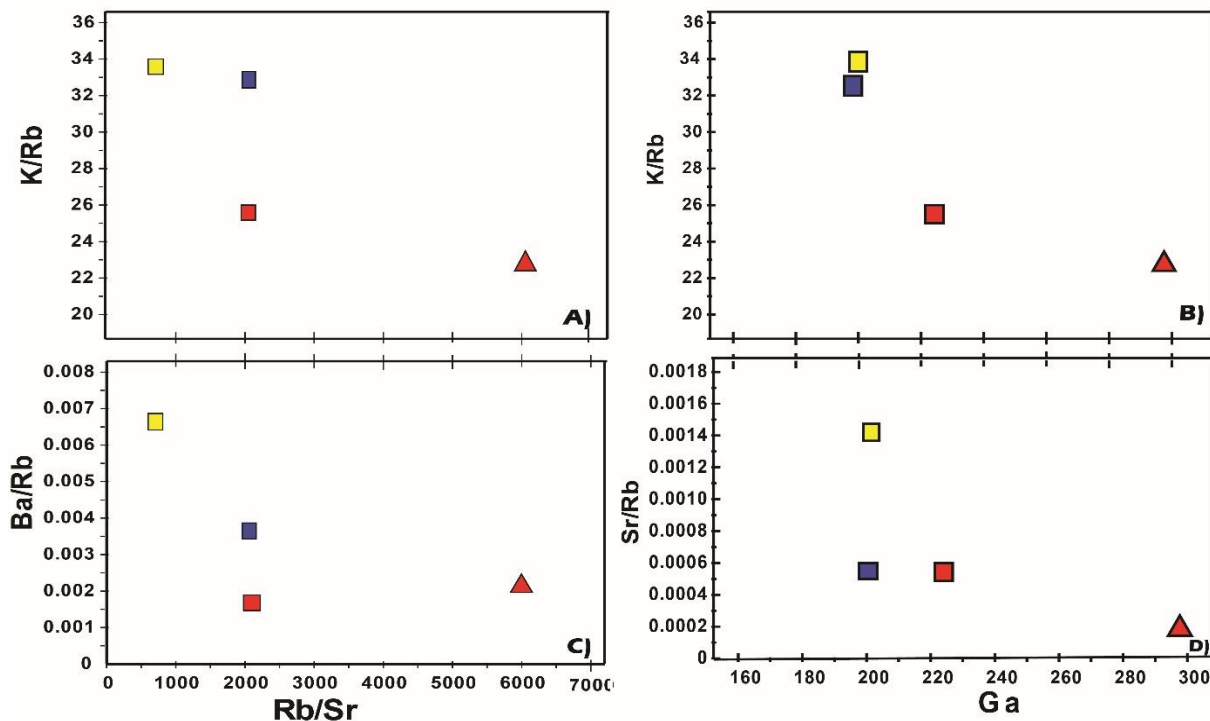


Figure 5.11. Ratio of traces element diagram. A) Rb/Sr versus K/Rb; B) Ga versus K/Rb; C) Rb/Sr versus Ba/Rb and D) Ga versus Sr/Rb. These plots help to infer the evolution of the granitic pegmatites because they are sensitive for igneous processes.

The plot of Rb/Sr ratio versus K/Rb and Ba/Rb, and Ga versus the ratios K/Rb, and Sr/Rb all show negative correlations.

Both tantalum and niobium are incompatible and lithophile high-field-strength elements (HFSE), both elements are enriched in highly differentiated in alkali granites and syenites, in carbonatites and in rare-metal bearing granitic pegmatites which develop intense electrostatic fields that strongly reduce their potential to substitute for more common elements in rock-forming minerals. This is further inhibited by high activity of complexing volatile compounds (B, C, Cl, F, P) that cause the HFS to concentrate in late liquid phases (Ballouard et al. 2016).

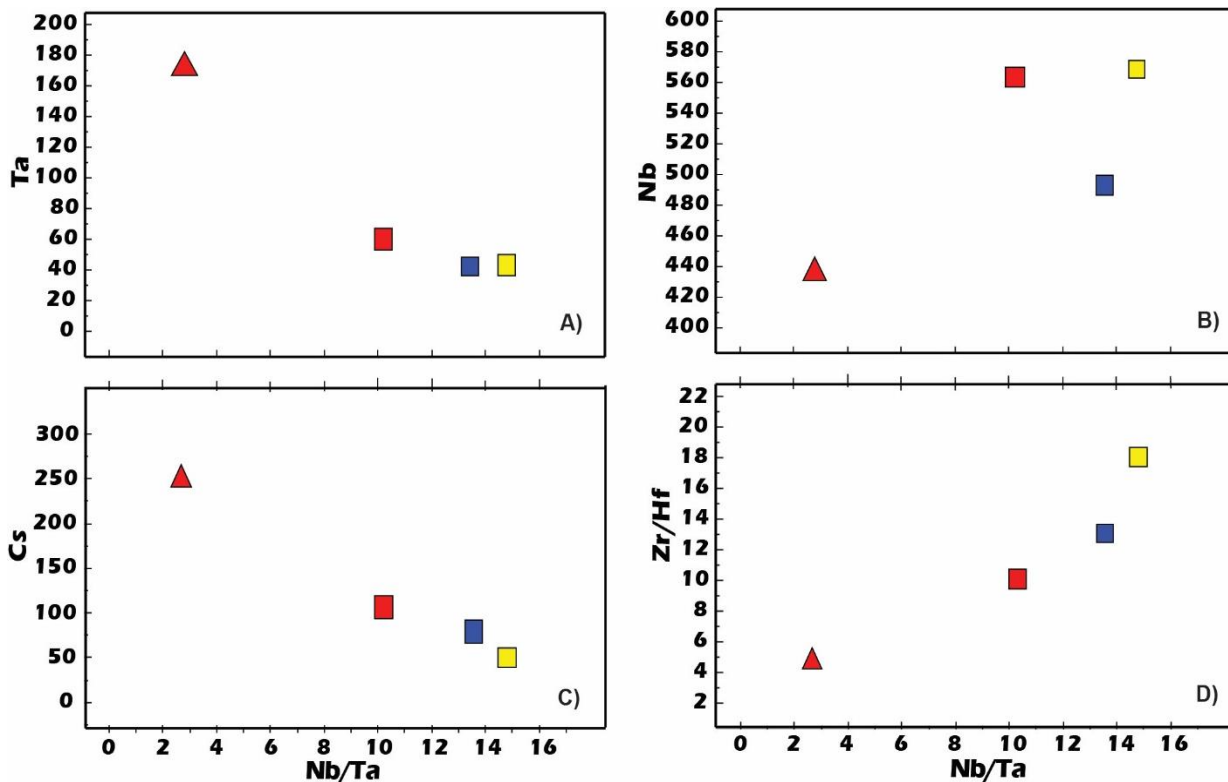


Figure 5.12. Trace element variation in muscovite samples of Kilkile area: A) Nb/Ta versus Ta; B) Nb/Ta versus Nb; C) Nb/Ta versus Cs and D) Nb/Ta versus Zr/Hf.

The Ta and Cs show linear negative correlation with Nb/Ta while the ratio of Zr/Hf versus Nb/Ta and Nb shows positive relationship.

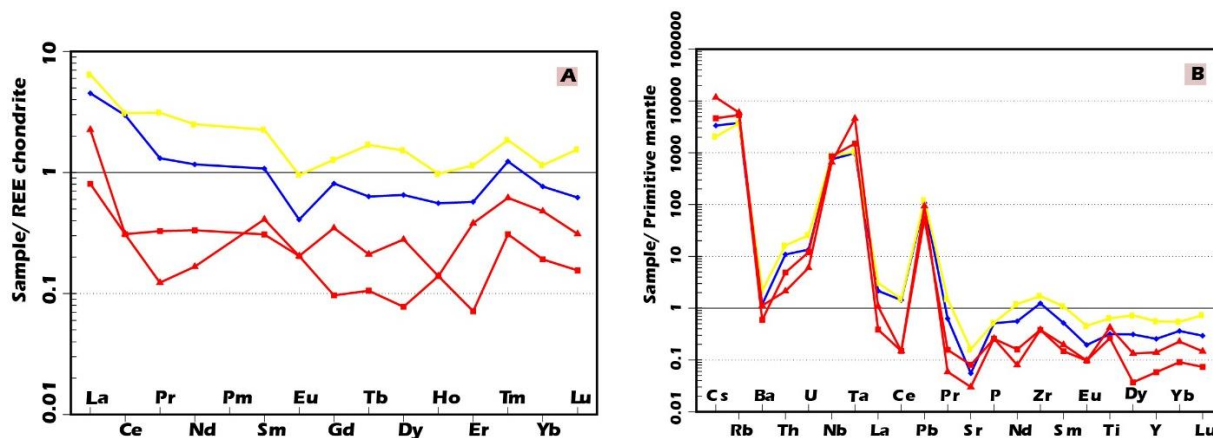


Figure 5.13. (A) Multi-element spider diagram (Sun and McDonough, 1995) and (B) Chondrite normalized REE pattern (Boynnton, 1984) of the Kilkile muscovite samples.

The trace element diagram of Kilkile muscovite show relatively higher Cs, Rb, Ta, Nb and Pb the remaining elements have relatively very low content nevertheless all the sample shows similar trend. Chondrite normalized REE pattern (Boynnton 1984) of the Kilkile muscovite sample show negative Eu anomaly.

CHAPTER SIX

6. Discussion

6.1. Geology of Kilkile rare metal deposit

Kilkile area consists a number of pegmatite veins (Fig 4.1). Some of them are mappable while others are not at the current mapping scale. Depending on their geographical location, these granitic pegmatites are divided in to three namely Kilkile I, II and III. Out of these, some of the pegmatites in the eastern part (Kilkile III and Kilkile II) have simple mineralogy like granites while those found in Kilkile I and some of Kilkile II and III pegmatites are complex. Kilkile pegmatites show columbite-tantalite minerals with different contents in different zone. According to EMPBC (1997) coarse columbite-tantalite crystals up to 5 cm in dimension were collected from the surface at Kilkile I, Kilkile II areas. Accordingly, Kilkile I and Kilkile IIC are rich in columbite-tantalite minerals.

The study area comprised various lithology that are affected by medium to low grade metamorphism. The pegmatite veins in this area have various internal structures characterized by different mineralogical assemblages and textural behavior. Degree of rare metal mineralization can be directly compared to that of the degree of fractionation, highly differentiated pegmatites are characterized by various mineralogical association, alteration features, structural complicity and zonation. As rare elements are highly incompatible elements, high content of Ta and Nb mineralization formed at last stage of magma. The final stage of rare metal forming process is developed in association with hydrothermal metasomatic minerals, such as albite, small flaky muscovite, lepidolite and, greisen. Those features are more abundant in Kilkile I than in kilkile II and III. As we go from Kilkile III to Kilkile II, the pegmatite becomes more evolved and contains high rare-metal mineralization. By inferring from their mineralogy, the Kilkile I pegmatite contains more complex mineralization relative to Kilkile III which contains mainly quartz, mica and feldspar (Fig 4.13).

The previous studies in Kenticha pegmatite near Kilkile show that the Ta content in the weathered mantle is reaching its maximum value in the zone of cleavelandite and greisen zone. Most of

Kilkile I and some of Kilkile II pegmatite shows albitization and greisenization. The concentration of columbite-tantalite increases in the zone where albitization and greisenization occurred as alteration upgrades the deposits in situ. During interaction between crystallized granites and acidic late magmatic fluids, secondary muscovitization and greisenization become prominent under sub-solidus conditions (Pirajno, 2013).

Alteration largely attracts interests of economic geologists because the altered rocks form natural halos adjacent to valuable ores, and they provide a host of valuable clues concerning the composition and physical parameters of the ore fluids (Taylor, 2009).

Pegmatite bodies in the study area developed different types of alteration. The degree and type of alteration features vary in different pegmatite veins and they may be produced by hypogene, mineral deposit formed by generally ascending solutions below surface of the earth and supergene alterations (Re-precipitation of sulphides and oxides by descending acidic ground water which has leached the surface zone of an ore deposit (Allaby, 2008). The degree of alteration varies from one vein to the other, pegmatites on the northern part of the study area is relatively more affected by alterations. Generally, alterations increase economic importance of the deposit because they accommodate economically important mineral in one specific place and by softening the hard rocks thereby making the mining expenses relatively cheaper. Therefore, columbite-tantalite crystal is expected more in Kilkile I and some of Kilkile II pegmatite whereas, minimum content of columbite-tantalite is expected in the zone where there is poor development of albitization and greisenization in Kilkile III.

6.2. Zoning

Most LCT pegmatite bodies show some sort of structural control. The specifics are a function of depth of emplacement and vary from district to district. At shallower crustal depths, pegmatites tend to be intruded along anisotropies such as faults, fractures, foliation, and bedding (Brisbin, 1986). In higher-grade metamorphic host rocks, pegmatites are typically concordant with the regional foliation, and form lenticular, ellipsoidal, or “turnip-shaped” bodies (Featherston, 2004).

Most LCT pegmatite bodies are concentrically, but irregularly, zoned (fig.6.2). Zoning is both mineralogical and textural. London (2008) identified four main zones: the border, wall, intermediate, and core.

The border zone is outer most zone, which is the contact between pegmatite and country rock. It is few centimeters thick, fine-grained, and usually composed of quartz, muscovite, and albite. Next to border zone, the wall zone follows, it covers less than or about 3-m thick, with crystals up to 30 cm large occasionally. The essential minerals are albite, perthite and muscovite. Graphic intergrowths of perthite and quartz are also common. Wall zones are mined for muscovite, tourmaline and occasionally beryl may also be found. Feldspars, micas, and quartz are essential minerals. Beryl, spodumene, elbaite, columbite-tantalite, pollucite, and lithium phosphates may also be available in more evolved LCT pegmatites, and the grain size becomes coarser than in the wall zone. At the central or core zone quartz is the dominant mineral but, in some case, quartz is joined by perthite, albite, spodumene or other lithium aluminosilicates, and (or) montebrasite and columbite-tantalite.

Nine boreholes were used for both Geochemical and petrological analysis from those three representative boreholes from each locality are shown below which shows zonation. From the mineralogical assemblages of kilkile borehole, albite is more common in the border and wall zones, feldspar and mica become dominant in the intermediate zone while quartz is dominant in the core zone (Figure 4.2). Fluxing components and some incompatible elements increase towards the center of the magma chamber resulting in increasing chemical fractionation from the margin to the center of the pegmatites (Cameron, 1949)

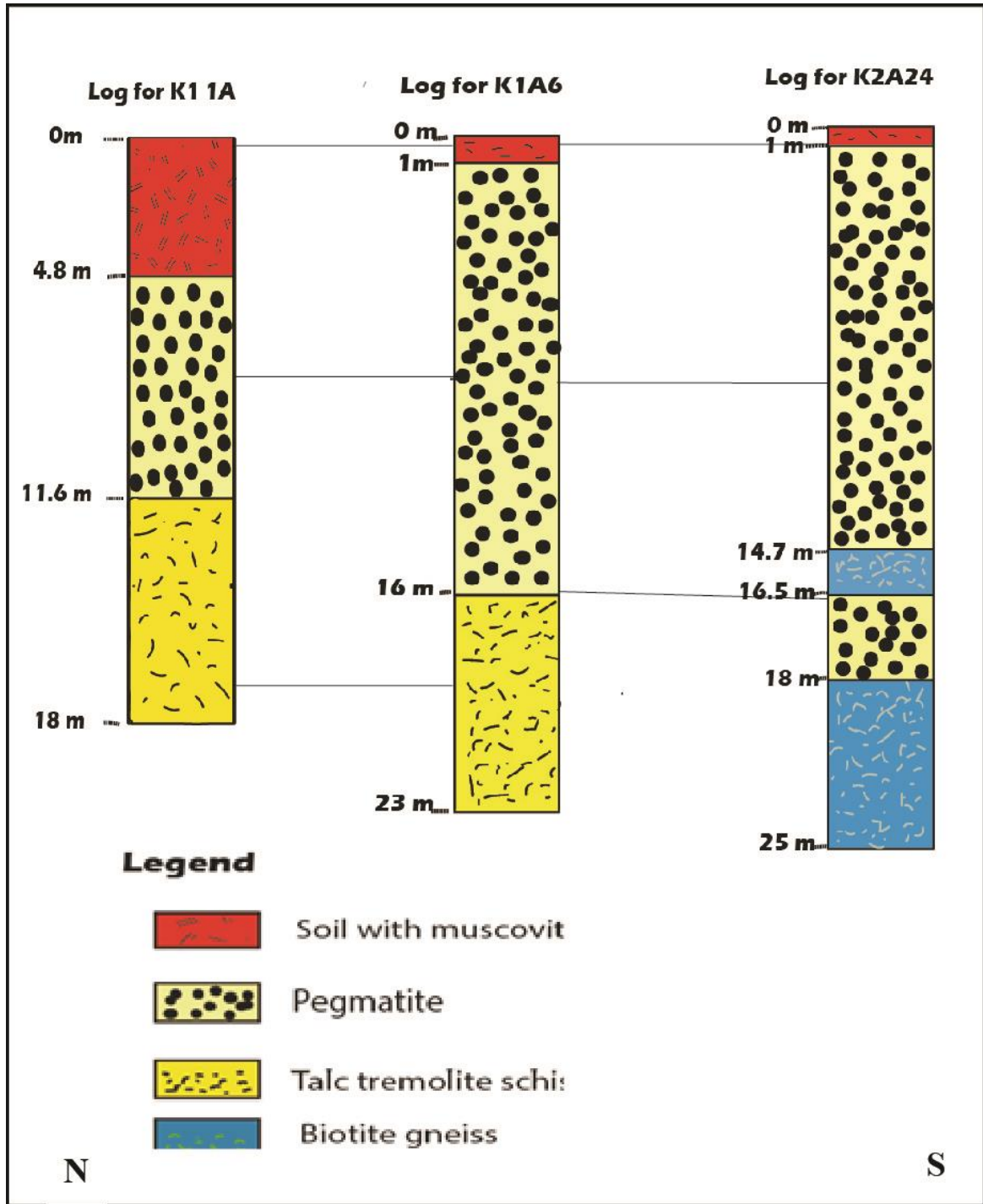


Figure 4.1. Borehole log of Kilkile I and II area.

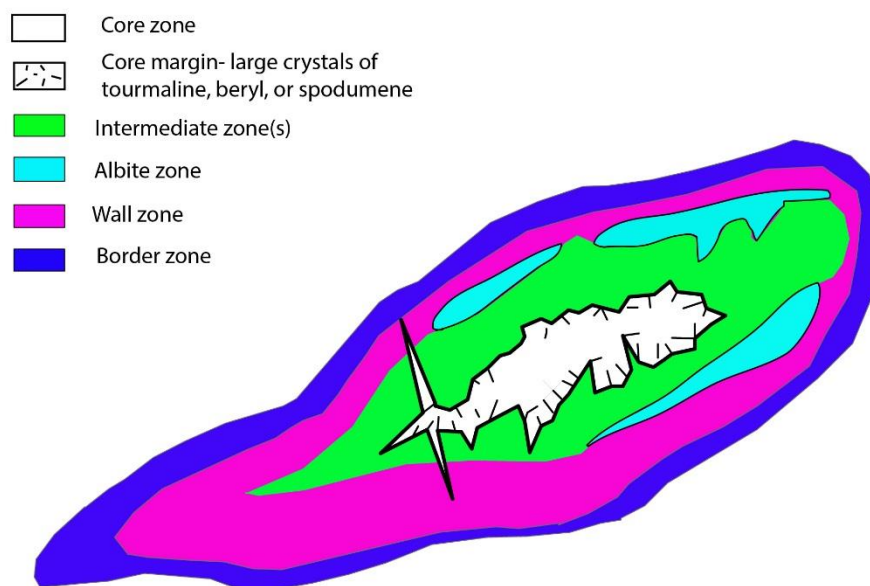


Figure 6.2. Deposit-scale zoning patterns in an idealized pegmatite, redrafted from Fetherston (2004) and Černý (1991).

6.3. Whole-rock geochemistry

6.3.1. Major elements

The above writer further illustrates that fractionation of alkali – feldspars will lead to the removal of Rb from the liquid where Rb is accommodated. Therefore, if there is decreasing of Rb with increasing SiO_2 , it indicates feldspar fractionation. Strontium preferentially enters the plagioclase structure or other Ca bearing phases and shows a negative correlation. Therefore, Sr fall is attributable to removal of feldspar and apatite. Vanadium is similar to TiO_2 , in which its fall is related to Fe–Ti oxide fractionation. The decreasing pattern of Nb is related to fractionation of sphene (Rollinson, 1993).

During partial melting P is concentrated in the melt because it is incompatible in mantle mineralogy. In granites, however, even though P is present as a trace element, it is compatible because it is accommodated in the structure of the minor phase apatite (Rollinson, 1993). Enriched Li, Rb, Cs, Ga, and Ta, low P_2O_5 contents of the pegmatite are akin to rare-metal granitoids of the low- to intermediate-P type (Küster et al., 2009). SiO_2 versus P_2O_5 diagram shows Kilkile granite pegmatite consists low P_2O_5 value (Fig. 5.3C).

In $\text{Al}_2\text{O}_3/\text{CaO}+\text{Na}_2\text{O}+\text{K}_2\text{O}$ versus SiO_2 and $\text{Al}_2\text{O}_3/\text{CaO}+\text{Na}_2\text{O}+\text{K}_2\text{O}$ versus SiO_2 diagrams, the granitic pegmatite plot is entirely within the field of S-type granitoids (Figure 5.4A and B). This suggests that the granites probably derived from the anatexis of schist or aluminous gneisses of sedimentary origin that is rich in rare metals.

6.3.2. Trace elements

Kilkile rare metal pegmatites are typically hosted by metavolcanics or metasedimentary rocks, and are located near peraluminous granite plutons ($A/\text{CNK} > 1.0$). After identifying peraluminous pegmatite pluton, next task will be whether the pegmatite is fertile or barren. According to Selway et al. (2005) fertile granites contain higher rare element contents, Mg/Li ratio less than 10, Nb/Ta ratio less than 8 and commonly they contain blocky K-feldspar and green muscovite. The presence of tourmaline, beryl, and ferrocolumbite; and Mg/Li (<10) and Nb/Ta (<10) ratios in bulk granite samples indicates the fertility of granitic pegmatite. Most of Kilkile I and some of Kilkile II pegmatite fulfill the above criteria (Table 4.1).

Incompatible elements which belong to the group Cs, Sr, K, Rb, Ba are mobile, whereas the HFS elements are immobile. This latter group includes the REE, Sc, Y, Th, Zr, Hf, Ti, Nb, Ta and P (Pearce, 1983). Key fractionation indicators incompatible elements, especially the immobile ones plotted to determine the fractionation direction. Fertility increases while we go from least to high fractionated pegmatite. In this sense, Kilkile III pegmatites are relatively least fractionated while Kilkile I pegmatite is relatively highly fractionated. Kilkile II is placed in the middle position and this can be observed on both whole rock diagrams. On the other hand, samples from boreholes were analyzed in order to identify differentiation direction. Even though those samples are not sufficient to get better result, they can give some clue about differentiation. Fractionation increases from surface to center(core) part of Kilkile one and two pegmatite specifically on K1B and K2A pegmatite occurrences (Fig 5.6 and 7).

The trend of Sr and Ba indicates the differentiation process and removal of feldspar (Rollinson, 1993). Rb-Ba-Sr plot (El Bouseily and El Sokkary, 1975) indicates a granitic trend typical of strongly differentiated granites with Rb enrichment and low Ba and Sr contents for whole-rock analyses of the Kilkile rock samples (Figure 6.1).

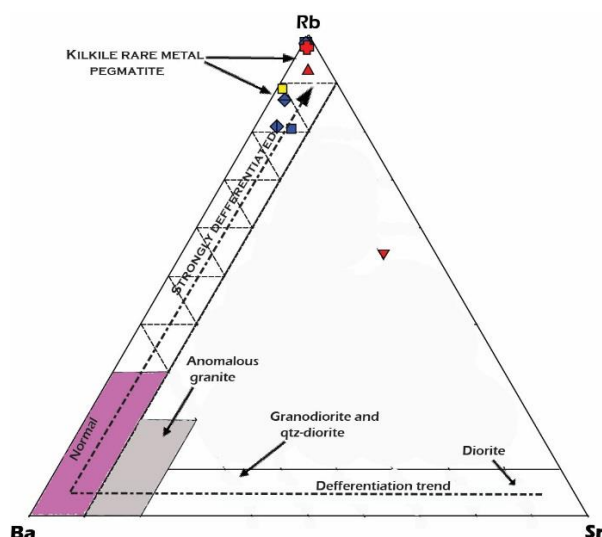


Figure 6.3: Differentiation indicator triangular plot of Rb-Ba-Sr (El Bouseily and El Sokkary, 1975) for granitic rocks.

6.3.3. REE pattern

The REE pattern of an igneous rock is controlled by the REE chemistry of its source and the crystal-melt equilibria which have taken place during its evolution (Rollinson, 1993). According to the above writer relative to other magmas, in felsic magmas, europium anomalies are mainly controlled by feldspars. Thus, the removal of feldspar from a felsic melt by crystal fractionation or the partial melting of a rock in which feldspar is retained in the source will give rise to a negative Eu anomaly in the melt. Almost all samples of the Kilkile area show high to moderate negative Eu anomalies which indicates the removal of feldspar from the melt by crystal fractionation. In felsic liquids, accessory phases such as sphene, zircon, allanite, apatite and monazite may strongly influence REE pattern (Rollinson, 1993).

LCT pegmatite displays moderately to slightly HREE-depleted patterns and low REE abundances and negative Eu anomaly is occasionally well expressed but in most cases absent (Černý, 1997). The chondrite-normalized REE pattern of Kilkile area (Figure 5.9; Boynton, 1984) indicates all the analyzed pegmatite rocks samples display slightly enrichment in light rare earth element (LREE: La, Ce, Pr, and Nd) relative to heavy rare earth elements (HREE: Er, Tm, Yb and Lu).

6.4. Muscovite chemistry

The distribution of trace elements can be used to identify geological processes and to test hypotheses. These elements are often studied in groups because trace elements have their own group and these respective groups have similar chemical properties. Therefore, they show similar geochemical behavior. Consequently, deviations from group behavior or systematic changes in behavior within the group are used as indicators of petrological processes (Rollinson, 1993). The element pairs Hf and Zr, and Nb and Ta, are very similar in size and charge and show very similar geochemical behavior that is why they form very good linear correlation (Figure 5.6 for Hf versus Zr and 5.12 for Nb versus Ta). Low field strength, large ion lithophile cations include Cs, Rb, K and Ba. They also have similar geochemical behavior. These elements increase while fractionation increases (Table 5.2). Sr, divalent Eu and divalent Pb - three elements with almost identical ionic radii and charge (Humphries, 1984). On Kilkile pegmatite those three elements decrease while fractionation increases.

The larger the ionic radii the more incompatible, the higher the ionic charge the more incompatible on this sense Cs, Rb, K, Nb and Ta concentration should be higher during fractionation similarly, the study area, from muscovite samples, comprises elevated amount of the above elements.

The muscovite samples ratio of Nb/Ta decrease during magmatic fractionation of a granitic melt. The decrease of Nb/Ta in columbite–tantallite and of Zr/Hf in zircon is consistent with fractionation of a silicate melt (Linnen and Keppler, 2002). Ta content increases while fractionation increases opposing to Nb, Nb content decreases on the last stage of magma evolution. From the study area muscovite samples, the highest Nb/Ta ratio is obtained in Kilkile III and the lowest figure obtained in the Kilkile I. This indicates Kilkile I pegmatite is highly evolved and has more rare metals than Kilkile II and III. Similarly, LIL elements like Cs, K and Rb concentration increases from Kilkile III to Kilkile I, accordingly, the ratio of Zr/Hf decreases from Kilkile three to Kilkile one.

K-feldspars and mica are the most important carriers of Rb in granitic pegmatite, Cs is only reluctantly admitted in to K-rich phase (Cerny, 1982). Ta and Nb are highly incompatible in quartz and feldspar; thus, their bulk distribution coefficients are typically very small. However, they are compatible in muscovite and partition strongly into Ti-bearing minerals, notably rutile and titanite

(Linnen and Cuney 2005). The Ta content of muscovite has been used as an exploration tool, and pegmatites that contain muscovite with greater than ~80 ppm Ta are considered to have economic potential for Ta (Černý, 1989). According to Beus (1966) and Gordiyenko (1971), the Ta content in muscovite should be above 20 ppm to be called Ta-prospective and called Ta-mineralization if it contains above 65 ppm of Ta. Ta contents in muscovite from the Kilkile pegmatite occurrences are all above the critical value of 20 ppm used in exploration to identify Ta-prospective pegmatites (Figure 5.10D). Muscovite from Kilkile I typically fall or above the limit of 65–70 ppm used to indicate Ta-mineralization whereas muscovite from Kilkile III and II falls within Ta-prospect region.

The role of fluids is still a matter of debate. London (1986) supposed that although hydrothermal fluids may not play a critical role in the transport of Ta, they may nevertheless be important in controlling mineralization by adding to the melt the divalent cations Fe, Mn, and Ca, which are essential components of columbite–tantalite-(Fe, Mn), wodginite ($\text{MnSnTa}_2\text{O}_8$), and microlite ($[\text{Ca, Na}]_2\text{Ta}_2\text{O}_6[\text{O, OH, F}]$). Tantalum minerals are also intimately intergrown with apatite and zircon, suggesting that the crystallization mechanism for different HFSE minerals may be interrelated (Černý et al. 2007). Metasomatized host rocks are an indication of a nearby rare-element pegmatite. Metasomatic aureoles can be identified by their geochemistry: elevated Li, Rb, Cs, B, and F contents; and by their mineralogy: presence of tourmaline, (Rb, Cs)-enriched biotite, holmquist, muscovite, and rarely garnet (Selway et al., 2005). Most of this criterion are fulfilled by Kilkile I and some Kilkile II muscovite (EMBPC, 1997 and Table 5.2).

Pegmatites with Ta mineralization usually contain Li-rich minerals (e.g., spodumene, petalite, lepidolite, elbaite, amblygonite, and lithiophilite) and may contain Cs-rich minerals (e.g., pollucite, Cs-rich beryl) (Selway et al. 2005). Kilkile pegmatite has relatively high concentration of Rb, Nb, Li, Ga, Cs, and Ta. Rare-element pegmatites may host several economic commodities, such as tantalum as Ta-oxide minerals, lithium as ceramic-grade spodumene, tin as cassiterite and petalite, and cesium as pollucite. While fractionation increases, the content of Rb/Sr ratio increases whereas the ratio of K/Rb and Ba/Rb decreases. Similarly, the content of Ga shows enrichment during fractionation, whereas the ratio of K/Rb and Sr/Rb decreases while the fractionation increases (Figure 5.11).

Kilkile muscovite's trace elements also show fractionation-related depletion and enrichment features. For example, high field strength element (HFSEs) U, Th, Pb, Y, REE, and Nb and Zr becomes depleted while Zn enriched with increasing fractionation (Table 5.2). Fractionation indicators of Nb/Ta versus K/Rb and Fe/Mn versus K/Rb shows positive correlation. Nb/Ta, Fe/Mn and K/Rb content decreases while fractionation increases. This reveals that the least differentiated part in the study area is Kilkile III where as Kilkile I pegmatite is highly differentiated (Fig. 5.10). This suggests that crystallization and solidification of the leucogranite to pegmatitic melt progressed mainly from Kilkile III the south to Kilkile I to the North

Systematic enrichment and depletion of incompatible trace element and a well-correlated suite the K/Tl versus Rb diagram (Figure 5.10) muscovite analyses from the Kilkile I Kilkile II and Kilkile III pegmatites shows progressive shifts from the least evolved Kilkile III to high evolved Kilkile I, the Rb content also increase from Kilkile III to Kilkile I due to increasing fractionation (Figure 5.10.), and the correlation of this diagram infers a cogenetic formation of all pegmatites in the study area from a common magma source. Muscovite chemistry (Fig. 5.11, 5.12 and especially 5.13) tells each pegmatite rather represents a separated batch of fractionated melt, with a common source but with individual fractionation histories and local inhomogeneities regarding trace element composition and accessory mineralogy.

The chondrite-normalized REE pattern of Kilkile area muscovite also shows (Figure 5.13; Boynton, 1984) that all the analyzed pegmatite rock samples display slight enrichment in light rare earth element (LREE) contents relative to heavy rare earth elements (HREE). However, all samples show more or less similar trend. This is also observed in trace element diagram and this consistency indicates that Kilkile pegmatites (I, II, and III) are sourced from the same magma source have similar petrogenetic process. The Kilkile muscovite Multi-element spider diagram Sun and McDonough (1995) shows similar trend to the whole rock multi-element spider diagram. Although REE contents basically decrease with increasing fractionation of the parental melt, total REE in Kilkile I are higher than total REE in Kilkile II and total REE in Kilkile II are higher than total REE in Kilkile III (table 5.2).

6.5. Comparison of pegmatites in the Adola belt

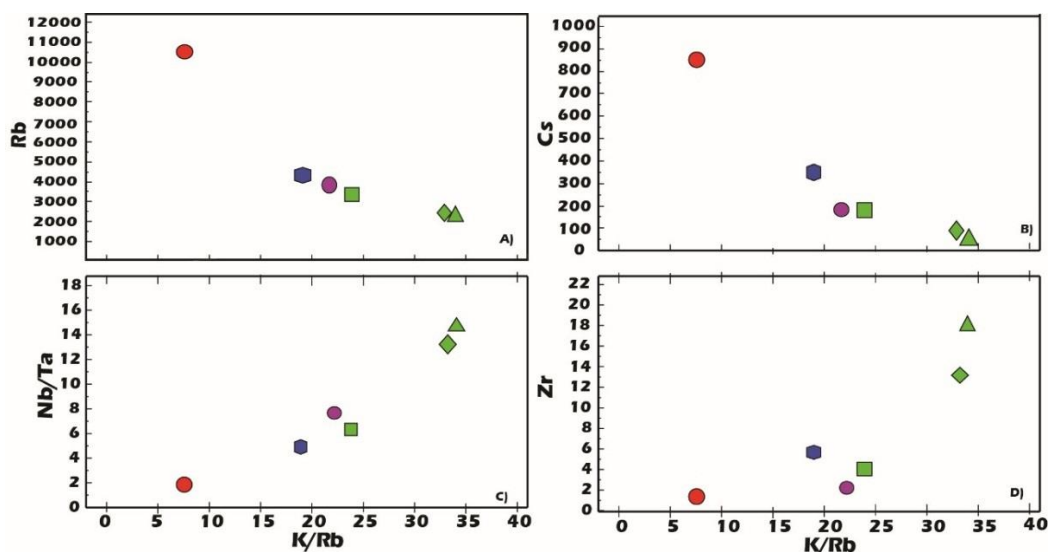
In addition to Kilkile area pegmatites, there are also a number of pegmatite veins in the fields of the Kenticha belt. Those pegmatites vary in size, fractionation as well as chemical composition. These include Bupo, and Shuni Hill, Kenticha, Kilkile and other granite pegmatite fields. Using U–Pb dating, the Kenticha pegmatite and the Bupo (9 km to the North of Kenticha) pegmatite were both emplaced around 530 Ma (Küster et al., 2009).

Samples	Kilkile			Shuni Hill	Kenticha	Bupo
	Kilkile III	Kilkile II	Kilkile I			
ICP-AES (Major oxides (wt.%))						
SiO ₂	45.5	48.3	45.9	46.7	48.64	45.4
TiO ₂	0.12	0.06	0.065	0.18	0.088	0.03
Al ₂ O ₃	32.9	31.9	32.55	32.6	31.87	36.4
Fe ₂ O ₃	4.57	4.25	4.54	3.06	1.33	0.96
MnO	0.04	0.04	0.065	0.08	0.197	0.24
MgO	0.64	0.34	0.5	1.25	0.63	0.05
CaO	0.05	0.01	0.01	0.01	0.042	0.03
Na ₂ O	0.51	0.57	0.675	0.52	0.55	0.66
K ₂ O	9.09	9	9.685	9.92	9.45	9.59
P ₂ O ₅	0.01	0.01	bdl	0.01	0.024	0.03
Lol	6.44	5.44	5.265	4.64	4.68	4.94
Total	99.87	99.92	99.25	94.33	92.82	93.39
ICP-MS (Trace element (ppm))						
Ba	14.4	7.8	5.65	111	10.33	7
Cs	42.8	70.2	171.65	166	338.3	838
Ga	205	199.5	259.5	233	228.9	283
Hf	1	1	0.6	0.5	0.92	0.3
Nb	567	491	497	407	346	144
Rb	2230	2260	3385	3600	4200	10395
Sn	316	355	238.5	322	169.9	205
Sr	3.2	1.1	1.1	12	11.6	22
Ta	38.7	36.5	112.4	75	82.1	90
Th	1.3	0.87	0.28	4.3	6.03	12
U	0.51	0.27	0.18	0	0.23	0
W	8	6	49.5	6	24.9	5
Zr	18	13	4	2	5.59	1.1
Li	310	250	665	840	2961	1773
Tl	10	10	15	12	15	45
Zn	192	304	380.5	297	661.5	636
K/Rb	33.82	33.04	23.8	22	18.9	7.4
K/Cs	1762.3	1063.8	574.6	619	380.8	92
K/Tl	7542.8	7468.1	6013.9	6716	5353.1	1,715
Rb/Tl	223	226	249.25	300	282.7	231
Nb/Ta	14.65	13.45	6.31	7.5	4.76	1.6
Fe/Mn	103.23	96	66.162	48.3	14.58	4.1
Mg/Li	12.38	8.16	4.87	13	4.05	5.6
Zr/Hf	18	13	7.5	3.9	5.8	4.3

Table 6.1. Average major and trace element composition of muscovite from Kilkile (I, II, III), Kenticha, Bupo and Shuni, pegmatites. Major elements in weight % (wt.%) and trace elements in parts per million (ppm). All the above secondary data (Kenticha, Bupo and Shuni hill muscovite composition) is taken from Küster et al., (2009).

The Bupo pegmatite is highly weathered and shows relatively simple zoning than the complex spodumene-type main Kenticha pegmatite, and is classified as Albite-Spodumene type (Zerihun et al., 1995; Solomon and Zerihun, 1996). Regionally, the fractionation trend, increases from list fractionated Kilkile III and Kilkile II to SKK (Shuni Hill, Kilkile I and Kenticha pegmatite) then further fractionated Bupo.

Muscovite from different area of Kenticha belt shows diverse chemical composition. The contents of the SiO₂ slightly vary in individual muscovite samples (45.4 in Bupo to 48.64 wt.% in Kenticha), Al₂O₃ (31.87 in Kenticha to 36.4 wt.% in Bupo), K₂O (9 wt.% in Kilkile II to 9.92 wt.% in Shuni hill). The content of Fe₂O₃ is relatively very small in Kenticha next to Bupo whereas all Kilkile have relatively higher value. The MgO content relatively small in Bupo (0.05wt. %) higher in Shuni hill (1.25wt.%). In the Kilkile muscovite, the rare alkali elements Rb and Cs show enrichment from Kilkile III to highly differentiated Bupo (Fig. 6.4). Pronounced enrichment of Rb (up to 10395 ppm in Bupo), Nb (up to 567 in Kilkile III) and Cs (up to 838 ppm in Bupo) whereas Ga (up to 283 ppm in Bupo) and Ta (up to 112.4 ppm in Kilkile I) are the highest from the above four occurrences in the Kenticha belt.



LEGEND
 ■ KILKILE I
 ▲ KILKILE III
 ◆ KILKILE II
 ■ KENTICHA
 ● SHUNI HILL
 ● BUPO

Figure 6.4. Bivariate plots showing geochemical variation in muscovite samples from Kenticha, Bupo, Shuni Hill, and Kilkile (I, II and III) pegmatites A) K/Rb Vs. Rb B) K/Rb Vs. Cs C) K/Rb Vs. Nb/Ta D) K/Rb Vs. Zr. N.B: Use symbols (Similar color and shapes) for all comparison Muscovite chemistry diagrams.

Fractionation indicates the ratio of K/Rb versus Nb/Ta, K/Rb versus Zr (Figure 6.4) and Rb versus Tl (Fig. 6.5) shows positive correlation, but those two are reverse in fractionation, which means that the ratio of K/Rb versus Nb/Ta and K/Rb versus Zr, decreases while fractionation increases. However, in Rb versus Tl diagram, fractionation increases while their content increases. K/Rb versus Rb and K/Rb versus Cs, shows negative correlation. While the fractionation increases the ratio of K/Rb content decreases, but Ta and Cs content increases from least evolved (Kilkile III muscovite) to most fractionated (Bupo muscovite, Table 6.4). But Ta content is higher in Kilkile I than further differentiated Bupo pegmatite. This might be lateral hydrothermal activity (Fig. 6.5).

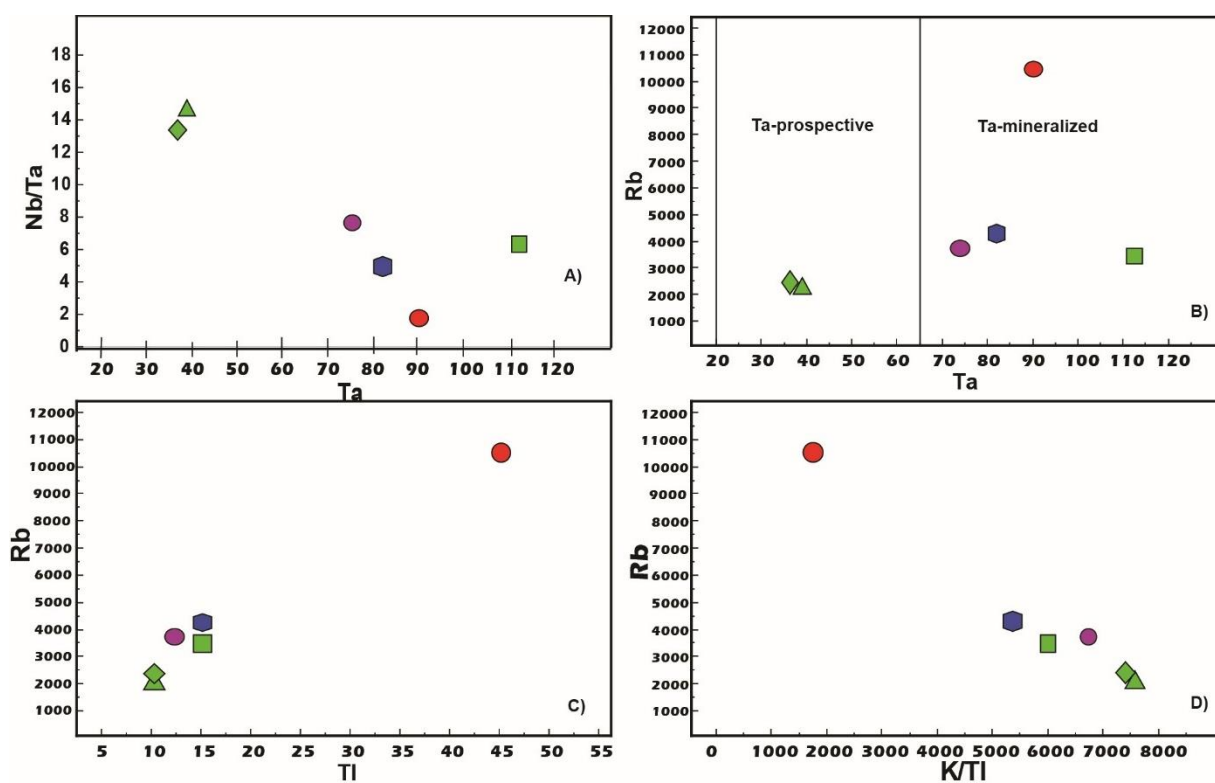


Figure 6.5. Bivariate diagrams showing chemical variation in muscovite from Kenticha, Bupo, Shuni, and Kilkile (I, II and III) pegmatites: A) Ta versus Nb/Ta B) Ta versus Rb (minimum Ta contents for Ta-prospective and Ta-mineralized pegmatites are from Beus 1966, and Gordiyenko 1971); C) Tl versus Rb D) Rb versus K/Tl.

In the Rb/Tl and Rb versus K/Tl diagram (Fig. 6.5) muscovite analyses from the Kilkile I, Kilkile II and Kilkile III Shuni, Kenticha and Bupo pegmatites form a well-correlated suite. The Rb/Tl ratio shows progressive shifts from the least evolved Kilkile III to highly evolved Bupo; the high Rb versus Tl and Rb versus K/Tl correlation refers to a co-genetic formation of all pegmatites.

Coherent Rb/Tl ratios in muscovite from Kenticha, Bupo, Shuni Hill, and Kilkele II pegmatites suggest a co-genetic formation of parts (Küster et al., 2009). By using Beus (1966) and Gordiyenko (1971), criteria all area samples (Kilkile I, Bupo, Kenticha and Shuni hill) except Kilkile II and III are under Ta-mineralization zone which is considered as economic for mining company.

6.6. Genesis and parageneses of Kilkile rare metal deposit

6.6.1. Genesis of Kilkile tantalite deposit

Mineralization as markers of the transition between primary magmatic fractionation and secondary hydrothermal-metasomatic replacement processes. Pegmatitic ores are endogenic. They are deposited within the igneous body from which they originate (Linnen et al., 2012). According to London and Morgan (2012), fractional crystallization of the melt and interaction of aqueous fluid with the melt are the two competing models for the formation of rare-element granitic pegmatites. These elements are formed mainly by fractional crystallization of a granitic melt in the magmatic process (Černý et al., 1992 and Linnen et al., 2011). These processes are very unusual because they contain high concentrations of fluxing compounds, which play key roles at both the primary magmatic and metasomatic stages (Cameron, 1949).

Geotectonic discrimination diagrams technique is used for classifying samples into groups of WPG, Syn-COLG, volcanic-arc granites (VAG) and ocean-ridge granites (ORG). Kilkile area pegmatite sample mainly lies within Plate Granites (WPG) (Figure 5.5) on which the granite pegmatite is probably sourced from in-situ partial melting of the meta-sedimentary rocks in the area (Bongiolo et al., 2016; Simmons, 2007).

The collision of two continental crusts (orogeny), increases basal heat flow beneath the earth surface and causes partial melting of the pre-existing meta-sedimentary rocks by ascending magmatic intrusion forms felsic magma during the ascent of the magma fractional crystallization and assimilation with the country rocks. This modifies the composition of the magma and results in different zonal mineral assemblages, geochemical variations as well as rare metals mineralization. Garnet in the study area shows relict texture. The relict textures in minerals such as relict of garnet in the studied samples can suggest for anatectic origin of granitic pegmatite (Simmons et al., 1995).

The Kilkile pegmatites are depleted in Eu, Ba and Sr and are rich in Rb, Nb, Ta, Hf and Cs (Table 5.2) with negative Eu anomaly (Fig 5.9 and 5.13). The significant depletion in Eu, Ba and Sr, and enrichment in Rb, Nb, Ta, Hf and Cs, and strong negative Eu anomaly on the REE patterns show that the fractional crystallization must occur within the crust, or that the magma must originate from partial melting of the continental crust (Li et al., 2015; Mi et al., 2015).

S-type (rich in B, P and F, derived from micas), mineral assemblages constitute of muscovite, garnet, cordierite, sillimanite or andalusite, tourmaline and gahnite (Chappell and White, 2001) and derived by partial melting of sedimentary and meta-sedimentary rock (Farahat et al., 2007). The Kilkile pegmatite is also S-type of granite (Fig. 5.3). They are peraluminous characterized by the presence of typical minerals such as muscovite, quartz feldspar group minerals, garnet, tourmaline and others accessory minerals.

The classification is made by Cerny and Ercit (2005) recognizes LCT (Li–Cs–Ta), NYF (Nb–Y–F), and mixed families of pegmatites. Pegmatites of the LCT family are strongly correlated with S-type granites, derived by partial melting of sedimentary and meta-sedimentary rock, they are peraluminous granites characterized by the presence of typical minerals such as muscovite, biotite and marginally elevated SiO₂ contents whose ultimate protoliths can be traced to chemically mature sedimentary sources, such as marine shales (London, 2012). The above writer further stated that in contrast to peralkaline and carbonatite melts, peraluminous melts are generated in orogenic settings (syn- to late tectonic) (London, 2005).

The pegmatites of the Kenticha field can temporally be related to the 550–520-Ma post-collisional phase of granitic magmatism in southern Ethiopia (Yibas et al. 2002). Küster et al. (2009) also stated that U–Pb dating of Mn-tantalite from Kenticha and Bupo pegmatite gave the same age i.e both were emplaced around 530 Ma. The above writer further stated that, coherent Rb/Tl ratios in muscovite from Kenticha, Bupo, Shuni Hill, and Kilkele II pegmatites as observed in this research too, all four area pegmatites are from a common magma source. Therefore, the Kilkile pegmatite is also expected to have similar age to Kenticha and Bupo or near to 530 Ma. As discussed in chapter two of this study, the East Africa Orogeny (EAO) represents a plate tectonic starting around 900 Ma, ending by about 550 Ma, (Vail, 1985; Berhe, 1990; Abdelsalam and Stern, 1996).

Thus, it can be deduced that the Kilkile pegmatite is formed after or near to the cease of East African Orogeny.

Taking also the coherent muscovite chemistry of REE diagram (Fig. 5. 13) show more or less similar trend which indicates those three-area pegmatites have similar petrogenetic process. However, Kilkile I, II, and III each of them shows distinct mineralogically different. These differences may result from formation of rare metals in different zone and at different stages of fractionation within the pegmatite(s) then these pegmatites rather represent a separated batch of fractionated melt, with a common source. Muscovite REE patterns also shows that those three-zone pegmatites have distinct amount. Kilkile I, shows very low REE than Kilkile II and Kilkile II shows lower REE than Kilkile III. This shows chemical evolution of rare metals. REE contents basically decrease with increasing fractionation of the parental melt. Very low REE can be found in the most fractionated parts of pegmatite (Kuster et al., 2009). This may also suggest that crystallization occurred distinctly.

Tin (Sn) is highly mobile at the magmatic-hydrothermal transition which is a good marker for magmatic fractionation and hydrothermal-metasomatic alteration. Therefore, enrichment in Sn, K/Rb values less than 150 (Shaw, 1968) and the ratios Zr/Hf ($< \sim 18$) with the corresponding low content of Nb/Ta (< 5) for rare metal granites are a good marker for magmatic-hydrothermal interactions (Ballouard et al., 2016). Ballouard also stated that magmatic differentiation and fractional crystallization decrease Nb/Ta ratio. Nb is slightly more mobile than Ta, suggesting that magmatic-hydrothermal processes account for the decrease of the Nb/Ta ratio to $< 5\%$ in peraluminous granites that may be related to Ta, Cs, Nb, Be, Sn and W mineralization (Ballouard et al., 2016).

The above criteria are fulfilled in most of Kilkile I and some of Kilkile II samples. Zr/Hf value starts from 18 on Kilkile three and becomes 13 in Kilkile II and finally it reaches up to 5 in Kilkile one. K/Rb value ranges from 22.66 to 33.82. Both Kilkile III and Kilkile II samples Nb/Ta ratio content is above 5 but in Kilkile I sample, it is below arbitrary number 5. This is also associated with an increase in secondary muscovitization and greisenization and can be a good marker for magmatic-hydrothermal transition in peraluminous granites. Textural attributes of tantalum minerals. I.e., magmatic growth zonation, euhedral grain shape, intergrowth with magmatic phases

such as K-feldspar, spodumene, coarse albite, quartz, and spessartine garnet, also support a magmatic origin (Küster et al., 2009).

Muscovite samples of Kilkile area show the decrease in Nb/Ta, Zr/Hf, K/R ratios. This can be an evidence for enrichment in rare metals. Therefore, the formation of Kilkile pegmatite is also magmatic. During magmatic differentiation, content of some elements decreases while content of other elements increases. Therefore, both magmatic and hydrothermal meta-somatic activities play great role in Kilkile rare metals accumulation.

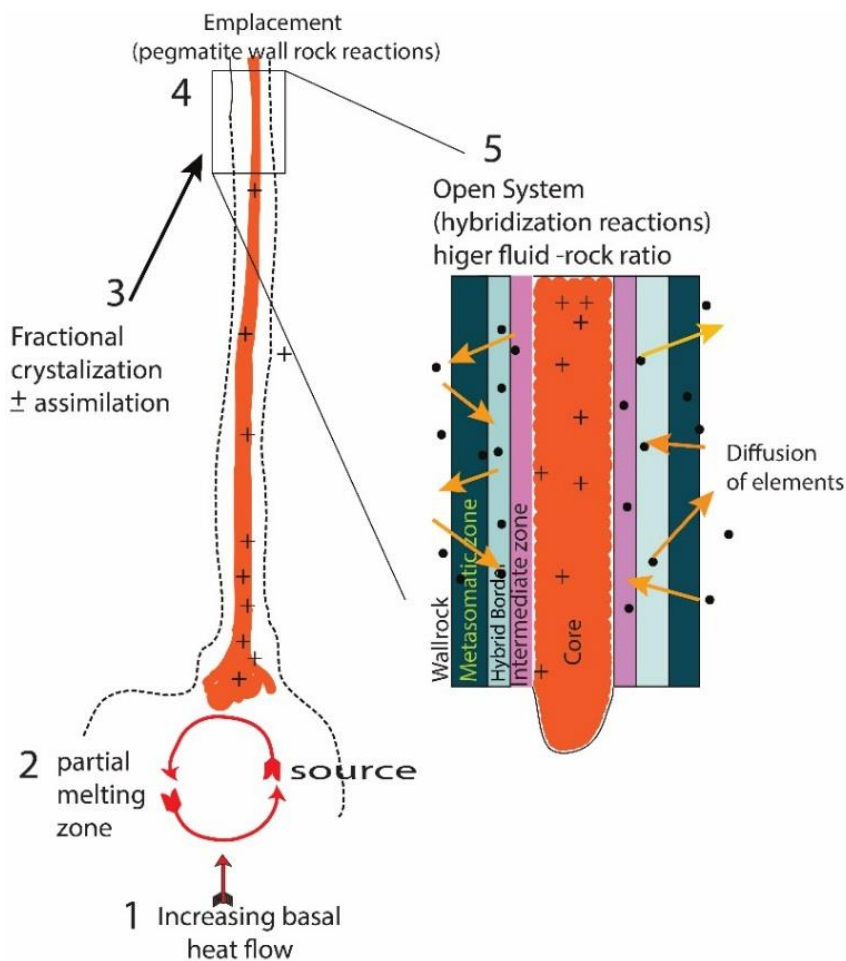


Figure 6.6. Conceptual diagram to illustrate the genesis of the Kilkile pegmatite (modified from McKeough et al., 2013).

6.6.2. Parageneses of Kilkile tantalite deposit

Despite the homogeneity of albite–spodumene pegmatites, their detailed study demonstrates that a great variety of mineral parageneses formed at different stages of their evolution. Thus, an argument goes for a protracted and complex crystallization history (Gordiyenko, 1970).

The time-successive order of formation of a group of associated minerals within a particular deposit implies that parageneses minerals that are formed under similar conditions constitute paragenetic series (Barsanov, 2010). Swrtzon, (1971) demonstrates three distinct stages of mineralization parageneses. Similarly, three distinct stages of mineralization parageneses occurred in Kilkile pegmatite. At the first stage, the magma does not reach high level of evolvement which represents the crystallization of a rest magma not significantly different in composition from a normal granitic magma. Graphic granite, tourmaline, as well as coarsely crystalline microcline, muscovite, and quartz minerals are the main pegmatite body crystallized at this stage.

In the second stage of mineralization, parageneses represent pneumatolysis that refers to changes in rock mineralogy and chemistry that are initiated by the action of a hot and chemically active, gaseous solution derived from magma during its final stages of crystallization. This initiates greisenization and tourmalinization at the roof-zone granite (Allaby, 2008). Large quantities of beryl, sericite, apatite, and albite were introduced at this time, their replacement play vital role.

The third stage refers hydrothermal stage of mineralization that results in the progressive introduction of a large number of minerals by hydrothermal solutions. The final action of the solutions, as their temperature approached that of meteoric waters near the surface was an alteration of previously formed minerals. quartz, muscovite and garnet can be examples for this stage. Kilkile III pegmatites were probably formed in the first stages because their composition is similar to this stage. Field study, petrographic study and chemical analysis show that Kilkile I and some of Kilkile II pegmatites were most probably formed in stages two and three.

The chemical action and geologic history of the environment and the physicochemical and thermodynamic conditions of mineral formation play a vital role in mineral parageneses (Barsanov, 2010). According to this writer, the study of mineral parageneses is very important to find mineral deposits in group. Careful investigation and analysis of mineral parageneses in rocks makes it possible to reconstruct the course of mineral-forming process and establish factors that cause regular and repeating combinations of minerals with similar geochemical history in deposits.

Temperature plays more vital role for the concentration of Ta than the source rock does. High temperature anatexis results in high Ta fractionate due to residual biotite. This biotite becomes lower and lower on the reverse of muscovite which becomes dominant at the end stage of magma evolution. At the most evolved stage of the pegmatite, Ti-bearing oxides (e.g., ilmenite, rutile and garnet) become hosts for the Ta and Nb (Stepanov et al., 2014). This indicates mineral parageneses. Because of their close relationship of mineral and elements, mineral parageneses is closely related to the parageneses of elements that participate in the formation of minerals. In Kilkile muscovite composition Nb and Ta show different contents in different evolution. Relatively less evolved pegmatite contains high amount of Nb than Ta whereas elevated amount of Ta found in highly evolved pegmatites. Therefore, their ratio of Nb/Ta tells the sequence and fractionation level of the pegmatite as well as mineral parageneses. In Kilkile III least evolved pegmatite, the Nb/Ta ratio is relatively higher (14.65). This shows that the Nb content is much higher than Ta content. After further evolution in the same magma the Nb/Ta ratio becomes lower and lower from 14.65 to 10.7 in Kilkile II. Finally, the ratio becomes 2.5 while Ta content increases exceedingly (from 38.7 Kilkile III to 169 in Kilkile I) whereas the Nb content decreases from 567 in Kilkile III to 432 in Kilkile I.

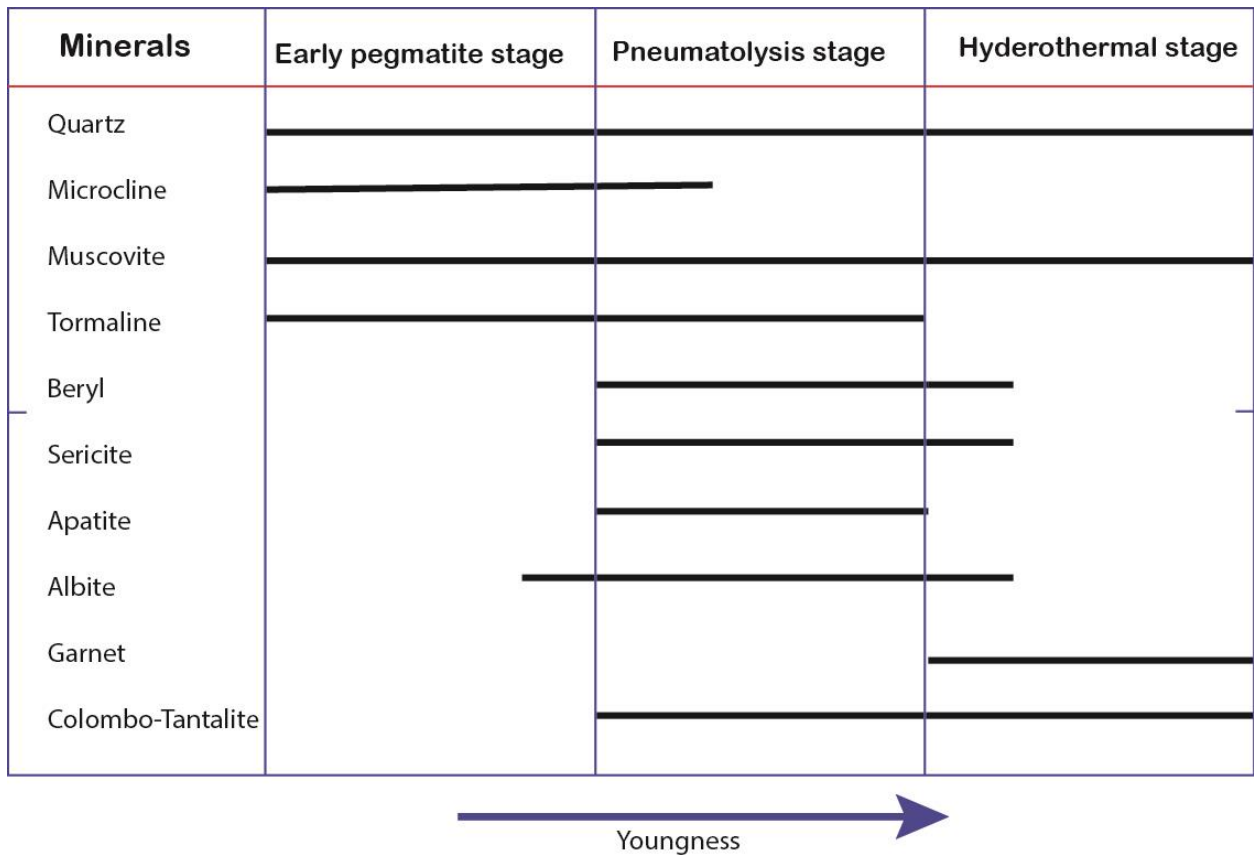


Figure 6.7. *Paragenetic scheme of Kilkile pegmatite.*

6.7. Others economic important commodities in Granitic Pegmatites of the study area

It is not expected all pegmatitic to comprises rare metals however, it can be the primary sources for industrial minerals like feldspar, quartz and mica. Feldspar uses for the glass and ceramics industries. In Kilkile area, feldspar is the most abundant next to quartz. The low iron and calcium contents of feldspars in pegmatite make these materials most desirable for glass and ceramics applications (London, 2012). Quartz used primarily in the manufacture of glasses, but ultra-high purity quartz from pegmatite is a fundamental material in the electronics industry. Boulder size variety quartz are like smoky, transparent and white quartz is available (Fig 6.6).

Some of Kilkile area granites are kaolinized. Thus, they can be used for clay (kaolinite) production. The clay minerals that are produced from weathered or hydrothermally altered pegmatites plays significant roles in the fabrication of microprocessors.

Many of the colored stones on the gem market today-varieties of beryl, topaz, tourmaline, garnet, emerald and others are produced mainly or solely from pegmatites. Most gem quality minerals come from open or clay-filled “miarolitic cavities” in pegmatite (Simmons et al., 2012). Gem varieties of beryl like emerald, tourmaline and beryl are available in Kilkile area especially in Kilkile I (Fig 6.7).



Figure 6.7. Gem and Industrial minerals of Kilkile area: A) and b) shows quartz, C) artesian miners on the way of extraction of emerald gem, D) artisional miners on rare metals, E) beryl minerals, F) emerald from Kilkile area and G) artisional miners on chromit mineral.

CHAPTER SEVEN

7. Conclusions and Recommendations

7.1. Conclusions

There are a number of rare metal occurrences in Kilkile area. Out of these, most of Kilkile I and some of Kilkile II (Kilkile IIc) pegmatites are found in the zone of Ta-mineralization. Almost all studies in pegmatite veins of Kilkile I area show positive in their rare metals mineralization as they are also the nearest to that of Kenticha rare metals bearing pegmatite. The Kilkile I and Kenticha area pegmatites have more or less similar geochemical behavior. However, relative to Kilkile II and III pegmatites, most of Kilkile I pegmatite veins are small in size.

The geotectonic discrimination diagrams show that majority of the Kilkile pegmatite samples fall within WPG. It is interpreted that the genesis of Kilkile rear metal bearing pegmatite, is related with the increase in basal heat flow beneath the earth surface causing partial melting of the pre-existing metasedimentary rocks which form felsic magma during post-Gondwana assembly, and later hydrothermal-metasomatic enrichment of rare metals deposit.

The result from Kilkile muscovite shows relatively high concentration in lithophile elements of Rb, Nb, Li, Ga, Cs, and Ta. The whole-rock geochemical composition of the Kilkile pegmatite corresponds to a peraluminous S-type granite composition and low content of P_2O_5 which shows mineralogical zonation with different concentration of major oxides, trace elements and REE.

Fractionation indicator elements in muscovite and their ratios indicate typical trend of magma fractionation on which fractionation increases from least evolved Kilkile III to relatively more evolved Kilkile I. This is also observed by fractionation indicator triangular (Rb-Ba-Sr plot) diagram by having high Rb and low Ba and Sr content. REE chondrite normalized diagram shows all samples have negative Eu-anomaly and their pattern indicates all the analyzed pegmatite rock samples display slight enrichment in light rare earth element (LREE) relative to heavy rare earth elements (HREE). This is a typical characteristic of evolved LCT-type granitic pegmatites. Most

of Kilkile I, and to some extent in Kilkile II pegmatites show albitization and greisenization, rare metals concentration also increases in this zone.

Muscovite chemistry, using Rb versus Tl and Rb versus K/Tl correlations, infers a cogenetic formation of Kilkile (I, II and III), Kenticha, Shuni and Bupo pegmatites and they are derived from same magma source most probably from Kilita Shumbela granite located on South of Kilkile III. Among These pegmatite Kilkile III pegmatites are the most evolved. Kilkile I, Kenticha and Shuni pegmatites show comparatively similar fractionation and geochemical behavior whereas the Bupo pegmatite is highly fractionated one.

7.2 Recommendations

Kilkile, Bupo, Shuni and Kenticha pegmatite have same magma source. From all pegmatites, Bupo is highly fractionated. But Ta content is higher in some of Kilkile I and Kenticha than further differentiated Bupo pegmatite. This might happen by latter hydrothermal activity and it needs further detailed studies.

The samples analyzed from these pegmatites were randomly taken and their quantity may not represent each pegmatite body. This is because the number of samples analyzed from each pegmatite veins is few in number. Therefore, further studies using robust sampling are needed for better understanding.

In addition to rare metals, the Kilkile pegmatites contain gemstones, such as beryl, tourmaline and recently discovered high-quality emerald. Some artisanal miners are producing these gems using backward technology. However, these gems especially emerald need special handling. As a result, there is a lot of wastage of commodity due to lack of knowledge and technical skill. Therefore, this situation calls for further studies by scholars and training for the local community members to capacitate them in using natural resource efficiently.

References

- Abdelsalam, M.G. and Stern, R.J. (1996). Sutures and shear zones in the Arabian–Nubian Shield. *Journal of African Earth Science*, **23**: 289–310.
- Abiola, O. (2014). Petrography and Petrochemical Characteristics of Rare Metal Pegmatites around Oro, Southwestern Nigeria, *Asia Pacific Journal of Energy and Environment*, 70-88.
- Allaby., M. (2 008) A Dictionary of Earth Sciences third edition, Oxford University Press, Oxford New York.
- Arundell, M. and Ronald, E. (2016). How To Make The Next Lithium Discovery, Mining Geology HQ.
- Asfawossen, A., Barbey, P. and Gleizes, G. (2001). The Precambrian geology of Ethiopia: a review, *Africa Geoscience Review*, **8**(3): 271-288.
- Ballouard, C., Poujol, M., Boulvais, P., Branquet, Y., Tartèse, R., Vignerresse, J.L., 2016. Nb-Ta fractionation in peraluminous granites: A marker of the magmatic-hydrothermal transition. *Geology* **44**, 231–234.
- Barsanov., G. P. (2010). Mineral Parageneses. The Great Soviet Encyclopedia, The Gale Group.
- Berhe, S. (1990). Ophiolites in Northeast and East Africa: implications for Proterozoic crustal growth. *Journal of Geological Society of London*, **147**: 647-657.
- Beus, A. (1966). Distribution of tantalum and niobium in muscovites from granitic pegmatites. *Geokhimiya* **10**:1216–1220, in Russian
- Beyth, M., Stern, R., Alther, R. and Kroner, A. (1994). The Late Precambrian Timna igneous complex, southern Israel: evidence for comagmatic type Sanukitoid monzodiorite and alkali granite magma. *Lithosphere*, **31**: 103-124.
- Blasband, B., White, S., Brooijmans, P., Boorder, H.D. and Visser, W. (2000). Late Proterozoic extensional collapse in the Arabian–Nubian Shield, *Journal of the Geological Society*, **157**: 615–628.
- Bongiolo, E.M., Renac, C., de Toledo Piza, P. d’Almeida, da Silva Schmitt, R., Mexias, A.S., 2016. Origin of pegmatites and fluids at Ponta Negra (RJ, Brazil) during late-to post-collisional stages of the Gondwana Assembly. *Lithos* **240**: 259–275.
- Boynton, W. (1984). *Cosmochemistry of the rare earth elements*. Elsevier.

- Bradley, D. and McCauley, A. (2013). *A Preliminary Deposit Model for Lithium-Cesium-Tantalum (LCT) Pegmatites*, U.S. Geological Survey, Open-File Report 2013–1008; Reston, Virginia, 10pp.
- British Geological survey (2011). *Niobium-Tantalum*, Natural Environmental Research Council. Nottingham, NG12 5GG, United Kingdom.
- Cameron, E.N., 1949. Internal structure of granitic pegmatites. Economic Geology Pub. Co.
- Černý, P. (1989). Characteristics of pegmatite deposits of tantalum. In: Lanthanides, Tantalum and Niobium. Springer, 195–239 pp.
- Černý, P. (1991). Rare-element granitic pegmatites. part I: Anatomy and internal evolution of pegmatitic deposits. *Geosci. Canada* **18**.
- Černý, P. (1997). REE trends in rare-element granitic pegmatites: enrichment vs. depletion in granite-to-pegmatite sequences. *J. Czech Geol. Soc.* **42**, 34.
- Černý, P. and Ercit, T.S. (2005). The classification of granitic pegmatites revisited. *Can. Mineral.* **43**.
- Cerny, P., 1982. Anatomy and classification of granitic pegmatites. *Min Soc Can Short Course Handb* 8, 1–39.
- Černý, P., London, D. and Novák, M. (2012). Granitic Pegmatites as Reflections of Their Sources, *New Hampshire and Maine*, **8**:289–294.
- Černý, P., Meintzer, R., Anderson, A. (1985). Extreme fractionation in rare-element granitic pegmatites: selected examples of data and mechanisms. *Can. Mineral.* 23.
- Chappell, B. and White, A. (2001). Two contrasting granite types: 25 years later. *Australian Journal of Earth Sciences*, **48**: 489-499.
- Desta, Z., Garbarino, C., Valera, R. (1995). Granite pegmatite system in Kenticha (Adola, Sidamo, Ethiopia) rare metal pegmatite belt: petro chemistry, regional pegmatite zoning and classification. *SINET Ethiop. J. Sci.* 18, 119e148.
- Eby, G. N. (1992). Chemical subdivision of the A-type granitoids: Petrogenetic and tectonic implications. *Geology* **20**:641–44.
- El Bouseily, A.M., El Sokyry, A.A. (1975). The relation between Rb, Ba and Sr in granitic rocks. *Chem. Geol.* **16**, 207–219.
- Ethiopian Geological Survey (2010), Opportunities for Tantalum resources development in Ethiopia, Addis Ababa, 3p.

- Ethiopian Mineral Development Enterprise, 1997. Background information on Kenticha Tantalum development, Volum I—Internal report (unpubl).
- Ethiopian Mineral, Petroleum and Bio-fuel Corporation (1982). Geological Map of Adola Area. 1:100,000.
- Ethiopian ministry of Mines (2002), Opportunities for investment in Ethiopia's Volume I Internal Report Addis Ababa.
- Eyob, A. (2013). Differentiating structures and litho-units of the Tsaliyet group around Negash area, Tigray, Northern Ethiopia. Unpublished MSc Thesis, Addis Ababa University, Addis Ababa, Ethiopia, 85pages.
- Farahat, E.S., Mohamed, H.A., Ahmed, A.F., El Mahallawi, M.M., 2007. Origin of I-and A-type granitoids from the Eastern Desert of Egypt: implications for crustal growth in the northern Arabian–Nubian Shield. *J. African Earth Sci.* 49, 43–58.
- Fertherson, J. M. (2004). Tantalum in Western Australia, Perth, *Geological Survey of Western Australia*.
- Fitches, W.R., Ajibade A. C., Egbuniwe I.G., Holt R. W., and Wright J.B. (1985): Late Proterozoic Schist Belts and Plutonism in NW Nigeria", *Geological Society of London*, **142**: pp. 319- 337.
- Genzebu, W. Hassen, N. and Yemane, T. (1994). Geology of the Agere Mariam area. Ethiopian Institute of Geological Surveys, memoir 8. Ethiopian Institute of Geological Surveys, Addis Ababa, 23p.
- Ginsburg, A.I., Timofeyev, I.N. and Feldman, L.G. (1979). *Principles of geology of the granitic pegmatites*. Nedra, Moscow, 296pp.
- Gordiyenko, V.V. (1971). Concentration of Li, Rb and Cs in potash feldspar and muscovite as criteria for assessing the rare metal mineralization in granitic pegmatites. *Int Geol Rev* 13:134–142.
- Hobart, M. (2018). Pegmatite An extreme igneous rock with large crystals and rare minerals. James R. C. (1994). Ore microscopy and ore petrography. Department of Geological Sciences.
- Johnson, P. and Woldehaimanot, B. (2003). Development of the Arabian-Nubian Shield: perspectives on accretion and deformation in the northern East African Orogen and the assembly of Gondwana. Supercontinent Assembly and breakup. *Geological Society of London*, Special Publication, **206**: 289-325.
- Kazmin, V. (1975). The Precambrian of Ethiopia and some aspects of the Geology of the Mozambique Belt. *Bulletin Geophysics. Obs.*, Addis Ababa University **15**: 27-43.

- Kazmin, V., Shiferaw, A., and Balcha, T. (1978). The Ethiopian basement and possible manner of evolution, *Geologische Rundschau* 67, 531-546.
- Kessel, R., Stein, M. and Navon, O. (1998). Petrogenesis of late Neoproterozoic dikes in the northern Arabian Nubian Shield: Implications for the origin of A-type granites. *Precambrian Research*, 92: 195-213.
- Kroner, A., and Stern, R.J. (2005). Africa/Pan- African Orogeny. Encyclopedia of Geology, v. 1. Elsevier, Amsterdam.
- Küster, D, Romer, R Toless, a D, Zerihun, D, Bheemalingeswara, K, Melcher, F & Thomas Oberthür (2009), *The Kenticha rare-element pegmatite, Ethiopia: internal differentiation, U–Pb age and Ta mineralization*, Porto.
- Küster, D., Rolf, L. Romer., Tolessa, D., & Zerihun, D., Bheemalingeswara, K., Melcher, F., and Oberthür, T. (2009). Granitoid-hosted Ta mineralization in the Arabian–Nubian Shield: ore deposit types, tectono-metallogenetic setting and petrogenetic framework. *Ore Geol. Rev.* 35: 68–86.
- Larsen, R.B., 2002. The distribution of rare-earth elements in K-feldspar as indicator of petrogenetic processes in granitic pegmatites: Examples from two pegmatite fields in southern Norway. *Can. Mineral.* 40: 137–151.
- Linnen, R., Lichtervelde, M. and Černý, p. (2011). Granitic Pegmatites as Sources of Strategic Metals, 8: 275–280.
- Linnen, R.L. and Cuney, M. (2005). Granite-related rare-element deposits and experimental constrains on Ta–Nb–W–Sn–Zr–Hf mineralization. In: Linnen, R.L., Samson, I.M. (Eds.), *Rare-element Geochemistry and Mineral Deposits: Geological Association of Canada. GAC Short Course Notes*, 17: 45–68.
- Linnen, R.L., Keppler, H., 2002. Melt composition control of Zr/Hf fractionation in magmatic processes. *Geochim. Cosmochim. Acta* 66: 3293–3301.
- Linnen, R.L., Lichtervelde, M. Van, Černý, P., (2012). Granitic Pegmatites as Sources of Strategic Metals. *Elements* 8: 275–280.
- London (2012) From vip Granitic Pegmatites: Scientific Wonders and Economic Bonanzas *Elements*, Vol. 8, pp. 257–261.
- London, D. (2008). Pegmatites. *Canadian Mineralogist Special Publication* 10, 347 pp.
- London, D., Morgan, G.B., (2012). The pegmatite puzzles. *Elements* 8, 263–268.

- London, D.(1982). spodumene, montebrasite and lithiophilite in pegmatites of the White Picacho District, Arizona. *Arizona State University*.**67**: 97-113.
- Martin, R. and De Vito, C. (2005). The patterns of enrichment in felsic pegmatites ultimately depend on tectonic setting. *Canadian Mineralogist* **43**: 2027-2048.
- McDonough, W., Sun, S. (1995). The composition of the Earth. *Chem. Geol.* 120, 223–253.
- McKeough, M.A., Lentz, D.R., McFarlane, C.R.M., Jarrod, B. (2013). Geology and evolution of pegmatite-hosted U–Th ± REE–Y–Nb mineralization, Kulyk, Eagle, and Karin Lakes region, Wollaston Domain, northern Saskatchewan, Canada: examples of the dual role of extreme fractionation and hybridization processes. *J. Geosci.* **58**: 321–346.
- Melcher, F., Graupner, T., Gäbler, H., Sitnikova, M., Henjes-Kunst, F., Oberthür, T., Gerdes, A. and Dewaele, S.(2013).Tantalum–(niobium–tin) mineralization in African pegmatites and rare metal granites: Constraints from Ta–Nb oxide mineralogy, geochemistry and U–Pb geochronology, *Ore Geology Reviews*, **64**:667–719.
- Mohammed, S. (2017). Geology, Geochemistry and Geochronology of the Kenticha Rare Metal Granite Pegmatite, Adola Belt, Southern Ethiopia: A Review, *International Journal of Geosciences*, 2017, **8**: 46-64, Debre Markos.
- New World Encyclopedia (2008). Pegmatite.
- O'Connor, J. T. (1965). A classification for quartz-rich igneous rocks based on feldspar ratios. *US Geological Survey, Professional Papers* 52(5): pp. 79-84.
- Pearce, J.A., Harris, N.B.W., Tindle, A.G., 1984. Trace element discrimination diagrams for the tectonic interpretation of granitic rocks. *J. Petrol.* **25**: 956–983.
- Poletayev, J., Verbvsky, O., Tew eldemedhin, T., Musa, E., Alemayehu, B. and Manaye, Y. (1991). The geology and rare metal potential of the Kenticha pegmatite deposit. Internal report (unpubl.) Ethiopian Mineral Resource Development Corp, Ministry of Mines and Energy, Addis Ababa, 113p.
- Rakovan, J. (2008). NYF-Type Pegmatite, Department of Geology, Miami University.
- Ralph, C. (2015). Prospecting for Pegmatites, *ICMJ's Prospecting and Mining Journal*, CMJ Inc.
- Robert, L, Marieke, V & Petr, C. (2011). *Granitic Pegmatites as Sources of Strategic Metals*, University of Western Ontario ON N6A 5B6, Canada.
- Rollinson, H.R. (1993). *Using geochemical data: evaluation, presentation, interpretation*: Routledge

- Selway, J., Breaks, F. and Tindle, A. (2005). A review of rare-element (Li-Cs-Ta) pegmatite exploration techniques for the Superior Province, Canada, and large worldwide tantalum deposits. *Exploration and Mining Geology* **14**: 1–30.
- Shaw, R.A., Goodenough, K.M., Roberts, N.M.W., Horstwood, M.S.A., Chenery, S.R. and Gunn, A.G. (2016). Petrogenesis of rare-metal pegmatites in high-grade metamorphic terranes: A case study from the Lewisian Gneiss Complex of north-west Scotland, *ScienceDirect*, **281**:338-362.
- Shearer, C.K., Papike, J.J., Jolliff, B.L. (1992). Petrogenetic links among granites and pegmatites in the Harney Peak rare-element granite-pegmatite system, Black Hills, South Dakota. *Can. Mineral.* **30**: 785.
- Simmons, S. (2007). Pegmatite genesis: Recent advances and area for future research. In: *Granitic Pegmatites: The State of the Art-International Symposium*. 06th – 12th May 2007, Porto, Portugal. p. 4.
- Simmons, W., Foord, E., Falster, A. and King, V. (1995). Evidence for an anatectic origin of granitic pegmatites, western Maine, USA. Geological Society of America Annual Meeting, New Orleans, Abstract Volume **27**:. p. A411.
- Simmons, W.B., Pezzotta, F., Shigley, J.E., Beurlen, H. (2012). Granitic pegmatites as sources of colored gemstones. *Elements* **8**: 281–287.
- Smith, R.E., Perdrix, J.L. and Davis, J.M. (1987). Dispersion into pisolitic laterite from the Greenbushes mineralized Sn-Ta pegmatite system, Western Australia: *Journal of Geochemical Exploration*, **28**: 251–265.
- Solomon, T. (2009). Mineral resource potential of Ethiopia. *Addis Ababa University Press, Ethiopia*, 1-50.
- Solomon, T. and Zerihun, D. (1996). Composition, fractionation trend and zoning accretion of the columbite-tantalite group of minerals in the Kenticha rare-metal field (Adola, southern Ethiopia). *J. African Earth Sci.* **23**: 411–431.
- Solomon, T. & Zerihun, D. (1996). Composition, fractionation trend and zoning accretion of the columbite-tantalite group of minerals in the Kenticha rare-metal field (Adola, southern Ethiopia). *J. Afr. Earth Sci.* **23**: 411e431.
- Stephanou, A., Mavrogenes, J.A., Meffre, S., David son, P. (2014). The key role of mica during igneous concentration of tantalum. *Contrib. to Mineral. Petrol.* **167**, 1009–1016.
- Stern, R.J. (1994). Arc assembly and continental collision in the Neoproterozoic East African Orogen: Implication for the consolidation of Gondwanaland, *Annual Review Earth Planetary Sciences*, **22**: 319–351.

- Stern, R.J. (2002). Crustal evolution in the East African Orogen: a neodymium isotopic perspective. *Journal of African Earth Sciences* **34**: 109–117.
- Swrtzon., G. (1971). The parageneses of the center strafford, new hampshire, pegmatite. Harvard University, Cambridge, Mass.
- Tadesse, T., Hoshino, M. and Sawada, Y. (1999). Geochemistry of low-grade metavolcanic rocks from the Pan-African of the Axum area-Northern Ethiopia. *Precambrian Research*, **99**: 101-124.
- Taylor,R. (2009). *Ore Textures*. Springer Dordrecht Heidelberg London New York, Australia, 282.
- Teklay, M. (1997). Petrology, Geochemistry, and Geochronology of Neoproterzoic Magmatic Arc Rocks from Eritrea: Implications for Crustal Evolution in the southern Nubian Shield. Eritrea Department of Mines Memoir, **1**: 125p.
- Trueman, D.L., and Černý, P. (1982), Exploration for rare-element granitic pegmatites: Mineralogical Association of Canada, *Short Course Handbook* **8**: 463–493.
- Trumbull, R. (1995): Tin mineralization in the Archean Sinceni rare-element pegmatite field, Kaapvaal craton, Swaziland *Journal of Economic Geology*, **90** (1): pp. 648-65
- Tsige, L. (2006). Metamorphism and gold mineralization of the Kenticha–Katawicha area, Adola Belt, southern Ethiopia. *Journal of Africa Earth Science*, **45**:16–23.
- Vail, J. (1985). Alkaline ring complexes in Sudan, *Journal of African Earth Sciences*, **3**. Virginia Polytechnic Institute and State University Blacksburg, Virginia.
- Woldai G. (1989). The Geological Evolution of Adola Precambrian Greenstone Belt, Southern Ethiopia. EIGS/UNDP Training for Mineral Exploration Project Eth/86/034, Addis Ababa.
- Worku., H. and Schandelmeier, H. (1996). Tectonic evolution of the Neoproterozoic Adola Belt of southern Ethiopia: evidence for a Wilson Cycle process and implications for oblique plate collision. *Precambr Res*, **77**:179–210.
- Yibas, B. (2000). The Precambrian geology, tectonic evolution, and controls of gold mineralization in southern Ethiopia. Ph.D. Thesis (unpublished), University of the Witwatersrand, Johannesburg, South Africa, 448 pp.
- Yibas, B., Reimold, W., Anhaeusser, C. and Koeberl, C. (2003). Geochemistry of the mafic rocks of the ophiolitic fold and thrust belts of southern Ethiopia: constraints on the tectonic regime during the Neoproterozoic (900–700 Ma). *Precambr Res* **121**:157–183.

- Yibas, B., Reimold, W.U. and Anhaeusser, C.R. (2000a). The geology of the Precambrian of southern Ethiopia: I—the tectonostratigraphic record. Information Circular 344, Economic Geology Research Institute, University of the Witwatersrand, Johannesburg, 21 pp.
- Yibas, B., Reimold, W.U., Armstrong, R., Koeberl, C., Anhaeusser, C.R. and Phillips, D. (2002). The tectonostratigraphy, granitoid geochronology and geological evolution of the Precambrian of southern Ethiopia, *Journal of Africa Earth Science*, **34**:57–84.
- Yihunie, T. (2002). Pan-African deformation in the basement of the Negele area, southern Ethiopia. *Int J Earth Sci (Geol Rundsch)*, **91**:922–933.
- Zerihun, D. (1991). Le mineralization a Ta-Nb: classification, propazine, valuations. Il caso di Kenticha (area di Adola, Sidamo, Ethiopia). —unpublished PhD.
- Zerihun, D. (1996). Mineralogical, geochemical, internal structure and metallogenetic relationship of granitite-pegmatite units in Kenticha area (Adola, Ethiopia). *Ethiop. Geosci. Miner. Eng. Assoc.* 251 – 280.
- Zerihun, D., Garbarino, C., Valera, R. (1995). Granite pegmatite system in Kenticha (Adola, Sidamo, Ethiopia) rare metal pegmatite belt: petro chemistry, regional pegmatite zoning and classification. *SINET Ethiop. J. Sci.* **18**, 119e148.
- Zhu, Y.F., Zeng, Y. and Gu, L. (2005). Geochemistry of the rare metal-bearing pegmatite No. 3 vein and related granites in the Keketuohai region, Altay Mountains, northwest China, *Journal of Asian Earth Sciences*, **27**: 61–77.

Appendix I

Structural data

№	structural element	Orientation			Location		Traverses	Unit
		Strike	Dip	Dip direction	Easting(x)	Northing(y)		
Fault								
1	fault	N12E	60	NW	501302	594206	1	Talc tremolite
2	fault	N15E	35	NW	502532	595401	2	Talc tremolite
3	fault	N10E	40	NW	503621	595372	2	Talc tremolite
4	fault	N15E	40	NW	502811	595932	3	Talc tremolite
5	fault	N8E	65	DUE EAST	501376	596652	4	Talc tremolite
6	fault	N5E	60	DUE EAST	502902	596392	4	Amphibolite
7	fault	N15E	60	NW	502902	596572	4	Talc tremolite
8	fault	N10E	70	DUE EAST	501801	597662	5	Amphibolite
9	fault	N20E	30	NW	502675	597296	5	Talc tremolite
10	fault	N20E	55	NW	503392	597716	5	Talc tremolite
11	fault	N10E	55	DUE EAST	501982	597442	5	Amphibolite
12	fault	N20E	60	NW	502880	597299	5	Talc tremolite
13	fault	N15E	20	NW	503274	598337	6	Serpentinite
14	fault	N30E	55	NW	502231	598335	6	Pegmatite
15	fault	NS	76	DUE EAST	501322	599764	7	Talc tremolite
16	fault	N22E	70	NW	501885	599263	7	Pegmatite
17	fault	N12E	40	NW	502782	599226	7	Talc tremolite
18	fault	N25E	55	NW	502811	599496	7	Amphibolite
19	fault	N5E	60	DUE EAST	504133	600374	8	Talc tremolite
20	fault	N5E	60	DUE EAST	503132	600665	8	Talc tremolite
Joints								

1	Joint	N15E	20	NW	503407	595601	2	Amphibolite
2	Joint	N10E	40	NW	503582	596176	3	Amphibolite
3	Joint	N10W	25	NE	501564	596880	4	Talc tremolite
4	Joint	N15E	60	NW	503276	597000	5	Amphib.. Schist
5	Joint	N20E	65	NW	502786	597545	5	Pegmatite
10	Joint	N25W	25	SW	597564	502301	5	Amphib. Schist
14	Joint	N35W	0	SW	597564	502405	5	Amphib. Schist
15	Joint	N5E	15	SW	597800	502563	5	Amphib. Schist
6	Joint	N8W	60	DUE EAST	503376	597923	6	Amphib. Schist
7	Joint	N5E	65	DUE EAST	501454	598704	6	Talc tremolite
8	Joint	N12W	50	NE	501778	598761	6	Biotite Gneiss
9	Joint	N5E	10	NW	501940	504942	6	Talc tremolite
11	Joint	N50W	10	SW	501943	504942	6	Talc tremolite
12	Joint	N30W	15	SW	501955	50470	6	Talc tremolite
13	Joint	N45W	20	SW	503443	59800	6	Amphib. Schist
Foliation								
1	Foliation	N25E	40	NW	501185	594601	1	Talc tremolite
2	Foliation	N30E	35	NW	502312	594470	1	Talc tremolite
3	Foliation	N28E	40	NW	500923	595568	2	Talc tremolite
4	Foliation	N18E	40	NW	501374	596861	4	Talc tremolite
5	Foliation	N24E	30	NW	503301	596538	4	Talc tremolite
6	Foliation	N12W	70	NE	502410	597651	5	Amphib. Schist
7	Foliation	N5E	65	DUE EAST	503813	597374	5	Talc tremolite
8	Foliation	N10W	70	SW	502565	597901	5	Amphib. Schist
9	Foliation	N20E	30	DUE EAST	503672	598106	6	Talc tremolite
10	Foliation	N25W	40	SW	501265	598854	6	Talc tremolite
11	Foliation	N10E	45	NW	502632	598430	6	Amphib. Schist
12	Foliation	N10W	70	SW	503870	598824	6	Talc tremolite

13	Foliation	N25W	40	SW	501265	598854	6	Talc tremolite
14	Foliation	N10E	45	NW	502632	598430	6	Amphib. Schist
15	Foliation	N10W	70	SW	503870	598824	6	Talc tremolite

Appendix II

CIPW norm of the analyzed pegmatite rocks

	Pegmatite rocks								
	K1A7	K1B14B	K1B14A	K2T6S2	K2A24A	K2A24B	K2C31	K2C30	K3T3S2
Quartz (Q)	32.19	28.95	27.75	76.67	35.22	49.88	57.04	26.81	92.41
Corundum(C)	1.65	2.26	4.76	5.36	3.47	5.37	10.94	1.98	1.81
Orthoclase(Or)	22.32	7.90	19.00	14.18	9.89	7.93	27.09	5.62	4.15
Albite(Ab)	41.42	55.09	44.63	1.73	47.82	32.71	2.51	61.89	0.51
Anorthite(An)	0.68	2.84	1.06	0.02	1.23	1.07	0.09	1.54	0.02
Hypersthene(Hy)	0.20	0.70	0.48	0.43	0.20	0.43	0.66	0.30	0.08
Magnetite(Mt)	0.07	0.48	0.48		0.73	0.45		0.33	0.00
Ilmenite(Il)	0.02	0.11	0.08	0.04	0.06	0.12	0.04	0.06	0.02
Apatite(Ap)	0.16	0.12	0.17	0.01	0.09	0.05	0.02	0.48	0.01
Hematite(Hm)	1.29	1.57	1.59	1.52	1.29	1.99	1.57	0.99	0.99
Rutile(Ru)				0.03			0.04		
Hypersthene en	0.20	0.70	0.48	0.43	0.20	0.43	0.66	0.30	0.08